

The Epigenetic and Neurodevelopmental Consequences of Maternal Tobacco Smoke
Exposure

by

Rashmi Joglekar

Environment
Duke University

Date: _____

Approved:

Joel N. Meyer, Advisor

Susan K. Murphy, Advisor

Edward D. Levin

Cynthia M. Kuhn

Dissertation submitted in partial fulfillment of
the requirements for the degree of
Doctor of Philosophy
in Environment
in the Graduate School
of Duke University

2019

ABSTRACT

The Epigenetic and Neurodevelopmental Consequences of Maternal Tobacco Smoke
Exposure

by

Rashmi Joglekar

Environment
Duke University

Date: _____

Approved:

Joel N. Meyer, Advisor

Susan K. Murphy, Advisor

Edward D. Levin

Cynthia M. Kuhn

An abstract of a dissertation submitted in partial
fulfillment of the requirements for the degree
of Doctor of Philosophy
in Environment
in the Graduate School of
Duke University

2019

Copyright by
Rashmi Joglekar
2019

Abstract

Maternal smoking is a deleterious and preventable risk to fetal health. Maternal tobacco smoke (TS) exposure in humans has been linked to impaired fetal growth, preterm birth, sudden infant death syndrome, and neurobehavioral disorders including cognitive dysfunction, attention-deficit hyperactivity disorder (ADHD) and autism spectrum disorder (ASD). In the United States, nearly 10% of pregnant women smoke despite ongoing public health efforts to reduce the incidence of smoking. Of additional concern is the steady rise of electronic nicotine delivery systems (ENDS) use among pregnant women over the past decade. Further, ENDS are often used in conjunction with tobacco cigarettes, compounding exposure effects. In animal models, both maternal TS and nicotine exposure lead to adverse neurodevelopmental outcomes, including increased anxiety and ADHD-like behavior, that are transmitted to subsequent generations. A likely explanation for this phenomenon lies in early developmental epigenetic programming. Epigenetic markers that are established early in development, like DNA methylation, can persist throughout somatic cell division and gametogenesis. During early development, zygotic DNA methylation is reprogrammed following a wave of global demethylation, and only re-established during the peri-implantation period. Environmental perturbations during these critical phases of reprogramming have been associated with persistent, and even transgenerationally-inherited effects,

underscoring the importance of examining these associations in the context of human health and disease.

The broader goals of this dissertation were to identify alterations in DNA methylation patterning in the brain as a result of maternal TS exposure, and assess their neurodevelopmental significance. In an effort to better understand the effects of nicotine alone, especially given the increasing usage of ENDS during pregnancy, we chose to examine developmental nicotine exposure in addition to TS exposure. Finally, we evaluated the translational significance of these alterations by examining correlations in humans developmentally exposed to TS. Using a rat model for gestational nicotine exposure, DNA methylation levels were measured in the brains of neonatal and adult rats to determine the persistence of exposure effects. Specific brain regions, including the rat preoptic area (POA), hippocampus and cortex were targeted for evaluation based on their neurobehavioral significance. A rat gestational exposure model for tobacco smoke extract (TSE) was further employed to determine potential overlap with methylomic regions affected by developmental nicotine exposure. Finally, to derive translational implications, DNA methylation was examined on both epigenome-wide and targeted levels in human cord blood from newborns exposed to maternal TS.

In neonatal rats developmentally exposed to nicotine, DNA methylation was reduced in regions implicated in masculinization of the preoptic area (POA), a region of the brain that requires epigenetic reprogramming events to sexually differentiate.

Subsequent behavioral analyses in adulthood revealed that these alterations may have contributed to the developmental masculinization of the POA in nicotine-exposed females. In adults males developmentally exposed to nicotine, alterations to DNA methylation were observed in the hippocampus and cortex, two brain regions that are also associated with ADHD- and ASD-like behaviors, respectively. Further, a comparison of differentially-methylated regions (DMRs) between the brains of animals exposed to developmental nicotine and TSE revealed significant overlap, indicating that nicotine is largely driving the developmental alterations to DNA methylation observed in TSE-exposed animals. Examination of DNA methylation alterations in human infant cord blood as a result of maternal TS exposure indicated significant overlap with those revealed in rats, supporting common impacts on developmental epigenetic reprogramming across species. Moreover, nearly half of these common regions were implicated in neurodevelopmental disorders, namely ASD and ADHD. Alterations to DNA methylation at human metastable epialleles, or regions for which DNA methylation is stochastically established during early development, were observed in the cord blood of infants exposed to TS *in utero*, supporting the ability of TS-exposure to alter vulnerable regions of the epigenome during early developmental reprogramming.

Dedication

This dissertation work is dedicated to my roots, The *Damles* and The *Joglekars*, for exemplifying the strength and power in education.

Contents

Abstract	iv
Contents	viii
List of Tables	xii
List of Figures	xiv
Acknowledgements.....	xvi
1. Introduction	1
1.1 Epigenetic Modifications.....	2
1.1.1 DNA Methylation.....	3
1.1.1.1 Detection Methods.....	5
1.1.1.2 Early Epigenetic Reprogramming.....	7
1.1.1.3 Neurodevelopment.....	9
1.2 Dissertation Objectives and Outline.....	10
2. Maternal nicotine exposure alters brain sexual differentiation in rats	15
2.1 Introduction	15
2.2 Materials and Methods	20
2.2.1 Animal Husbandry and Behavioral Testing.....	20
2.2.2 Immunofluorescence Microscopy	24
2.2.3 Whole Genome Bisulfite Sequencing Analysis.....	25
2.2.4 Targeted DNA Methylation Quantification.....	26
2.2.5 Quantitative Real-Time PCR.....	27

2.2.6 Statistics	29
2.3 Results	30
2.3.1 Birth Outcomes and Weight Characteristics.....	30
2.3.2 Maternal nicotine exposure evokes upregulation of epigenetic mechanisms required for POA masculinization.....	31
2.3.3 Maternal nicotine exposure eliminates structural and functional sex differences in the adult POA	34
2.3.4 Maternal nicotine exposure masculinizes the female POA	36
2.4 Discussion	37
3. Maternal tobacco smoke exposure alters DNA methylation at genomic regions implicated in neurobehavioral disorders.....	64
3.1 Introduction	64
3.2 Materials and Methods	69
3.2.1 Animal Husbandry and Gestational Treatment.....	69
3.2.2 Study Population: NEST	71
3.2.2.1 NEST Maternal Plasma Cotinine Measurement & Cord Blood Collection	71
3.2.3 DNA Isolation.....	72
3.2.4 Whole Genome Bisulfite Sequencing (WGBS) of Rat Hippocampus, Cortex, and Peripheral Blood	73
3.2.4.1 Methyl-MaxiSeq® library construction	73
3.2.4.2 Methyl-MaxiSeq® sequence alignments and data analysis	74
3.2.5 Reduced Representation Bisulfite Sequencing (RRBS) of NEST Cord Blood...	74
3.2.6 Data Analysis.....	75

3.3 Results	77
3.3.1 Overlap in genomic targets of altered methylation across peripheral blood, hippocampus, and cortex elicited by developmental TSE and nicotine exposure... ..	77
3.3.2 Developmental TSE and nicotine exposure-associated DMRs correlate to common functional clusters in male rats.....	78
3.3.3 Overlap in genomic targets of altered methylation associated with developmental TS exposure in rats and humans.....	78
3.3.4 Developmental TSE exposure induces tissue-specific changes in the number of differentially methylated CpGs within DMRs common to rats and humans.....	79
3.4 Discussion	80
4. Maternal tobacco smoke is associated with increased DNA methylation at human metastable epialleles in infant cord blood	97
4.1 Introduction	97
4.2 Materials and Methods	99
4.2.1 Study Specimens: Human Conceptual Tissues	99
4.2.2 Study Population: NEST	99
4.2.2.1 Maternal Plasma Cotinine Measurement	100
4.2.2.2 Maternal Whole Blood Micronutrient Measurement	101
4.2.2.3 Umbilical Cord Blood Collection.....	102
4.2.2.4 Umbilical Cord Fractionation	102
4.2.3 DNA/RNA Isolation and Bisulfite Modification	102
4.2.4 DNA Methylation Analyses.....	103
4.2.5 Gene Expression Analyses	104
4.2.6 Statistics	104

4.3 Results	105
4.3.1 Validation of metastable epialleles at BOLA3, PAX8, and ZFYVE28	105
4.3.2 NEST maternal demographics and smoking status.....	106
4.3.3 Maternal micronutrient levels, smoking status, and sociodemographic variables	107
4.3.4 Maternal tobacco smoke exposure is associated with increased infant ME DNA methylation.....	109
4.3.5 PAX8 and BOLA3 methylation are negatively associated with maternal micronutrient levels	110
4.3.6 PAX8 mRNA levels are negatively associated with DNA methylation.....	111
4.4 Discussion	112
5. Conclusion.....	141
5.1 Summary	141
5.2 Implications, Limitations, and Future Directions	144
5.2.1 The Masculinizing Effects of Developmental TS Exposure.....	145
References	148
Biography.....	168

List of Tables

Table 1: Pyrosequencing assays used in targeted DMR validation	60
Table 2: Birth outcomes stratified by gestational exposure.....	61
Table 3: DAVID Functional Annotation Clustering of Top DMRs.....	62
Table 4: Genomic location and function of target DMRs.....	63
Table 5: DAVID Functional Annotation Clustering of DMRs Common to Peripheral Blood, Hippocampus, and Cortex of Male Rats Exposed to 0.2 mg/kg/day TSE.	92
Table 6: DAVID Functional Annotation Clustering of DMRs Common to Peripheral Blood, Hippocampus, and Cortex of Male Rats Exposed to 0.2 mg/kg/day Nicotine.....	93
Table 7: DAVID Functional Annotation Clustering of DMRs Common to Peripheral Blood, Hippocampus, and Cortex of Male Rats Exposed to 2.0 mg/kg/day Nicotine.....	94
Table 8: DAVID Functional Annotation Clustering of DMRs Common Across Blood, Hippocampus, and Cortex of Rats	95
Table 9: 115 DMRs Common to Rats and Humans Developmentally Exposed to TSE or Components of TS, Stratified by Neurodevelopmental Disorder Implication	96
Table 10: Pyrosequencing assays for human metastable epialleles.	129
Table 11: NEST cohort maternal sociodemographic data stratified by plasma cotinine levels.	130
Table 12: NEST gestational characteristics stratified by tobacco smoke exposure status.	132
Table 13: Maternal plasma cotinine distribution in the full NEST cohort.....	133
Table 14: NEST infant birth weight stratified by maternal tobacco smoke exposure status.....	134
Table 15: NEST cohort maternal micronutrient levels stratified by tobacco smoke exposure.	135

Table 16: NEST maternal micronutrient levels stratified by education level.....136

Table 17: NEST maternal micronutrient levels stratified by pre-conceptional BMI.....137

Table 18: NEST maternal micronutrient levels stratified by predominant race.138

Table 19: NEST maternal micronutrient levels stratified by maternal age.....139

Table 20: DNA methylation at human metastable epialleles stratified by NEST maternal micronutrient levels.....140

List of Figures

Figure 1: Types of Epigenetic Modifications.	13
Figure 2: Schematic of Dissertation Aims.	14
Figure 3: Birth outcomes are unaffected by gestational treatment.	47
Figure 4: Body weight measurements taken between PND1 and PN77 in male and female offspring indicate both sex- and treatment-specific effects.	48
Figure 5: Sex differences in brain weight emerge in adulthood in all groups except estradiol-treated animals.	49
Figure 6: Distribution of epigenome-wide CpG methylation (represented as percent methylation) in neonatal male, female, and estradiol-masculinized female POA.	50
Figure 7: Nicotine exposure evokes upregulation of epigenetic mechanisms required for POA masculinization in neonates.	52
Figure 8: Maternal nicotine exposure eliminates sexual dimorphisms in male sexual behavior and SDN area.	55
Figure 9: Variability across additional sexual behavior parameters observed during PND60 male sexual behavior assays.	57
Figure 10: Novel methods for assessing masculinization of the rat POA.	58
Figure 11: Schematic of tissue collection for bisulfite sequencing in humans and rats exposed <i>in utero</i> to TS or its constituents.	87
Figure 12: Overlapping DMRs identified through WGBS across peripheral blood, hippocampus, and cortical tissue in male rats exposed to TSE or nicotine.	88
Figure 13: Overlapping DMRs identified through WGBS and RRBS in rat tissues and human umbilical cord blood.	89
Figure 14: Frequency and Relative Genomic Location of CpGs within Target DMRs.	90
Figure 15: Pyrosequencing assay validations for human MEs.	122

Figure 16: Inter-tissue correlation and inter-individual variation verify BOLA3, PAX8, and ZFYVE28 as human metastable epialleles (MEs).....	123
Figure 17: Characterization of ME status for the putative human ME SLITRK1.....	124
Figure 18: NEST maternal tobacco smoke (TS) exposure is associated with increased infant cord blood DNA methylation at MEs.	127
Figure 19: Association of PAX8 mRNA levels and ME DNA methylation in conceptual kidney tissue.	128

Acknowledgements

To my educators, mentors, and classmates at Duke and past academic institutions, thank you for encouraging and supporting me throughout my academic pursuits.

To the collaborators near and far that contributed to this work, thank you for sharing the facilities and expertise that were critical to this research.

To my thesis committee, thank you for your insight and collaboration over the past four years. Your dedication has not only shaped my dissertation work, but also my growth as a scientist.

To my graduate research mentors Joel Meyer and Susan Murphy, your guidance, patience, and unwavering support are the reasons that I was able to grow and thrive at Duke. I am forever grateful to you both for enabling me to transform not only as a scientist, but as a Duke citizen and Durham community member. You both are extraordinary examples of kindness, balance, and determination that I will always look up to.

To my mom, dad, and brother, your constant love keeps me afloat.

Finally, and most certainly not least, to my partner Will. For being my source of stability in the most uncertain of times, a shoulder to cry on, and my biggest fan. To the late nights you spent with me in lab, your smiling face in the audience during my

proudest moments, and the umpteen batches of homemade popcorn. To your voice of reason when nothing seemed reasonable, and your constant sense of strength. I can never truly express how grateful I am for your support throughout this journey.

1. Introduction

Epigenetic reprogramming during early development is critical to normal development [1-14]. Following fertilization of the egg, epigenetic markers in the early developing zygote are erased, with new markers established at the blastocyst stage. Perturbations to these reprogramming processes can adversely impact fetal development, with effects lasting into adulthood and even into subsequent generations. Exposure to environmental compounds during early epigenetic reprogramming has been shown to adversely affect development. A multitude of studies examining gestational exposure to compounds like polycyclic aromatic hydrocarbons (PAHs) were shown to alter early epigenetic reprogramming, and subsequently affect developmental phenotypes later in life [14, 15].

Gestational exposure to tobacco smoke (TS) has also been associated with alterations in epigenetic makeup, namely DNA methylation, in the fetus [1, 6, 16-23]. These alterations have been further associated with adverse behavioral outcomes later in life [1, 21, 23, 24]. However, most of these studies relied on the examination of epigenetic markers in the cord blood or leukocyte fractions of exposed offspring. Such studies identified long-term developmental effects of gestational TS exposure including biases towards neurobehavioral disorders such as ADHD and ASD [25-28]. As such, to fully understand the connection between methylation and gestational TS exposure, it is critical to examine epigenetic alterations in the brain, with focus on regions implicated in

these neurobehavioral disorders. In order to validate current findings and identify epigenomic regions that could serve as potential biomarkers of exposure, it is important to correlate exposure-induced alterations in the brain with those in the blood.

The focus of this research was to identify alterations in neuro-epigenetic patterning across multiple developmental timepoints as a result of maternal TS exposure, and assess corresponding neurodevelopmental significance.

1.1 Epigenetic Modifications

Canonically, epigenetic modifications are heritable changes made to genomic DNA that alter gene expression or chromatin structure without changing the genomic sequence itself [3, 7, 12-14, 29, 30]. Conrad Waddington first described this phenomenon in 1942 as the mechanism that enables irreversible cell type differentiation, in a process he defined as “canalisation.”[31] Currently, epigenetic modifications are considered a collection of covalent and non-covalent heritable modifications that alter gene expression and chromatin structure; however, this understanding is continuously advancing. Non-covalent epigenetic modifications include non-coding RNAs, such as long-non coding RNAs, microRNAs and circular RNAs [13]. Covalent modifications, which are perhaps the most widely-studied forms of epigenetic modifications, include DNA methylation and post-translational histone modifications (Figure 1). Epigenetic modifications like DNA methylation and histone acetylation are enzymatically added to their respective substrates (via methyltransferase and histone acetyltransferase

enzymes), and can be enzymatically removed [1, 5, 7, 9, 13]. The ability to enzymatically add and remove modifications on DNA and chromatin underscores the plasticity of the epigenome.

1.1.1 DNA Methylation

DNA methylation typically refers to the covalent bonding of a methyl group (-CH₃) to the 5' carbon of the cytosine nitrogenous base found in DNA. These methylated cytosine residues at the 5' carbon position, referred to as 5-mC, often precede guanine residues and are collectively referred to as CpG methylation [32]. While CpG methylation is the most common form of DNA methylation, other forms of 5-mC (CpC, CpA, or CpT) have been reported [32], although at a much lower frequency. 5-mC has also been reported in its oxidized state, 5-hydroxymethylcytosine (5-hmC), although this modification is relatively uncommon throughout the genome [33, 34]. The enzymes responsible for methylating DNA are collectively referred to as DNA methyltransferase enzymes (DNMTs) [8, 35]. These enzymes catalyze DNA methylation of hemimethylated DNA strands in a process referred to as maintenance methylation, or alternatively, they target fully-unmethylated DNA strands in a process referred to as *de novo* methylation [36]. DNMTs performing both maintenance (DNMT1) and *de novo* (DNMT3a, 3b) cytosine methylation rely on the universal methyl group donor, S-adenosylmethionine (SAM).

CpG dinucleotides are vastly underrepresented in the genome (comprising only 1% of the human genome) likely due to the high rate of C→T transition mutations that occur spontaneously via deamination of cytosine [37]. Because methylated cytosines are protected from deamination, CpG methylation is highly favorable in the genome. In fact, 70% of genomic CpG dinucleotides are methylated [38]. CpG dinucleotides often exist in clusters known as CpG islands. CpG islands are defined as CpG clusters over segments of DNA (spanning 0.5-2-kb in length) that contain >50% CG content, and contain CpGs at a ratio of observed to expected CpG that is greater than 0.6 [32, 37]. CpG islands are often found in proximal gene promoter regions or heterochromatin [39], and less commonly found within gene bodies themselves [40]. CpG methylation is often implicated in gene regulation due to the localization of CpG islands to gene promoter regions. Promoter CpG methylation levels are commonly negatively correlated with expression of the downstream gene, although this correlation can be positive [12].

CpG methylation is the most well studied epigenetic modification, likely due to its chemical stability and persistence across cell division [13]. CpG methylation plays crucial roles in critical cellular and developmental process, including cellular differentiation, gene expression, X-chromosome inactivation, chromatin stability, and parental gene imprinting [30, 41, 42] As such, it remains one of the most plausible mechanisms for inter-and trans-generational transmission of environmentally altered or disrupted epigenetic patterning [15].

1.1.1.1 Detection Methods

In general, DNA methylation levels can be quantified in vertebrates at targeted epigenomic regions, or epigenome-wide. In order to assess whole-genome methylation levels without regional specificity, high performance liquid chromatography-ultraviolet (HPLC-UV) [43], liquid chromatography and tandem mass spectrometry (LC-MS/MS) [44-47] and enzyme-linked immunosorbent assay (ELISA) detection techniques can be employed [48]. HPLC-UV detection relies on the hydrolyzation of input DNA into nucleoside monomers, and the quantification of chromatographically-separated methylated cytosines (5mCs) [43]. While HPLC-UV detection methods are considered the “gold standard” for quantifying overall 5-mC content, the technique requires a large amount of input DNA, and can be costly. In ELISA detection methods, antibodies targeting 5-mC are used to colorimetrically quantify genomic 5-mC content. Similar to HPLC-UV, ELISA-based techniques require large amounts of input DNA. Additionally, ELISA detection techniques have very low sensitivity, and are only capable of detecting relatively large differences in DNA methylation [48]. LC-MS/MS relies on mass spectrometry to detect 5-mC. Although this technique requires costly and highly-specialized expertise, it is capable of detecting as low as 0.05% global 5-mC levels and requires very little input DNA [44-47]

Broadly, bisulfite sequencing is the most commonly-used method for assessing region-specific differences in DNA methylation and defining differentially-methylated

regions (DMRs). Bisulfite sequencing relies on the bisulfite modification of DNA, a chemical process that converts all unmethylated cytosine residues to uracils, which then appear as thymines following PCR amplification and sequencing. As methylated cytosines are protected from bisulfite conversion, they remain as cytosines and are thus distinguishable from unmethylated cytosines using either small- or large-scale sequencing technologies [49].

Bisulfite-modified DNA can be assessed for epigenome-wide or targeted 5-mC methylation using next generation sequencing (NGS) technologies. Whole genome bisulfite-sequencing (WGBS) is much like whole-genome sequencing, but relies on bisulfite-modified DNA input. WGBS is capable of detecting differential methylation levels between two or more samples at all genomic CpGs with very little input DNA required. However, this methodology is costly and is often only used in the case of non-targeted, hypothesis-generating analyses [50]. Reduced-representation bisulfite sequencing (RRBS) is another larger-scale bisulfite sequencing technique, but only examines a fraction of the genome, and particularly selects for regions that are CG-enriched [51-53]. RRBS relies on enzymatic digestion of DNA at CCGG sites *prior* to bisulfite-modification. Following digestion, fragments are bisulfite-treated and sequenced using NGS techniques. Although RRBS requires more input DNA than WGBS, it can be performed for a fraction of the cost and still covers nearly 85% of all genomic CpG islands [51-53].

Bisulfite pyrosequencing is a small-scale sequencing technology used to examine 5-mC across short, targeted stretches of DNA (upwards of 100bp) [50]. Pyrosequencing relies on the detection of light signals produced following nucleotide inclusion during primer-guided elongation of bisulfite-modified DNA that has been PCR-amplified. Although the window of examination is magnitudes smaller than in whole-genome approaches, pyrosequencing is able to detect methylation differences as low as 5% [50], and even down to 0.5% in one reported case [54].

In addition to bisulfite sequencing technologies, microarray and bead hybridization techniques are also common large-scale CpG quantification methods. Both rely on the hybridization of pre-designed oligos complementary to either uracil (indicative of unmethylated cytosine) or cytosine (indicative of methylation) to assess methylation status at up to 850k genomic CpGs [55, 56]. Microarray methylation assays are among the most cost-efficient large-scale methylation sequencing techniques, but have primarily been developed for human samples. Further, because CpGs of interest are predetermined, this technique allows for little flexibility in investigating genomic CpGs in non-functional genomic regions [50].

1.1.1.2 Early Epigenetic Reprogramming

DNA methylation levels are highly dynamic during embryonic development [13, 57], specifically during stages of epigenetic reprogramming. In mammals, there are two primary windows for epigenetic reprogramming: 1) immediately following fertilization

and 2) during primordial germ cell maturation [9, 15]. Both reprogramming windows are critical to normal development: the first for establishing totipotency required for cellular differentiation, and the second for the completion of germ cell differentiation [5, 58]. DNA methylation reprogramming events during the early developmental period are particularly critical, as embryonic stem cells (ESCs) lacking DNMTs can proliferate, but fail to differentiate [57]. Following fertilization, DNA methylation patterns are globally erased in the developing zygote, except at regions that escape this wave of demethylation, and are re-established following implantation of the blastocyst [9]. Re-established DNA methylation in the implanted blastocyst closely resembles that of adult somatic cells [59].

Although demethylation of the early zygote is widespread, regions of the epigenome that escape demethylation are often referred to as “escapees.” Allelic escapees that normally resist zygotic reprogramming and maintain the DNA methylation patterning of the parent-of-origin are referred to as imprinted loci [4]. More specifically, CpG methylation patterning at imprinted loci is either maternally or paternally inherited, and persists throughout reprogramming-associated demethylation events [60]. Genomic deletion mutations within imprinted loci are associated with intellectual disability syndromes, including the Prader-Willi and Angelman Syndromes, underscoring the significance of genomic imprinting in normal development [61]. Moreover, the fact that epigenetic regions escape developmental epigenetic

reprogramming under normal conditions supports the notion that DNA methylation patterning across these regions can be transmitted from one generation to the next.

Mammalian metastable epialleles (MEs) are regions of the epigenome where DNA methylation is stochastically established during the early epigenetic reprogramming window, before the separation of the germ layers that occurs during gastrulation. [62-65]. As such, DNA methylation patterning that is established at MEs persists throughout all cell types of the body and is consistent across tissues [64]. However, because the methylation establishment at these regions is stochastic, ME methylation is also characterized by strong interindividual variation [64]. In the context of environmental exposures during early epigenetic reprogramming, ME methylation has served as one of the most reliable early developmental epigenetic biosensors and indicator of early developmental epigenetic disruption [62, 65-67].

1.1.1.3 Neurodevelopment

Although mammalian neurodevelopment largely occurs after early epigenetic reprogramming, DNA methylation levels are nonetheless highly dynamic during normal neurodevelopment. In fact, the brain is characterized by some of the highest 5-mC levels of all organ tissues. Fluctuations in DNA methylation were found to be responsive to long-term potentiation, and thus thought of as critical for normal neuronal function [13]. Cell-type specific alterations to DNA methylation levels are critical for normal astrocytic [68] and neuronal [57] differentiation during late embryonic

development. Imprinted loci also play a critical role in neurodevelopment [12, 69]. Imprinted genes that are expressed in both the placenta and the fetal brain during development are almost all overwhelmingly maternally imprinted and paternally expressed. One such gene, *Peg3*, plays a critical role in hypothalamic development. Mutations in *Peg3* that led to maternal expression not only altered the ability of pregnant mice to raise their pups, but prevented normal neurodevelopment in the developing pups [12, 69]. These phenotypes in both the mother and pups resembled those of hypothalamic lesions [12, 69]. Such investigations underscore the critical roles that imprinted gene dosage and establishment, especially of maternally-imprinted genes, play in normal neurodevelopment. This is of particular relevance given the heritable nature of DNA methylation patterning at imprinted loci [10, 70, 71].

1.2 Dissertation Objectives and Outline

The broader goals of this dissertation are to identify alterations in DNA methylation patterning in the brain as a result of maternal TS exposure, assess their neurodevelopmental significance, and derive translational implications. I hypothesized that maternal TS exposure would lead to alterations in fetal DNA methylation patterns that would 1) disrupt larger, neurodevelopmental processes like the sexual differentiation of the brain, and 2) lead to behavioral consequences later in life in rodents. In order to better understand the translational implications of these findings, I further sought out to examine whether or not maternal TS exposure in humans could

alter DNA methylation in corresponding regions to those in rodents, particularly regions that are known to undergo early epigenetic reprogramming (research schematic depicted in Figure 2).

This dissertation is organized into the following research chapters which each address critical elements of these objectives and hypotheses:

Chapter 2: Maternal nicotine exposure alters brain sexual differentiation in rats.

Alterations to DNA methylation in epigenomic regions required for brain masculinization were examined in the rodent preoptic area (POA), a brain region characterized by robust sexual dimorphism. Using a rat gestational model for nicotine exposure, pups were exposed to nicotine throughout the window for brain sexualization. Following the examination of epigenetic endpoints, adult sexual behavior was assessed to examine behavioral correlations with developmental nicotine exposure. Finally, a statistical analysis method was developed to comprehensively assess POA masculinization across multiple measurements.

Chapter 3: Maternal tobacco smoke exposure alters DNA methylation at genomic regions implicated in neurobehavioral disorders.

Using next-generation sequencing techniques, genome-wide DNA methylation patterning was assessed in blood, hippocampal, and cortical tissues taken from adult

male rats developmentally exposed to nicotine and tobacco smoke extract (TSE). Differentially methylated regions (DMRs) were identified across tissues and treatments, and overlapping regions were evaluated for functional significance. Finally, DMRs common to rats were compared to those identified in humans developmentally exposed to TS in order to derive translational relevance and potential biomarkers of exposure.

Chapter 4: Maternal tobacco smoke is associated with increased DNA methylation at human metastable epialleles in infant cord blood

Cord blood obtained from infants developmentally exposed to TS was examined for DNA methylation levels at human metastable epialleles, or epigenomic regions stochastically established during early epigenetic reprogramming. Bisulfite pyrosequencing techniques were employed to evaluate DNA methylation at MEs in a targeted fashion, and examine whether or not developmental TS exposure could alter DNA methylation in the fetus during the earliest epigenetic reprogramming window.

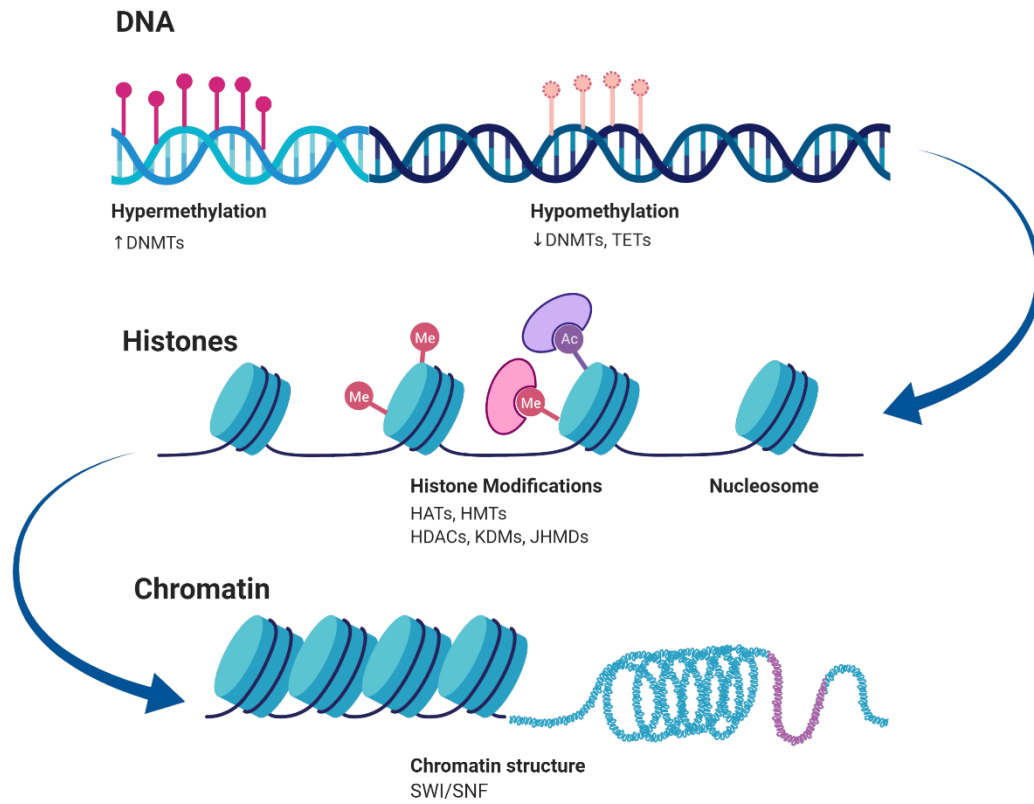


Figure 1: Types of Epigenetic Modifications.

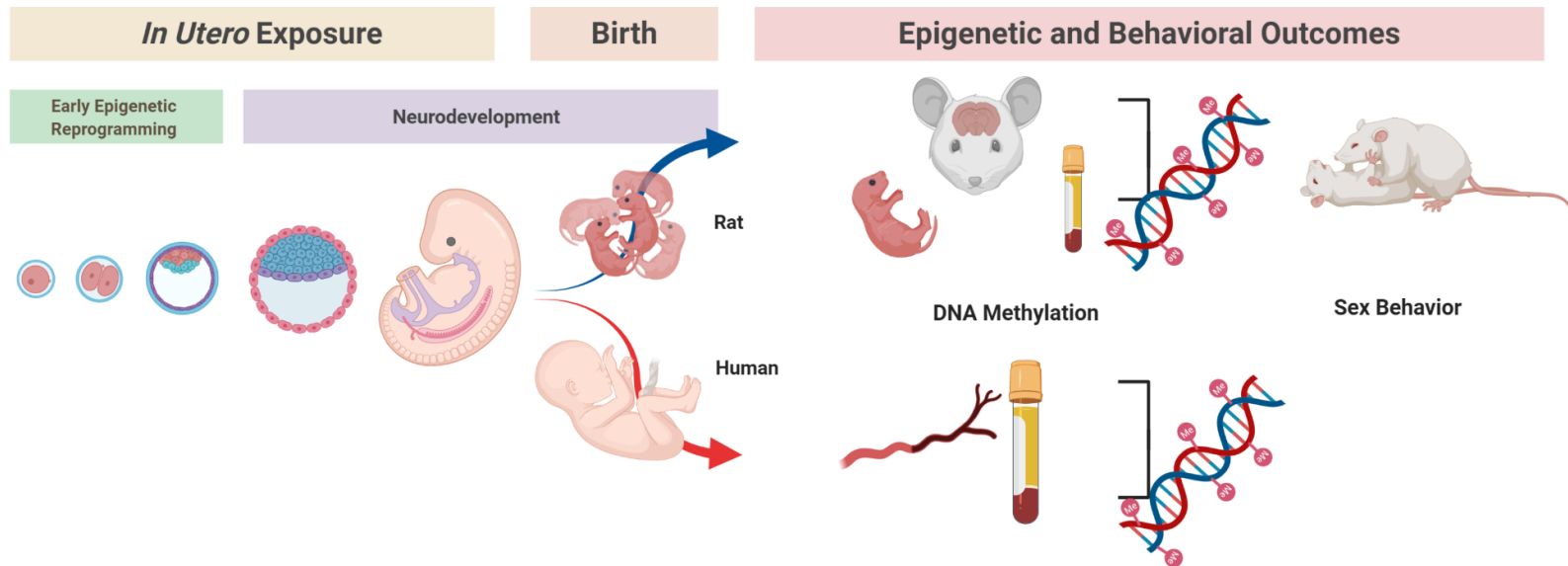


Figure 2: Schematic of Dissertation Aims.

2. Maternal nicotine exposure alters brain sexual differentiation in rats

2.1 Introduction

Maternal tobacco smoke (TS) exposure has been extensively characterized as a major risk to fetal health. Epidemiological studies have found that smoking tobacco during pregnancy is not only related to increased infant mortality and decreased birth weight [72-78] but also to cognitive and behavioral deficits [77, 79-86]. Children born to women who smoke are more likely to display ADHD-like behaviors [25, 28, 77, 81, 87-89] and suffer learning impairment [90-92]. Moreover, the behavioral effects of prenatal TS exposure are long-lasting and likely permanent [93]. Despite the known detrimental effects of maternal TS exposure and ongoing public health efforts, nearly 9% of women smoke cigarettes while pregnant in the United States, according to recent reports [94].

Adult women are particularly vulnerable to the effects of tobacco smoking [93, 95]. Not only do they experience more difficulty with smoking cessation [96, 97]; females experience higher rates of anxiety and depression associated with tobacco withdrawal than males [95, 98, 99]. Following acute nicotine exposure, females display a heightened hypothalamic pituitary adrenal (HPA) axis response and cortisol secretion compared to males [100, 101]. These effects are in part explained by sex hormones. Nicotine, the most addictive and neuroactive substance in tobacco smoke, exerts its effects via activation of the nicotinic acetylcholine receptor (nAChR). Estradiol and progesterone, the

predominant circulating female hormones, are allosteric modulators of the human nAChR [102, 103], and have marked effects on nAChR expression in rats [104]. In general, estrogens potentiate nAChR expression [104] and activity [103, 105, 106], while progesterone inhibits activity [102, 107]. Following the onset of estrous cycling during adolescence, fluctuations in estrogens and progesterone can have opposing effects on nAChR activity or expression [93].

Estrogens are also critical to early developmental processes, including the sexual differentiation of the brain in rodents [2, 108-121], a process initiated towards the end of gestation, well after sex determination, and continuing throughout early postnatal life (PND10) [116, 120-122]. The estrogens are derived locally in the brain following aromatization of androgens derived from the fetal testis. The differentially higher exposure of the developing male brain to estrogens results in brain regions that are sexually-dimorphic in both structure and function [113-118, 120, 122, 123]. nAChR activity is detectable in the rodent brain as early as gestational day (GD) 11 in rodents [93], well before the critical period for sexual differentiation [86, 116, 120-122]. Exposure to nicotine during early development has been associated with sex-specific effects on neurotransmitter function [124], dendritic complexity [125], and even the inclusion of membrane potassium-chloride transport channels [126]. While previous studies have examined the effects of nicotine exposure throughout the critical developmental period for brain sexual differentiation (GD18-PND10) [86, 127-129], little is known about

nicotine's effects on the differentiation of highly sexually-dimorphic brain regions, such as those that comprise the diencephalon [108].

The preoptic area (POA) is one such region that displays robust structural and functional dimorphisms in rodents [114-117]. The rodent POA lies just anterior of the hypothalamus, and largely controls male sexual behavior [116, 118, 130-134]. It is comprised of two neighboring subnuclei: the sexually dimorphic nucleus (SDN), which is embedded with the larger medial preoptic nucleus, and the anteroventral periventricular nucleus (AVPV). Sexual differentiation of the POA is initiated around GD18, when testosterone released by the developing testes is aromatized into estrogen in male POA neurons [108, 120, 121]. This local estradiol surge triggers a downstream cascade promoting neuronal survival in the SDN [116-118]. The absence of estradiol in the developing female POA leads to programmed cell death in the SDN, resulting in dramatically smaller sub-nucleic size [116, 134]. After sexual differentiation, the POA-SDN displays marked size differences between males and females: the male SDN reaches nearly 5-7 times the volume of the female SDN [114, 116-118, 134, 135].

Activation of the masculinized rodent POA via testosterone in adulthood results in male sexual behavior in the forms of mounting, intromissions, and ejaculations [115, 116]. Electro-stimulation of the medial POA increases male-like sexual behavior in both males [136] and females [137]. Correspondingly, adult males with lesioned POA lose their ability to perform copulatory behavior [132, 136, 138]. Females who were

developmentally masculinized by estradiol treatment during the critical window for brain sexualization and gonadectomized as adolescents also display male-like sexual behavior if administered testosterone in adulthood [113-115, 120, 121, 134, 139]. As such, adult male sexual behavior serves as a reliable readout for the masculinization status of the sexually-differentiated POA in both males and females.

Masculinization of the rodent POA was recently shown to require the inhibition of DNA methyl-transferase enzymes (Dnmts), and an overall hypomethylated epigenetic state [139]. In contrast, active DNA methylation during the critical period was required for feminization of the POA. Estradiol mediates these effects; administration of estradiol during the critical window for POA sexual differentiation significantly reduces Dnmt activity in females, and masculinizes sexual behavior in adulthood [139]. Pharmacological inhibition of Dnmt activity in the female POA during this window similarly results in masculinized POA DNA methylation levels and adult sexual behavior [139]. Of note, Dnmt inhibition additionally upregulated expression for 24 of the 34 genes identified as sexually-dimorphic in the POA, with higher expression in males [139]. This subset of 24 genes, termed methylation-dependent masculinizing genes (MDMGs), included *Cyp19a1* encoding aromatase, the cytochrome p450 enzyme responsible for converting testosterone into estradiol in the masculinizing POA [116, 117, 120, 139]. These findings suggest that hormone-induced alterations to DNA methylation in the developing POA are critical to POA sexual differentiation.

Nicotine exposure has been linked to alterations in DNA methylation patterning in the rodent brain in a limited number of studies. Developmental nicotine exposure is associated with a reduction in global 5-methyl cytosine levels in both male and female mouse striatum and frontal cortex (FC) [140]. A study examining DNA methylation patterns in mouse hippocampal and frontal cortex (FC) neurons noted that nicotine exposure down-regulated *Dnmt1* expression in both brain regions, and reduced promoter-specific CpG methylation in the FC. Of note, this downregulation was prevented in the FC following administration with mecamylamine, a noncompetitive nAChR channel blocker [141], suggesting nicotine's ability to reduce *Dnmt1* transcript levels is mediated via the nAChR, and providing important mechanistic links between nicotine, the nAChR, and DNA methylation.

Given the modulatory effects of hormones on nAChR expression, and their critical role in the sexual differentiation of the rodent POA, we investigated the effects of developmental nicotine exposure on POA sexual differentiation by examining both structural and functional outcomes in adults. Due to nicotine's ability to alter methylation levels in the rodent brain [140, 141], we further examined the epigenetic state of the neonatal rodent POA to elicit potential developmental mechanisms underlying changes to the adult POA.

Here, we report masculinization of the nicotine-exposed female POA based on observed changes in 1) adult male-like sexual behavior and 2) adult SDN area,

supporting developmental impacts to POA structure and function. Nicotine-induced alterations to neonatal DNA methylation levels and masculinizing gene expression levels further suggest that epigenetic mechanisms may at least partially underlie the phenotypes observed in the adult POA. Our findings are the first description of these associations, and provide additional evidence corroborating females' enhanced vulnerability to nicotine's neuropsychological effects. This research not only contributes to our understanding of nicotine's ability to alter neurodevelopment, but also the sex-specific vulnerability of these alterations.

2.2 Materials and Methods

2.2.1 Animal Husbandry and Behavioral Testing

All experiments involving the handling of animals or processing of animal tissues were conducted in compliance with Duke Institutional Animal Care and Use Committee (IACUC). Young adult male and female Sprague-Dawley rats between the weights of 225-250g were ordered from Charles River Laboratories (Wilmington, MA, USA). Following two weeks of acclimation to our facilities, females were anesthetized (60 mg/kg ketamine + 0.15 mg/kg dexmedetomidine administered i.p., followed by 0.15mg/kg atipamezole + 5 mg/kg ketoprofen administered s.c.) as previously described [142], and surgically fitted with a subcutaneous Alzet 2ML4 mini-osmotic infusion pump (Durect Corp.; Cupertino, CA, USA) delivering either vehicle (dimethyl sulfoxide;

DMSO), or nicotine (nicotine hydrogen tartrate salt, Sigma-Aldrich; Saint Louis, MO, USA) at a dose of 2 milligrams per kilogram body weight per day (2mg/kg/day) via subcutaneous diffusion.

This dose was chosen to model moderate maternal smoking based on previous reports that a subcutaneous dose of 2.0-3.0 mg/kg/day nicotine by osmotic minipump produces plasma nicotine levels in rats similar to those observed in pregnant moderate smokers [143-145]. A continuous infusion model of nicotine exposure was chosen to eliminate episodic hypoxia and ischemia that are associated with nicotine injections [143, 146], as well as the confound of maternal stress that accompanies forced smoke inhalation in rodents [86, 147]. Further, a gestational dose of 2 mg/kg/day of nicotine has been shown to cause neurochemical and behavioral changes in exposed offspring without impairing growth in either the exposed offspring [146, 148] or the dam [149].

Nicotine dose was prepared based on the weight of the female on the day of surgery, and adjusted for tartrate salt weight. Previous studies using an identical infusion model confirmed that despite pregnancy-related weight gain (at 2.0 mg/kg/day, dose drops about one-third during pregnancy), dose was maintained within a range comparable to moderate smoking [142]. For early postnatal exposure, we relied on the lactational transfer of maternal nicotine to the pups [150] based on observations that the Alzet mini-osmotic pump continues to dose well past the 28-day marketed timeline (previous reports indicated up to a 39-day dose delivery period) [142]. Following

surgery, females were allowed to recover for three days. A subset of females did not undergo surgery and were not fitted with pumps, and served as our “no pump” controls.

Immediately following the three-day surgical recovery period, all females were mated with a naïve adult male rat for 5 days. Females were kept in isolation throughout pregnancy, and allowed to undergo normal birthing processes. Cages were monitored for pups daily to detect timing of birth, and day of birth was considered PND0. Litter size and pup sex distributions were assessed on PND0. On PND0 and PND1, pups were subcutaneously injected with 100 μ L of either vehicle (sesame oil) or 100 μ g estradiol benzoate (Sigma-Aldrich) as previously described [139]. Litters were culled to three males and three females on PND4, and POA was harvested from culled animals for examination of epigenetic endpoints. Whole brain weight was also measured at this time. At PND21, pups were weaned and housed in same sex groups of three. At PND40, two males and two females were chosen from each litter to be surgically gonadectomized and subcutaneously implanted with a silastic capsule (30-mm length, 1.6-mm inner diameter, 3.17-mm outer diameter) containing crystalline testosterone (Sigma-Aldrich) to mimic male circulating levels of testosterone, as previously described [139]. Testosterone replacement is necessary to activate male sexual behavior in females masculinized during development [139]. All animals were single-housed following gonadectomy.

At PND50, animals were assessed for anxiety-like behavior and locomotion using the elevated plus maze apparatus (Med Associates, Inc.; Fairfax, VT, USA). Briefly, animals were placed in the center of the plus, and allowed to freely roam the apparatus for five minutes under dim light. Time spent in the open arms and the number of center crosses were recorded for each animal. At PND60, all animals were assessed for male sexual behavior. Gonadectomized males and females were paired with a sexually receptive female in a glass arena (50cm x 25cm x 30cm) for 30 minutes under red light during the dark phase, and video recorded. Videos were later manually scored in a blinded fashion for male sexual behavior parameters, including the number of mounts and latency to first mount. Videos were also manually scored for female sexual behavior parameters (number of lordoses) in hormonally-primed females to ensure sexual receptivity. Lordosis quotients ($LQ = \text{number of receptive female lordoses per 10 mounts of paired animal}$) were calculated for all pairings to assess sexual receptivity, and those with $LQ < 1$ were discounted in subsequent analyses. Following sexual behavior assays, adult whole brain weight was measured after euthanasia between PND61 and PND72. All behavioral data was averaged across sexes within each litter, and represented as a single data point for each sex and litter. All animals were maintained on a reverse 12-hour light/dark cycle, and provided with food and water *ad libitum*. Body weight was measured roughly twice per week between PND1-77.

2.2.2 Immunofluorescence Microscopy

Male and female adults (PND75-77) were anesthetized and transcardially perfused with 200mL of cold PBS, followed by 250mL of either 4% formalin or 10% neutral buffered formalin. Perfused brains were removed and placed in formalin overnight. Brains were then cryoprotected in 30% sucrose for four days, and subsequently freeze-stored in Tissue Tek O.C.T. freezing medium (Sakura Finetek USA; Dublin, OH, USA) at -80°C. Brains were cryo-sectioned at 40µm, and slices containing the POA-SDN were stored as floating sections in 0.02M KPBS (1x). Following an overnight block with 0.03% Triton™ X-100 (Sigma-Aldrich) and 2% normal goat serum (NGS, Sigma-Aldrich) overnight at 4°C, sections were incubated with monoclonal mouse anti-calbindin D 28K antibody (CB-955) (Sigma-Aldrich), a reliable and specific marker for the SDN, diluted 1: 20,000 in 2% NGS for 72 hours at 4°C. Sections were then washed with 1x KPBS, and incubated for two hours at room temperature (RT) in goat anti-mouse IgG secondary antibody cross-adsorbed to Alexa Fluor 488 (Thermo Fisher Scientific; Waltham, MA, USA) diluted 1:200 in 2% NGS. Following incubation, sections were washed and mounted to glass microscope slides using ProLong Gold Antifade Mountant with DAPI (Thermo Fisher Scientific) and coverslipped. Mounted sections were dried overnight at RT, and subsequently imaged using the Keyence Fluorescence Microscope BZ-X800. Multiple sections were imaged per animal with both 4x and 10x objectives to capture the entirety of the POA-SDN. POA-SDN area was measured in 10x

images using the area measurement tool in Image J (Image Processing and Analysis in Java, NIH). The largest area measurement for each animal was used in final quantification.

2.2.3 Whole Genome Bisulfite Sequencing Analysis

Whole genome bisulfite sequencing (WGBS) data collected from male, female, and estradiol-masculinized PND4 POA [139] was obtained from NCBI's Short Read Archive under BioProject ID 275796. Reads were mapped to the Rnor6 version of the rat genome using the Bismark [151] alignment algorithm. Percent methylation was called via the *MethylKit* [152] package from the R statistical programming environment (available at www.r-project.org). Due to the low coverage, percent methylation was called using 250 nucleotide-long bins tiling the whole genome every 50 nucleotides. Only windows that had at least four (un)methylated calls in each of the eight samples were considered for further analysis. Hierarchical clustering using a correlation distance with complete linkage was performed on the top 25% most variable sites to identify outlier samples and establish genome-wide similarity across samples. Sites were reported as differentially methylated if 1) all replicates of one condition were higher or lower than all replicates of the other condition, 2) the difference in percent methylation between all replicates was less than 25%, and 3) the difference in average percent methylation between the conditions was at least 60%. Using these thresholds, 285 differentially-methylated regions (DMRs) were identified, which mapped to 134 unique

genes. Functional clusters from this gene list were derived using the DAVID Functional Annotation Tool (DAVID Bioinformatics Resources 6.7, NIAID/NIH) [153, 154].

2.2.4 Targeted DNA Methylation Quantification

Genomic DNA and total RNA were co-extracted from PND4 POA samples pooled in groups of two using the Qiagen AllPrep DNA/RNA Mini Kit (Qiagen; Valencia, CA, USA). DNA and RNA samples were eluted in nuclease-free water, and assessed for concentration and purity using the NanoDrop 2000 spectrophotometer (Thermo Fisher Scientific). From each sample, 800ng of genomic DNA was bisulfite-modified using the Zymo EZ DNA Methylation Kit (Zymo Research, Inc.; Irvine, CA, USA) for subsequent DNA methylation analyses. Bisulfite-treated samples were eluted in 40 μ L nuclease-free water to achieve a final concentration of 20 ng/ μ L, assuming 100% recovery. CpG methylation was examined at the *Dlgap1*, *Kcnn3*, *Nkain3*, and *Tab1* DMRs using bisulfite pyrosequencing as previously described [18]. Pyrosequencing assays for each DMR were validated for quantitative performance using methylation standards (EpigenDx Rat Methylation Standards, Cat No. 80-8060R-PreMix) of defined methylation levels: 0%, 25%, 50%, 75%, and 100% methylated. Assay validation further informed the linearity and range of each assay. Validated pyrosequencing assay primers and PCR conditions are listed in Table 1. All pyrosequencing was performed using the Qiagen PyroMark Q96 MD Pyrosequencer, and percent CpG methylation was calculated using the PyroQ CpG Software (Qiagen) as an average across all CpGs within each

sequence analyzed. Each pyrosequencing sample contained 7 μ L PCR product generated using the following PCR conditions: 95°C for 15m, then 55 cycles of 94°C for 30s, [assay-specific] annealing temperature for 30s, 72°C for 30s, followed by 72°C for 10m. Assay-specific annealing temperatures were as follows: *Dlgap1*, 58°C; *Kcnn3*, 62°C; *Nkain3*, 62°C; *Tab1*, 62°C (Table 1).

2.2.5 Quantitative Real-Time PCR

Gene expression levels for *Cyp19a1*, *Dnmt1*, *Dnmt3a*, *Ebf2*, *Ebf3*, and *Nr2f2* in PND4 POA were assessed using quantitative real-time PCR (RT-PCR) relative to the housekeeping gene *Gapdh*. Prior to quantification of experimental samples, RT-PCR assay efficiency and specificity were validated. Assay efficiency was calculated using a standard curve comprised of cDNA serial dilutions of 16, 8, 4, 2, 1, 0.5, and 0.25 ng/ μ L. Standard curve amplicons were subsequently run on a 2% agarose gel to verify amplification specificity. Assays with targeted amplification of >90% efficiency were used for subsequent analyses. Total RNA extracted from PND4 POA tissue was converted to cDNA using the High Capacity cDNA Reverse Transcription Kit (Applied Biosciences; Thermo Fisher Scientific). For each sample, 500-700ng of extracted RNA diluted in 13.2 μ L nuclease-free water was combined with 2 μ L 10x RT buffer, 0.8 μ L 25x dNTP mix, 2 μ L 10x random primers, 1 μ L reverse transcriptase, 1 μ L RNase inhibitor, and nuclease-free water to achieve a total reaction volume of 20 μ L. Samples were reverse transcribed under the following conditions: 25°C hold for 10m, 37°C hold for

120m, and 85°C hold for 5m. Converted cDNA samples were diluted to a concentration of 2ng/μL in nuclease free water prior to use in RT-PCR. RT-PCR assays were conducted using the SYBR Green reporting dye with ROX passive reference dye. 4ng of cDNA (2 μL) were combined with 12.5 μL *Power*SYBR Green PCR Master Mix (Applied BioSystems; Thermo Fisher Scientific), 10.3 μL nuclease-free water, 0.1 μL of 10 μM forward primer and 0.1 μL of 10 μM reverse primer to achieve a total reaction volume of 25 μL. RT-PCR was conducted using the QuantStudio 6 Flex Real-Time PCR System (Thermo Fisher Scientific) and the following thermal cycler conditions: 50°C hold for 2m, 95°C hold for 10m, then 40 cycles of 95°C for 15s and 62°C (annealing temperature) for 1m, followed by 95°C for 15s, 60°C for 30s, and 95°C for 15s to generate a melting curve. Cycle threshold (Ct) values were obtained for each sample, and difference in cycle threshold (Delta Ct) relative to *Gapdh* was used to determine fold change in expression. Fold change values for each gene were normalized to the control males. Primer sequences designed previously [139] were used as follows: *Cyp19a1* Fwd 5' GCAAACCTCACCTTCAAGAGT 3', Rev 5' ATCTTGTGCTATTTTGCCTCAGAA 3'; *Dnmt1* Fwd 5' GCTTTGACGGTGGCGAGAA 3', Rev 5' TCTGCAAGAACTCGACCACAATC 3'; *Dnmt3a* Fwd 5' TTTCTTGAGTCTAACCCCGTGATG 3', Rev 5' TGCAACTCCAGCTTATCATTACAA 3'; *Ebf2* Fwd 5' ATGAGACGGTTTCAGGTCGTGTT 3', Rev 5' TTTGATGCAGGGTGTAGCTTCTG 3'; *Ebf3* Fwd 5'

ACGCTTTGTCTACACTGCCCTTAA 3', Rev 5' TGCCGCCCTCTTCAGTAACA 3';
Gapdh Fwd 5' TGGTGAAGGTCGGTGTGAACGG 3', Rev
5'TCACAAGAGAAGGCAGCCCTGGT 3'; *Nr2f2* Fwd 5'
CACGTCGACTCCGCCGAGTAC 3', Rev 5'ACGAAGCAAAGCTTTCCGAACCGT 3'.

All assays were optimized to an annealing temperature of 62°C.

2.2.6 Statistics

Prior to all statistical analyses, data sets were assessed for normality using the Shapiro Wilk's test. Normally-distributed data were analyzed using parametric statistics, including analysis of variance (ANOVA), analysis of covariance (ANCOVA), multivariate analysis of variance (MANOVA), and t-tests. Data that were not normally distributed were analyzed using non-parametric tests including the Kruskal-Wallis test. *Student's t-test* was used in *post hoc* analyses of multiple comparisons when appropriate. To account for testosterone-induced mounting behavior in females occurring as a result of testosterone replacement rather than developmental masculinization [155], females with a mount count greater than – and SDN area less than – the average of the control males were excluded from all analyses. Four females met these criteria for exclusion. Prior to our comprehensive masculinization analyses, data were normalized to percent of the control males within each endpoint and log transformed. Variance within data sets was examined to ensure similarity across endpoints prior to combined repeated measures analysis. A mixed model approach was employed to examine repeated

measures in our comprehensive masculinization analysis since we were only able to examine SDN area in half of the animals evaluated for male sexual behavior. The mixed model approach is ideal for assessing repeated measures across incomplete data sets since individuals with missing values are not excluded from the analysis, like in the MANOVA approach. In order to ensure that our masculinization parameters (male sex behavior and SDN area) differed from non-masculinization parameters (anxiety-like behavior), our mixed model tested the interaction between three main effects: treatment, sex, and measure type (positive or negative) with positive measure indicating masculinizing parameters and negative measure indicating non-masculinizing parameters. Due to the fact that our gene expression data sets were nearly complete, we employed a MANOVA approach for repeated measures analysis.

Statistical analyses were performed using either JMP Pro Version 13.0 (SAS Institute Inc.; Cary, NC, USA) or GraphPad Prism Version 7.00 for Mac OS X (GraphPad Software; LaJolla, CA, USA) software.

2.3 Results

2.3.1 Birth Outcomes and Weight Characteristics

Birth outcomes and offspring weight were evaluated across all litters to examine potential confounding treatment effects. In alignment with previous findings, [146, 156] gestational treatment with 2mg/kg/day nicotine had no effect on the number of pups

born, the distribution of male and female pups within litters, (Table 2, Figure 3A-B), sex-specific body weight (Figure 4), or the emergence of sex differences in adult brain weight (Figure 5A-B) relative to vehicle controls. In contrast, perinatal treatment with estradiol (PND0-PND1) affected body weight outcomes in both males and females (Figure 4), and normal sex differences in adult brain weight (Figure 5A-B), suggesting off-target developmental effects.

2.3.2 Maternal nicotine exposure evokes upregulation of epigenetic mechanisms required for POA masculinization

To identify candidate mechanisms underlying nicotine-induced POA masculinization, we investigated DNA methylation levels in the neonatal POA based on evidence suggesting that developmental alterations to DNA methylation are critical to POA masculinization [139]. Using publicly-available whole genome bisulfite-sequencing (WGBS) data obtained from neonatal male, female, and estradiol-masculinized female POA (see Figure 6 for full methylation distributions), we first identified differentially methylated regions (DMRs; 250 nucleotides in length) between males and females unexposed to nicotine. Specifically, we analyzed those that were hypomethylated in males, based on previous work outlining POA masculinization to be, in part, due to the suppression of global DNA methylation [139]. To select for regions that were associated with masculinization, regions in which methylation levels were similar between males and estradiol-masculinized females were further prioritized. Finally, a stringent

differential methylation threshold of 60% between unexposed males and females was employed to examine the most highly differentially-methylated, masculinizing regions. 285 DMRs were identified as statistically significant using these criteria. Using distance to nearest gene as a proxy for genomic location, we mapped 46% of these 285 DMRs to functional regions of the genome, including the proximal promoter region (up to 1000 bp upstream of gene), 5'UTR, 3' UTR, intron, and exon (Figure 7A). Based on nearest gene name, our top 285 DMRs mapped to 134 unique genes. Using the DAVID Functional Annotation Tool (DAVID Bioinformatics Resources 6.7, NIAID/NIH)[153, 154], we identified the following enriched functional clusters among these genes: phosphatidylinositol binding, the phox homologous domain, and synapse/cell junction formation (Table 3). However, only the phox homologous domain functional cluster maintained statistical significance following Benjamini correction for multiple comparisons.

DNA methylation levels were examined at four of the top identified DMRs in neonatal (PND4) POA (Figure 7B), based on their genomic locations, levels of differential methylation, and cellular function (Table 4). Bisulfite pyrosequencing assays were optimized within these DMRs (#CpGs): *Dlgap1* (2 CpGs), *Kcnn3* (2 CpGs), *Nkain3* (2 CpGs), and *Tab1* (1 CpG) (Table 1), and subsequently validated for their ability to detect a wide range of methylation (Figure 7C). In examination of DNA methylation levels, we were not able to validate the expected magnitude of sex difference among

control animals (Figure 7D). However, exposure and sex effects, albeit of smaller magnitude, were detected at *Nkain3* (Figure 7D). At *Nkain3*, DNA methylation was significantly increased in the control females relative to all other groups ($p < 0.05$, *Student's t post hoc* analysis following two-way ANOVA: $p = 0.0061$, sex*treatment $p = 0.0097$; Figure 7D), suggesting masculinization of the *Nkain3* DMR DNA methylation levels in both estradiol-masculinized and nicotine-treated neonatal females.

Expression of methylation-dependent masculinizing genes (MDMGs), or genes upregulated by *Dnmt* inhibition in the masculinized POA [139], were additionally evaluated given their association with alterations to neonatal global DNA methylation in the POA. Normalized gene expression levels were measured across four previously identified MDMGs: *Cyp19a1*, *Ebf2*, *Ebf3*, and *Nr2f2*. Expression levels of *Dnmt1* and *Dnmt3a* were concurrently quantified based on our expectation that their expression should not be altered by treatment or sex [139]. While expected sex differences in MDMG expression were not statistically resolved among control animals (Figure 7E) trending sex differences were observed when relative expression values were normalized as a ratio of male to female expression (Figure 7F). This ratio was diminished in both estradiol-masculinized and nicotine-treated animals compared to controls in all four genes examined, supporting a treatment-induced loss of normal sex difference in MDMG expression. This trend was significant in only one case, *Nr2f2* (*a-*

priori t-test, $p=0.0499$) (Figure 7F). As expected, *Dnmt1* and *Dnmt3a* expression levels were similar across sexes and treatments (Figure 7E-G).

Repeated measures analysis indicated that MDMG expression levels across *Cyp19a1*, *Ebf2*, *Ebf3*, and *Nr2f2* were higher in nicotine-exposed animals compared to controls (two-way MANOVA $p=0.0716$, treatment main effect $p=0.0113$, sex main effect $p=0.9752$, sex*treatment $p=0.8749$) (Figure 7G). This trend was significant at *Ebf2* (two-way ANOVA between nicotine and control groups, $p=0.1146$, treatment main effect $p=0.0259$) (Figure 7D,G), underscoring nicotine's ability to collectively alter MDMG expression in the developing POA.

2.3.3 Maternal nicotine exposure eliminates structural and functional sex differences in the adult POA

Male sexual behavior and SDN area were evaluated in adults developmentally exposed to either vehicle or nicotine in order to examine both the structural and functional masculinization of the POA. Animals perinatally exposed to estradiol (PND0-PND1) served as a positive control for POA masculinization. Prior to sexual behavior assessment, all animals were surgically gonadectomized and subcutaneously implanted with testosterone capsules, delivering adult male circulating levels of testosterone required to activate the masculinized POA in females (Figure 8A). Three weeks following gonadectomy and testosterone replacement, animals were paired with a sexually receptive female, and scored for male sexual behavioral endpoints, including

the number of mounts and latency to first mount. Female sexual behavior (number of lordoses) was simultaneously assessed among the sexually receptive females to examine potential confounding effects by treatment on their receptivity. We verified that receptive female lordosis quotient ($LQ = \# \text{ lordoses} / 10 \text{ mounts}$) was unaffected by the treatment of the paired animal (Figure 9A), although sex of the paired animal did have an effect (Figure 9B). Across both male sexual behavioral endpoints examined, we observed trending, expected sex differences among control animals that were lost in both estradiol-masculinized and nicotine-treated groups (Figure 8B). The ratio of male to female mounts was significantly reduced in estradiol-masculinized and nicotine-treated animals compared to controls ($p < 0.05$; Figure 8C) due to an increase in mounting behavior in the females of both groups, supporting nicotine's ability to functionally masculinize the POA. In order to assess the selectivity of our experimental paradigm for testosterone-mediated behaviors, we additionally examined two non-testosterone mediated behaviors: anxiety-like behavior and locomotion (Figure 8D). Sex differences in behavior were not observed among controls in either anxiety-like behavior or locomotion, validating the testosterone-mediated selectivity of our experimental paradigm (Figure 8D). Shortly following the behavioral assays, the SDN area was measured in all animals using immunofluorescent staining. Trending sex differences in adult SDN area observed among control animals were not evident in either estradiol-

masculinized or nicotine-treated groups (Figure 8E), supporting nicotine's ability to eliminate structural sex differences in the POA.

2.3.4 Maternal nicotine exposure masculinizes the female POA

Masculinization of the POA was comprehensively assessed by combining metrics of POA structure (SDN area) and function (male sexual behavior). We implemented two novel methods to comprehensively assess POA masculinization across multiple measurements (Figure 10A). Using the first method, masculinization parameters (including male sex behavior and SDN area) and non-masculinization parameters (including anxiety-like behavior) were normalized, log transformed, and combined in a mixed model repeated measures analysis. Within the repeated structure, the interaction between treatment, sex, and measure (masculinization or non-masculinization) was evaluated as a three-way ANOVA (Figure 10A). This approach resolved POA masculinization in both nicotine-treated and estradiol-masculinized females, relative to control females (Figure 10B). Further, control female masculinization parameters significantly differed from all other groups across masculinization and non-masculinization parameters ($p < 0.05$), underscoring the ability of this model to differentiate between the two parameter types. Using the second approach, a masculinization index was calculated for each animal based on normalized and log transformed masculinization parameters (male sex behavior and SDN area). This approach similarly resolved POA masculinization in nicotine-treated and estradiol-

masculinized females, although to a lesser degree of statistical significance (Figure 10B). Our findings support that both analysis methods are capable of statistically resolving POA masculinization in a comprehensive manner.

2.4 Discussion

Nicotine induces sexually-dimorphic changes during neurodevelopment, likely through interactions between sex hormones and the nicotinic acetylcholine receptor (nAChR), as both estradiol and progesterone directly modulate nAChR expression and activity [93]. These interactions support the notion that hormonally-regulated developmental windows like the sexual differentiation of the brain might be particularly vulnerable to nicotine exposure. In this study, the effects of developmental nicotine exposure on the sexual differentiation of the POA were investigated using a rat model for developmental nicotine exposure. We report that exposure to nicotine during the critical window for brain sexual differentiation masculinized the female POA by 1) eliminating normal sex differences in POA structure and function and 2) altering the epigenetic mechanisms that induce POA masculinization during perinatal development. In order to comprehensively evaluate masculinization, we combined behavioral and structural endpoints into both a repeated measures analysis and masculinization index. Both approaches revealed significant masculinization of the nicotine-exposed female POA. We are the first to demonstrate that exposure to nicotine during the perinatal

period for brain sexual differentiation is capable of comprehensively masculinizing the female rodent POA, both in structure and function.

There were several advantages to evaluating POA masculinization across neonatal and adult timepoints. In addition to demonstrating the persistence of developmental alterations to SDN structure, we were able to examine the extent to which testosterone replacement following surgical gonadectomy induced mounting behavior in females, independent of developmental POA masculinization. This additional measure is imperative, as testosterone-induced mounting behavior in females has been reported [155] and yet is seldom controlled-for in masculinization studies. Both the repeated measures analysis and masculinization index enabled the assessment of multiple measurements across individual animals, all of which contributed to the same phenotype of POA masculinization. The masculinization index analysis approach is best applied to data sets with missing values, whereas the repeated structure is ideal for complete data sets. Despite having data sets for behavior and SDN area that were not equal in size, we resolved slightly higher statistical significance among the nicotine-treated female group using the repeated measures approach. To account for missing values in our repeated measures analysis, we employed a mixed model approach, as opposed to the traditional MANOVA. We encourage future studies examining POA masculinization to adopt a comprehensive analytical approach as described above, and

to use these measurements to control for testosterone-induced mounting behavior in female subjects.

Another strength of our experimental model was our ability to examine exposure effects during both the organizational and activational periods of POA sexual differentiation. While structural differences within the POA appear by the end of the organizational period in early development, functional differences, such as the ability to perform male sexual behavior, can only be resolved following hormonal activation in adolescence and adulthood, or the activational period [116, 117, 120, 123, 134, 139]. Indeed, our findings underscore the idea that deleterious exposure during critical, organizational periods of development can exhibit persistent, functional outcomes later in life. This phenomenon, known as the Developmental Origins of Health and Disease, or DOHaD [157], has not been previously examined within the context of nicotine and the sexual differentiation of the POA.

This study was additionally strengthened by our targeted approach to identifying differentially methylated regions across the POA epigenome. Using publicly-available WGBS data and stringent thresholds for differential methylation, we mapped highly differentially methylated-regions to functional areas of the genome. A previous examination of these data using lower thresholds for differential methylation (>10%) mapped less than 25% of differentially-methylated CpGs to functional genomic locations [139]. Almost half of the masculinizing DMRs identified in this study using more

stringent thresholds for differential methylation (>60%) mapped to functional genomic regions in the POA. Our results suggest that masculinizing DMRs characterized by high levels of differential methylation more strongly localize to functional genomic regions than those with low differential methylation, potentially underscoring their increased functional relevance in the POA. These results not only guided our targeted studies, in which we validated sex differences and treatment-associated masculinization at one of the four DMRs examined, but also revealed potential mechanistic underpinnings of altered DNA methylation in the masculinizing POA. Functional annotation clustering of the top masculinizing DMRs in the POA revealed the phox homologous domain as the most highly enriched functional cluster. The phox homology (PX) domains interact with the cell membrane and bind phosphatidylinositol phospholipids, often used as organelle identity markers [158]. Genes associated with top identified masculinizing DMRs that were enriched in this cluster included those from the sorting nexin (Snx) protein family, all of which contain PX domains [158, 159] and are implicated in membrane signaling and trafficking [158].

Snx proteins have also been associated with neurological function [159-161].

Snx27, a gene that was among our top masculinizing DMRs, was found to localize to the post-synaptic density and facilitate excitatory glutaminergic neurotransmission via AMPA-type glutamate receptors [160], which are also critical to the early organization of the masculinizing POA in which dendritic spine density is increased [114, 119].

Although not among our list of top DMRs, *Snx9* and *Snx12* have been associated with presynaptic vesicle endocytosis [159] and neurite outgrowth [161], respectively. *Snx12* was further implicated in cortical neurodevelopment, with expression levels increasing during embryogenesis, and decreasing shortly after birth, closely following the developmental period for brain sexual differentiation [161]. Although we did not perform targeted DNA methylation analyses on *Snx* genes, results from our functional annotation clustering can inform future studies examining epigenome-wide changes in the neonatal POA.

In the neonatal POA, we determined that nicotine-induced masculinization might be the result of developmental alterations to DNA methylation patterning and MDMG expression that are characteristic of the masculinized POA. These findings corroborate the limited evidence supporting nicotine's ability to alter DNA methylation patterns in the rodent brain, specifically via downregulation of *Dnmt1* expression [141] and CpG methylation levels [140, 141]. Although we did not observe exposure-induced changes to *Dnmt1* transcript levels in the POA, it would be of interest to examine nAChR expression and activity in the developing rodent POA given the reported associations between nAChR activity and CpG methylation, albeit tissue-specific [141]. This is especially important in light of 1) nAChR's mechanistic links to estradiol, the sex hormone responsible for developmentally masculinizing the POA [2, 108-121], 2) nAChR's mechanistic links to *Bcl2* [162], an anti-apoptotic protein involved in POA

masculinization [117], and 3) nAChR activity detected in the developing rodent brain as early as GD11 [93], nearly a week before the sexual differentiation of the brain is initiated. Nicotine exposure inhibits aromatase, the enzyme critical to the conversion of testosterone into estradiol, in hypothalamic-related brain regions including the POA [163]. As aromatization is necessary for POA masculinization [117, 118, 139], this interaction would potentiate a phenotype opposite to that described in this study. However, as reported aromatase inhibition was not POA-specific, it is possible that nicotine does not inhibit aromatization in the POA, or at least to an extent that does not impede brain masculinization.

In our model, nicotine exposure was administered during the early, organizational window for POA sexual differentiation, spanning from late gestation through the early postnatal period. With osmotic diffusion of nicotine during gestation and lactational transfer during early postnatal development, our exposure model was ideal for covering the full developmental window for POA sexual differentiation (GD18-PND10) [116, 120-122]. However, recent evidence suggests this window may extend beyond the perinatal period [139]. While adulthood has been traditionally considered the “activational” period for brain sexual differentiation, organizational events can occur up until, and even during, adolescence [164-171]. This idea is supported by the fact that exposure to nicotine during adolescence alone can have sex-specific effects in the brain [93], simultaneously challenging the permanence of developmentally-established sex

differences in the brain, as well as understandings of the DOHaD phenomenon [157]. Given our findings, it will be of utmost importance to examine the effects of exposure during adolescence both as a separate exposure window, and in combination with developmental exposure, especially given the recent uptick of nicotine use during adolescence via electronic nicotine delivery systems (ENDS) [172].

Limitations to this study include that DNA methylation and gene expression were analyzed in POA tissue samples containing both neurons and glia, which display considerable differences in DNA methylation patterning [173], potentially reducing ability to detect changes in the reported differential methylation [139]. Additionally, because examination of adult male-like sexual behavior required testosterone administration during adolescence, we were limited in our ability to detect potential exposure-related disruptions to endogenous hormone levels during adolescence and adulthood. This is of particular relevance as prenatal nicotine exposure has been correlated with reduced testosterone levels in adult male rats [174].

As mentioned previously, adult women are particularly vulnerable to nicotine's psychopharmacological effects, experiencing more difficulty with smoking cessation and abstinence than men. Although the underlying mechanisms remain unclear, this sex-specific vulnerability is suspected to have developmental origins, particularly during the perinatal and adolescent hormone-mediated sexual differentiation of the brain [93]. Our findings support this idea by demonstrating that an additional sex-specific outcome in

adult females is linked to developmental exposure: nicotine-associated reorganization during the early perinatal period for brain sexual differentiation resulted in pronounced behavioral impacts later in life. While drawing parallels in humans is difficult, especially given the fact that eliciting male sexual behavior in our model required activation via exogenous hormones in females, there are human studies that corroborate the phenotypes observed in this study. First, the higher incidence of same-sex sexual orientation among women suffering from congenital adrenal hyperplasia (CAH), a genetic abnormality that leads to hyper-elevated androgen production throughout life [175], suggests that constant, elevated androgen levels can both developmentally-masculinize and adolescently-activate sexual behavior.

Same-sex sexual orientation in young adult females is additionally associated with gestational exposure to tobacco smoke [176]. This association is derived using robust surveying methods across over 7,000 mother-offspring pairs to assess the incidence of tobacco use, and other stressors, during pregnancy [176]. Complementing this finding, recent genome-wide association studies (GWAS) and phenotypic-wide association studies (PheWAS) across large human cohorts reveal that maternal smoking at the time of birth is associated with the same single nucleotide polymorphisms (SNPs) implicated in adult same-sex sexual behavior [177]. Although sex-specific effects were not elucidated, the observed associations were directionally similar, suggesting that

maternal smoking at the time of birth could be associated with same-sex preference in human adults [177].

In conclusion, our results indicated that exposure to nicotine during the critical window for brain sexual differentiation is capable of masculinizing the female POA, both in structure and function. These phenotypes were further associated with disruption of epigenetic mechanisms required for POA masculinization during perinatal development, providing insights into organizational mechanisms and the persistence of developmental effects. Using novel statistical approaches, we combine multiple measurements of masculinization to demonstrate comprehensive exposure-associated effects. Results from this study underscore our previous understanding of female's enhanced vulnerability to nicotine's effects, and importantly provide developmental links to these events. Examining estradiol's interaction with the nAChR in the developing POA might provide causative mechanistic insights into the phenotypes observed here. This would be of particular interest given estradiol's critical role in POA masculinization [2, 108-121], and established modulatory effect on nAChR expression in the rodent brain [93, 104]. Finally, further examination of the effects of other common environmental compounds or mixtures on POA sexual differentiation is needed to widen our understanding of DOHaD. Such studies are likely to improve our understanding of the processes associated with the sexual differentiation of the brain,

and how the environment, long suspected of being a contributing factor [123], can impinge on these pathways.

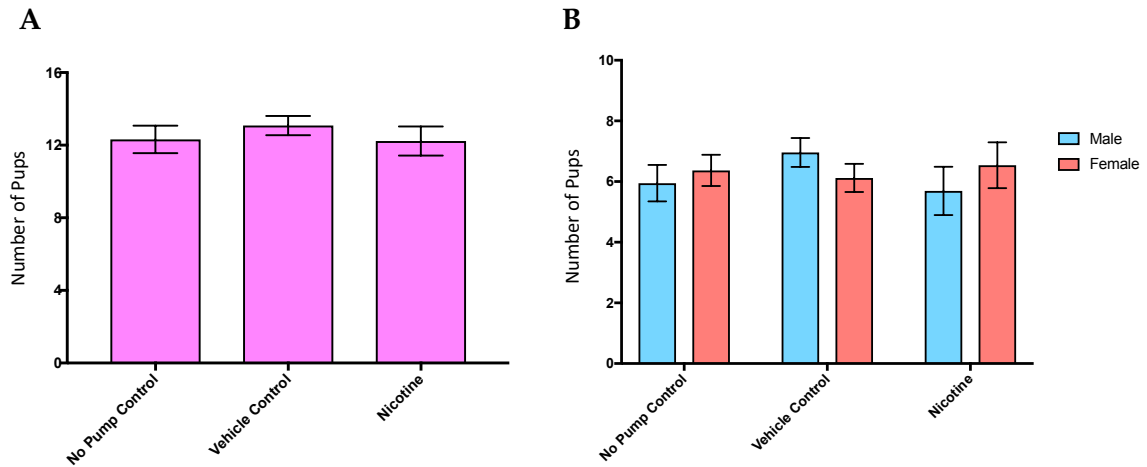


Figure 3: Birth outcomes are unaffected by gestational treatment.

Dams were either surgically fitted with a subcutaneous mini-osmotic pump delivering vehicle (DMSO) or nicotine (2mg/kg/day), or received no pump (No Pump Controls). Surgeries were performed pre-conceptionally to allow for exposure throughout the entirety of gestation. A) Gestational exposure had no effect on litter size (Kruskal-Wallis test $p=0.6438$) or B) distribution of males and females within litters (one-way ANOVA males $p=0.1167$, one-way ANOVA females $p=0.8412$). B-C) *No Pump Control*: $N=19$ litters; *Vehicle Control*: $N=25$ litters, *Nicotine*: $N=13$ litters. Error bars represent the standard error of the mean.

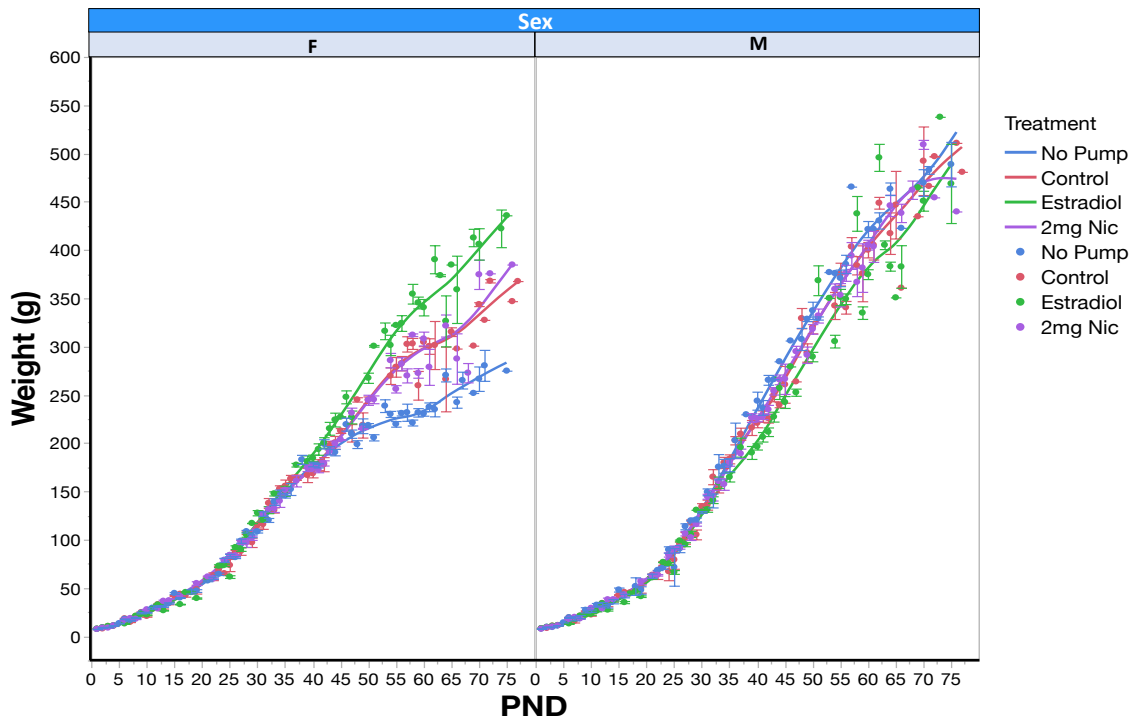


Figure 4: Body weight measurements taken between PND1 and PN77 in male and female offspring indicate both sex- and treatment-specific effects.

Body weight, treatment type, and age (PND#) were combined in an analysis of covariance (ANCOVA) for each sex, where age was considered the covariate. Across all timepoints, male offspring were heavier than females (ANCOVA, $p < 0.0001$, sex main effect $p < 0.0001$, PND# main effect $p < 0.001$). Within each sex, weight was significantly affected by treatment and age (Male: ANCOVA $p < 0.0001$, treatment main effect $p < 0.0001$, PND# main effect $p < 0.0001$; Female: ANCOVA $p < 0.0001$, treatment main effect $p < 0.0001$, PND# main effect $p < 0.0001$). *Post-hoc* analyses for multiple comparisons revealed vehicle control and nicotine-treated animals did not differ in body weight within each sex (*Student's t-post hoc test* between nicotine vs control males, $p = 0.2192$; nicotine vs control females, $p = 0.7800$). Males lacking gestational exposure and surgical gonadectomy (No Pump Control) were heavier than all other treated males (*Student's t-post hoc tests*, $p < 0.02$). Females from this group were lighter than all other treated females (*Student's t-post hoc tests*, $p < 0.0001$). In contrast, males given perinatal estradiol injections were smaller than all other male groups (*Student's t-post hoc tests*, $p < 0.02$), while females injected with estradiol were larger than all other female groups (*Student's t-post hoc tests*, $p < 0.0001$). No Pump Control: $n = 19$ male, $n = 19$ female; Vehicle Control $n = 13$ male, $n = 13$ female; Estradiol $n = 12$ male, $n = 12$ female; Nicotine $n = 13$ male, $n = 13$ female. *N* indicates the number of litters.

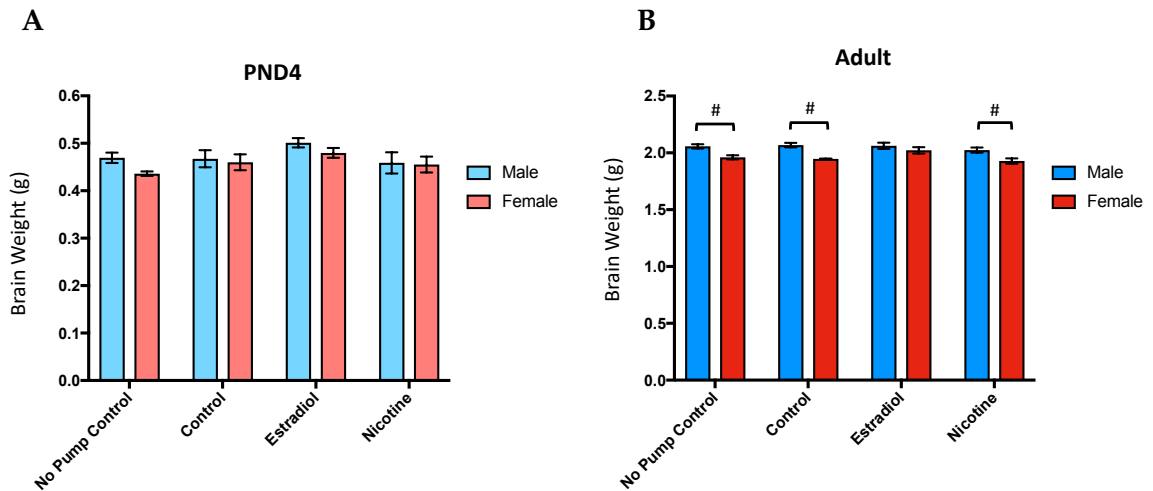


Figure 5: Sex differences in brain weight emerge in adulthood in all groups except estradiol-treated animals.

Sex differences in brain weight emerge in adulthood in all groups except estradiol-treated animals. Whole brain weight (g) measurements were collected from neonates (PND4) and adults (PND61-72). A) There were no significant sex or treatment differences in brain weight at PND4 (two-way ANOVA $p=0.2593$, sex main effect $p=0.1476$, treatment main effect $p=0.0792$, sex*treatment $p=0.7968$). No Pump Control $n = 15$ male, $n = 5$ female; Control $n = 10$ male, $n = 11$ female; Estradiol $n = 11$ male, $n = 10$ female; Nicotine $n = 10$ male, $n = 10$ female. B) Sex differences in brain weight were apparent in adulthood, although the sex*treatment interaction was not significant (two-way ANOVA $p<0.0001$, sex main effect $p<0.0001$, treatment main effect $p=0.0381$, sex*treatment $p=0.3893$). *A-priori t-tests* revealed significant sex differences in adult brain weight among no pump controls ($p=0.0026$), vehicle controls ($p=0.0003$), and nicotine-treated animals ($p=0.0119$), but not estradiol-treated animals ($p=0.3182$). No Pump Control $n = 7$ male, $n = 10$ female; Control $n = 5$ male, $n = 5$ female; Estradiol $n = 7$ male, $n = 7$ female; Nicotine $n = 8$ male, $n = 8$ female. A-B) # $P<0.02$ *a-priori t-test* between males and females. *N* indicates the number of litters. Error bars represent the standard error of the mean.

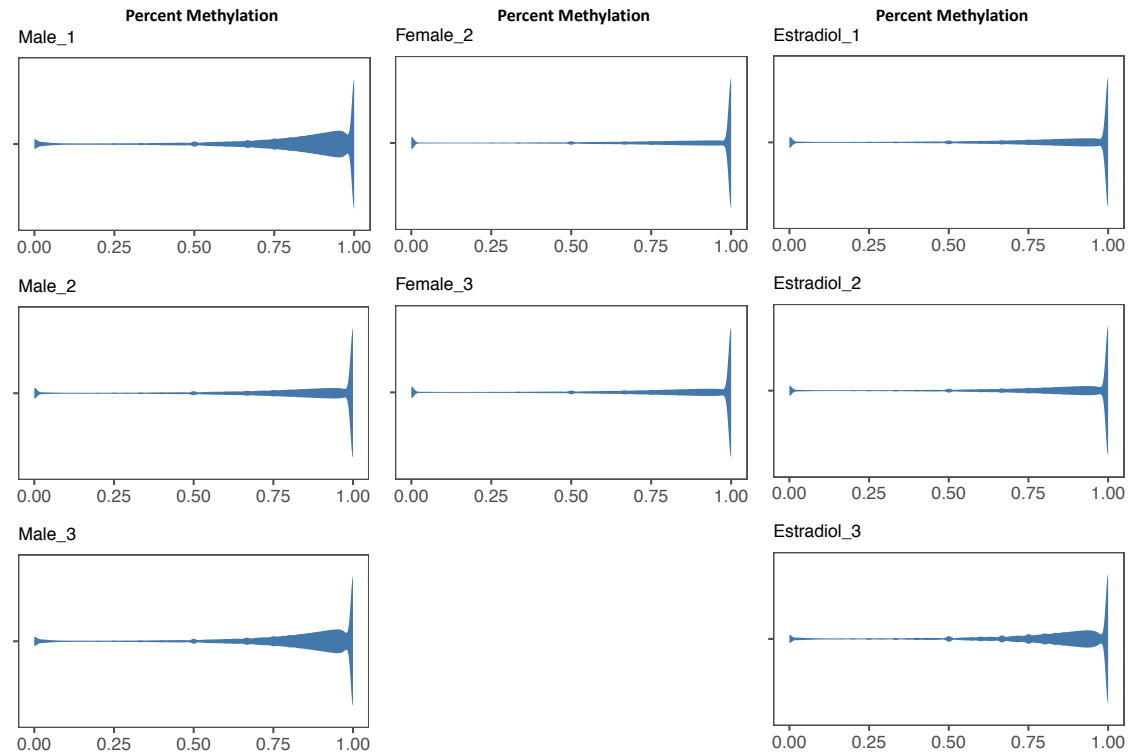
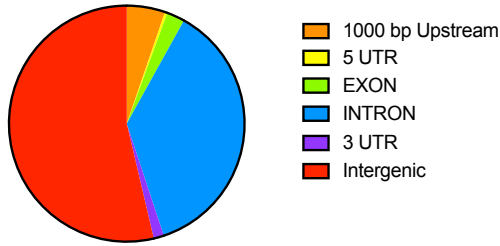
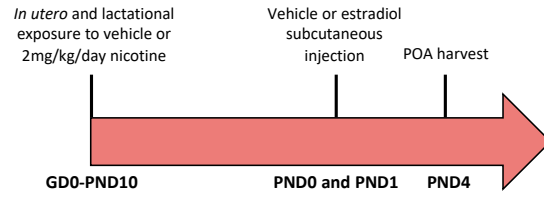
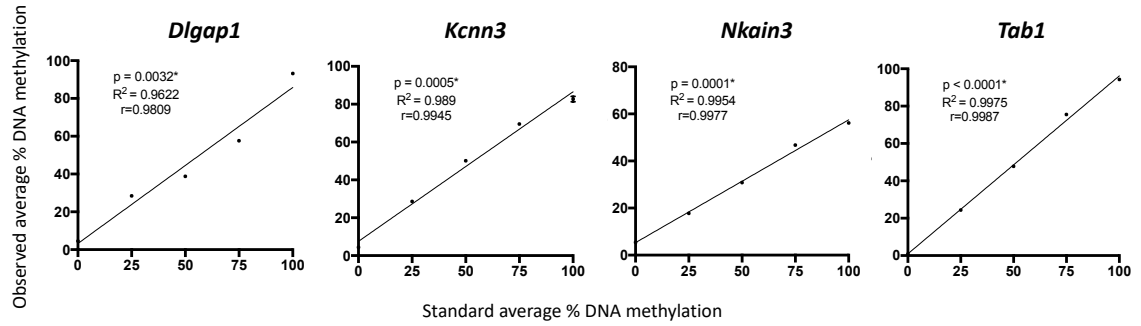
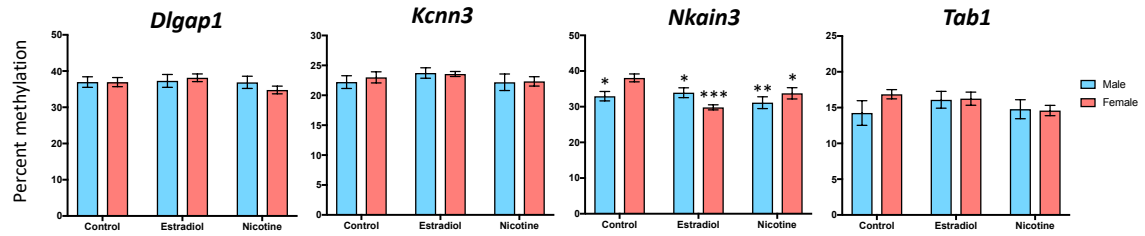
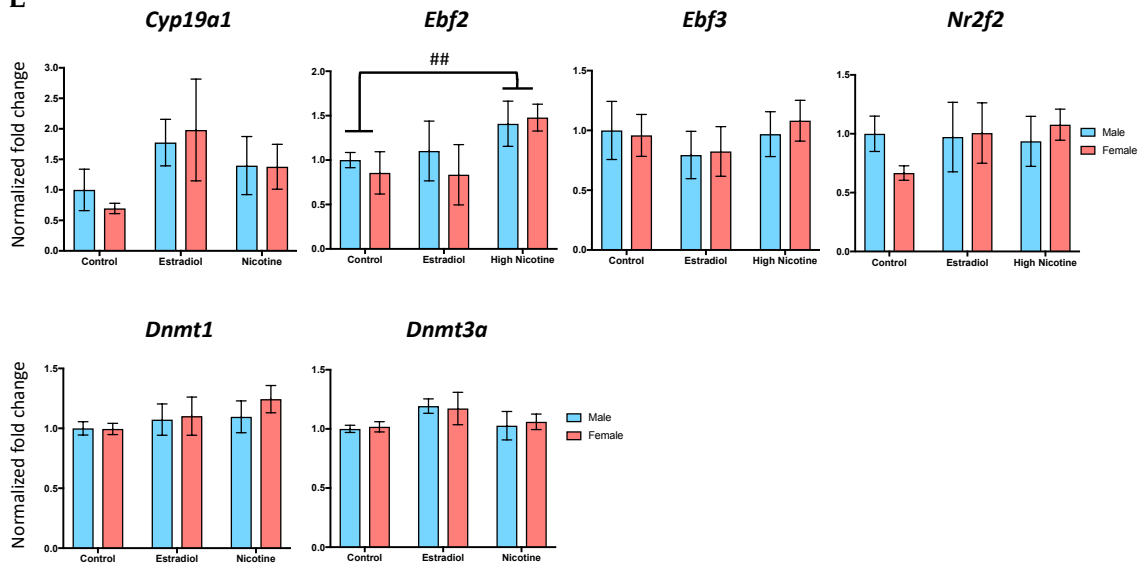


Figure 6: Distribution of epigenome-wide CpG methylation (represented as percent methylation) in neonatal male, female, and estradiol-masculinized female POA.

Violin plot distributions of epigenome-wide CpG methylation (represented as percent methylation) in neonatal male, female, and estradiol-masculinized female POA. All distributions were generated using whole genome bisulfite sequencing (WGBS) data previously collected from male, female, and estradiol-masculinized female POA at PND4 [139] and accessed from NCBI's Short Read Archive under BioProject ID 275796. N=3 males; N= 2 females; N= 3 estradiol-masculinized females.

A**B****C****D****E**

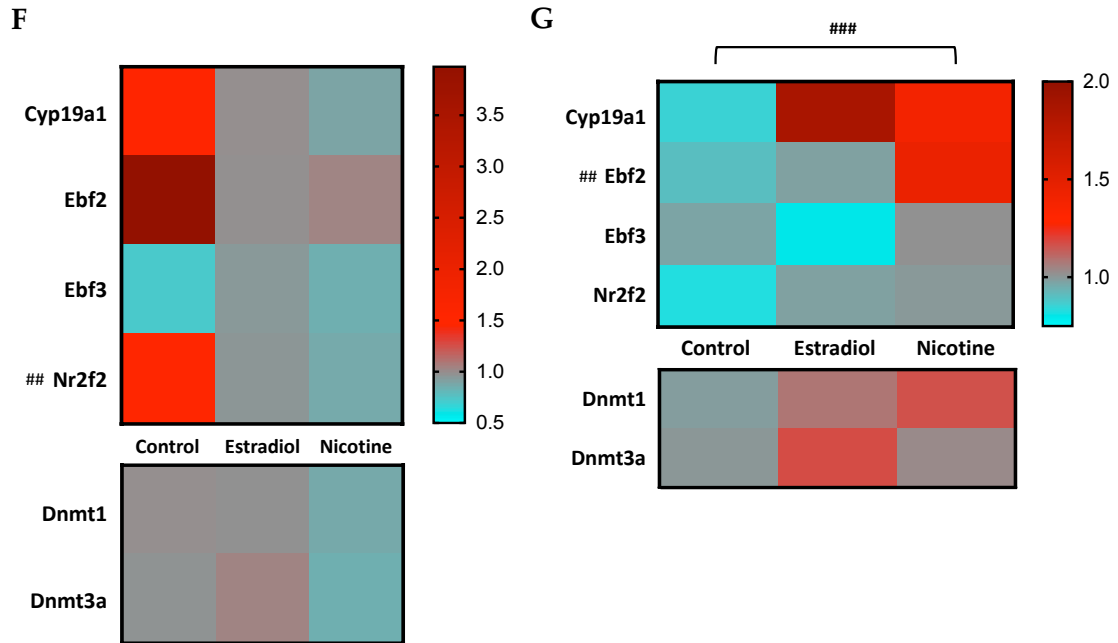


Figure 7: Nicotine exposure evokes upregulation of epigenetic mechanisms required for POA masculinization in neonates.

A) Pie chart outlining genomic location distribution of the top 285 masculinizing differentially-methylated regions (DMRs) between male and female POA. Differential methylation was calculated using publicly available WGBS data obtained from neonatal male, female, and estradiol-masculinized female POA [139]. B) Prior to targeted validation of DMRs, animals were developmentally exposed to either vehicle (DMSO) or nicotine (2mg/kg/day) throughout the window for POA sexualization (GD18-PND10). At PND0 and PND1, animals were subcutaneously injected with either vehicle (sesame oil) or estradiol to induce masculinization. At PND4, POA was isolated in male and female pups, and co-extracted for DNA and RNA. C) Validation of range and linearity of bisulfite pyrosequencing assays designed for four of the top 285 DMRs. Bisulfite-treated rat DNA methylation standards serially prepared at 0%, 25%, 50%, 75%, and 100% were used to correlate the input versus measured methylation values for the following DMRs: *Dlgap1*, *Kcnn3*, *Nkain3*, and *Tab1*. Data generated was analyzed using Pearson's correlation (r). *Dlgap1*: $r=0.9808$, $p=0.0032$; *Kcnn3*: $r=0.9945$, $p=0.0005$; *Nkain3* $r=0.9977$, $p=0.0001$; *Tab1*: $r=0.9987$, $p<0.0001$. $N = 3$ replicates for each serial DNA standard. D) Average percent DNA methylation across each DMR measured in control and treated PND4 POA. DNA methylation at the *Nkain3* DMR was significantly hypermethylated in control females compared to all other groups (two-way ANOVA $p=0.0061$, $\text{sex} \times \text{treatment } p=0.0097$). *Dlgap1*: Control $n = 6$ male, $n = 6$ female; Estradiol $n = 5$ male, $n = 5$ female; Nicotine $n = 6$ male, $n = 7$ female. *Kcnn3*: Control $n = 6$ male, $n = 6$

female; Estradiol n = 5 male, n = 5 female; Nicotine n = 6 male, n = 7 female. *Nkain3*: Control n = 6 male, n = 6 female; Estradiol n = 5 male, n = 5 female; Nicotine n = 6 male, n = 7 female. *Tab1*: Control n = 6 male, n = 6 female; Estradiol n = 5 male, n = 5 female; Nicotine n = 6 male, n = 7 female. E) Expression of methylation-dependent masculinizing genes (MDMGs=*Cyp19a1*, *Ebf2*, *Ebf3*, and *Nr2f2*) and Dnmts (*Dnmt1* and *Dnmt3a*) in control and treated PND4 POA. For each gene, expression was measured across multiple cohorts as fold change relative to the control male within each cohort, and subsequently normalized as percent of the control males across combined cohorts. Although there was no significant main effect of sex, *Ebf2* expression was significantly higher in nicotine treated animals compared to controls (two-way ANOVA between nicotine and control groups p=0.1146, sex main effect p=0.8612, treatment main effect p=0.0259, sex*treatment p=0.6165). *Cyp19a1*: Control n = 6 male, n = 5 female; Estradiol n = 5 male, n = 4 female; Nicotine n = 7 male, n = 6 female. *Ebf2*: Control n = 4 male, n = 6 female; Estradiol n = 4 male, n = 3 female; Nicotine n = 4 male, n = 5 female. *Ebf3*: Control n = 6 male, n = 6 female; Estradiol n = 5 male, n = 5 female; Nicotine n = 6 male, n = 6 female. *Nr2f2*: Control n = 6 male, n = 6 female; Estradiol n = 5 male, n = 5 female; Nicotine n = 7 male, n = 7 female. *Dnmt1*: Control n = 6 male, n = 6 female; Estradiol n = 5 male, n = 5 female; Nicotine n = 7 male, n = 7 female. *Dnmt3a*: Control n = 6 male, n = 6 female; Estradiol n = 5 male, n = 5 female; Nicotine n = 7 male, n = 6 female. F) Heat map representing sex differences in normalized fold change values across MDMGs and Dnmts. Expression represented as the ratio of male to female normalized fold change values. M:F expression of *Nr2f2* was significantly higher in controls compared to nicotine treated animals (*a-priori t-test*, p=0.0499). *Cyp19a1*: Control N=5 litters; Estradiol N=4 litters; Nicotine N=6 litters. *Ebf2*: Control N=4 litters; Estradiol N=3 litters; Nicotine N=4 litters. *Ebf3*: Control N=5 litters; Estradiol N=5 litters; Nicotine N=6 litters. *Nr2f2*: Control N=6 litters; Estradiol N=5 litters; Nicotine N=7 litters. *Dnmt1*: Control N=6 litters; Estradiol N=5 litters; Nicotine N=7 litters. *Dnmt3a*: Control N=6 litters; Estradiol N=5 litters; Nicotine N=5 litters. G) Heat map representing treatment differences in normalized fold change values across MDMGs and Dnmts. MDMG expression was significantly increased in the POA of nicotine-treated neonates as compared to controls (two-way MANOVA p=0.0716, treatment main effect p=0.0113, sex main effect p=0.9752, sex*treatment p=0.8749). *Cyp19a1*: Control n = 6 male, n = 5 female; Estradiol n = 5 male, n = 4 female; Nicotine n = 7 male, n = 6 female. *Ebf2*: Control n = 4 male, n = 6 female; Estradiol n = 4 male, n = 3 female; Nicotine n = 4 male, n = 5 female. *Ebf3*: Control n = 6 male, n = 6 female; Estradiol n = 5 male, n = 5 female; Nicotine n = 6 male, n = 6 female. *Nr2f2*: Control n = 6 male, n = 6 female; Estradiol n = 5 male, n = 5 female; Nicotine n = 7 male, n = 7 female. *Dnmt1*: Control n = 6 male, n = 6 female; Estradiol n = 5 male, n = 5 female; Nicotine n = 7 male, n = 7 female. *Dnmt3a*: Control n = 6 male, n = 6 female; Estradiol n = 5 male, n = 5 female; Nicotine n = 7 male, n = 6 female. C-G) *P< 0.05, **P< 0.01, ***P < 0.001 Student's t-test post hoc analysis compared to vehicle-treated females

following significant two-way ANOVA. ## $P < 0.05$ treatment as main effect between control and nicotine-treated groups following two-way ANOVA. ### $P < 0.05$ treatment as main effect between control and nicotine-treated groups in a repeated structure. N indicates the number of litters. Error bars represent standard error of the mean.

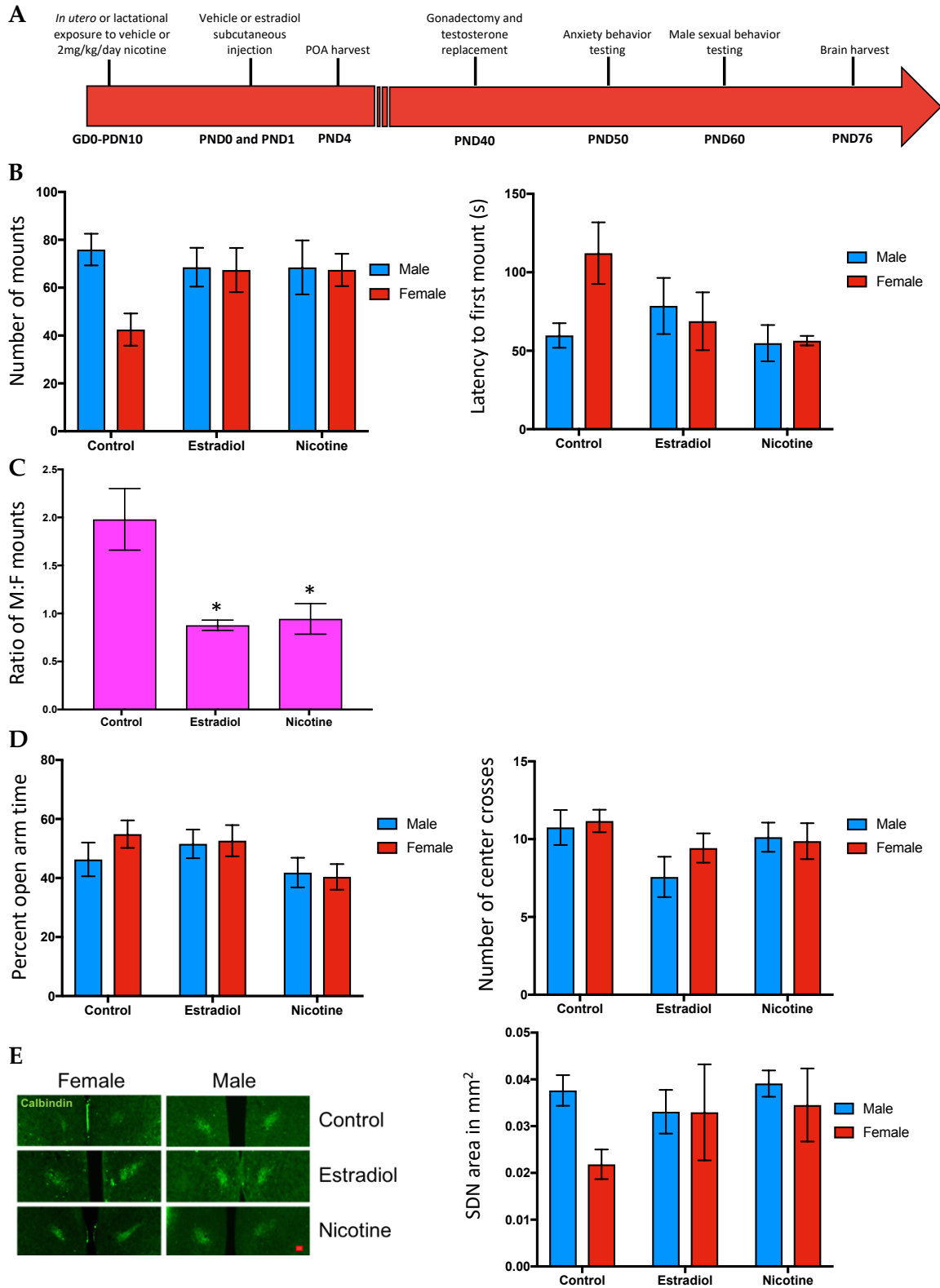


Figure 8: Maternal nicotine exposure eliminates sexual dimorphisms in male sexual behavior and SDN area.

A) Animals were developmentally exposed to either vehicle (DMSO) or nicotine (2mg/kg/day) throughout the window for POA sexualization (GD18-PND10). At PND0 and PND1, animals were subcutaneously injected with either vehicle (sesame oil) or estradiol to induce masculinization. Animals were gonadectomized at PND40, and fitted with a testosterone replacement. In all animals, anxiety-like behavior and locomotion were assessed at PND50, and male sexual behavior at PND60. Brains were harvested at PND76 to examine POA-SDN area. B) Male sexual behavior parameters measured in PND60 animals in the presence of a sexually-receptive female. Number of mounts: Control n = 9 male, n= 7 female; Estradiol n = 9 male, n= 8 female; Nicotine n = 8 male, n= 7 female. Mount latency: Control n = 8 male, n= 7 female; Estradiol n = 8 male, n= 8 female; Nicotine n = 8 male, n= 6 female. C) The ratio of male to female mounts was significantly reduced in nicotine-treated and estradiol-masculinized animals (one-way ANOVA $p=0.03$). Mount ratio: Control n = 7 litters; Estradiol n =7 litters; Nicotine n = 7 litters. D) Parameters of anxiety-like behavior and locomotion measured at PND50 using the elevated plus maze apparatus. Percent time in open arm: Control n = 6 male, n= 6 female; Estradiol n = 7 male, n= 7 female; Nicotine n = 8 male, n= 8 female. Center Crosses: Control n = 6 male, n= 6 female; Estradiol n = 7 male, n= 7 female; Nicotine n = 8 male, n= 8 female. E) POA-SDN area visualized in 40 μm sections using immunofluorescent staining for calbindin. Scale bar represents 100 μm . SDN Area (mm^2): Control n = 4 male, n= 4 female; Estradiol n = 3 male, n= 3 female; Nicotine n = 5 male, n= 4 female. B-E) $*P < 0.05$ Student's *t*-test post hoc analysis compared to vehicle-treated females following significant one-way ANOVA. N indicates the number of litters. Error bars represent standard error of the mean.

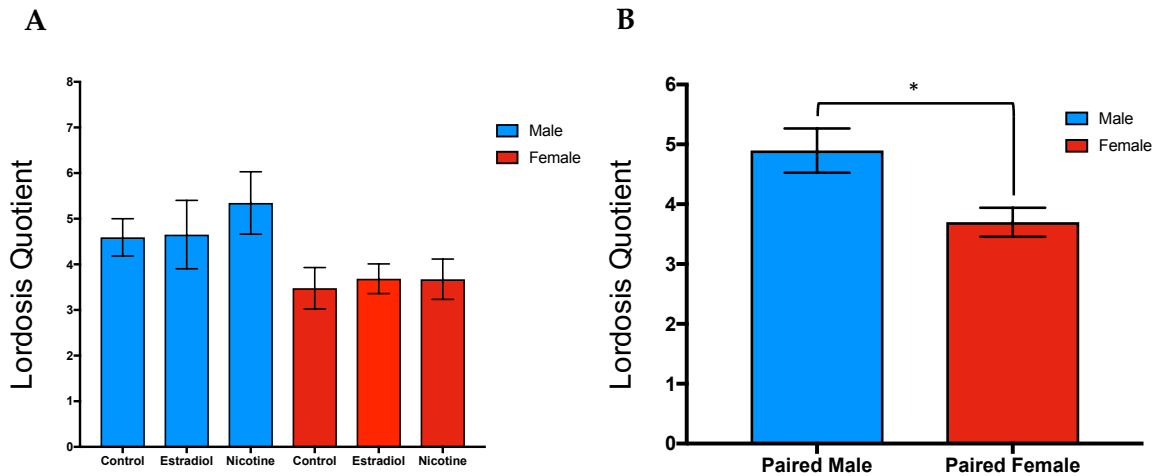


Figure 9: Variability across additional sexual behavior parameters observed during PND60 male sexual behavior assays.

A-B) Female sexual behavior (number of lordoses) was scored in all sexually-receptive females used in male sexual behavioral assays. For each assay pairing, the lordosis quotient (LQ=number of receptive female lordoses/10 mounts of paired animal) was calculated. A) Treatment of paired animal had no effect on LQ (two-way ANOVA $p=0.0867$, sex main effect $p=0.0052$, treatment main effect $p=0.6452$, sex*treatment $p=0.7710$). Lordosis Quotient: Paired males $n = 11$ Control, $n = 12$ Estradiol, $n = 14$ Nicotine; Paired females $n = 13$ Control, $n = 14$ Estradiol, $n = 16$ Nicotine. B) LQ was higher in paired male assays compared to paired females (t-test, $p=0.0066$). A-B) $*P < 0.05$ one-way ANOVA between paired males and females. N indicates the number of litters. Error bars represent the standard error of the mean.

A

1. Measure multiple masculinization endpoints across individual animals.
Include negative controls.



2. Normalize data to percent of the control male for each respective endpoint, log transform.



3.



Repeated Measures ANOVA

Perform 3-way repeated measures ANOVA across all normalized endpoints for each individual animal. Assess sex, treatment, and measure type (positive or negative) as main effects.

and/or

Masculinization Index

Average normalized endpoint values for each individual animal to determine the masculinization index. Run ANOVA to determine sex and treatment differences.

B

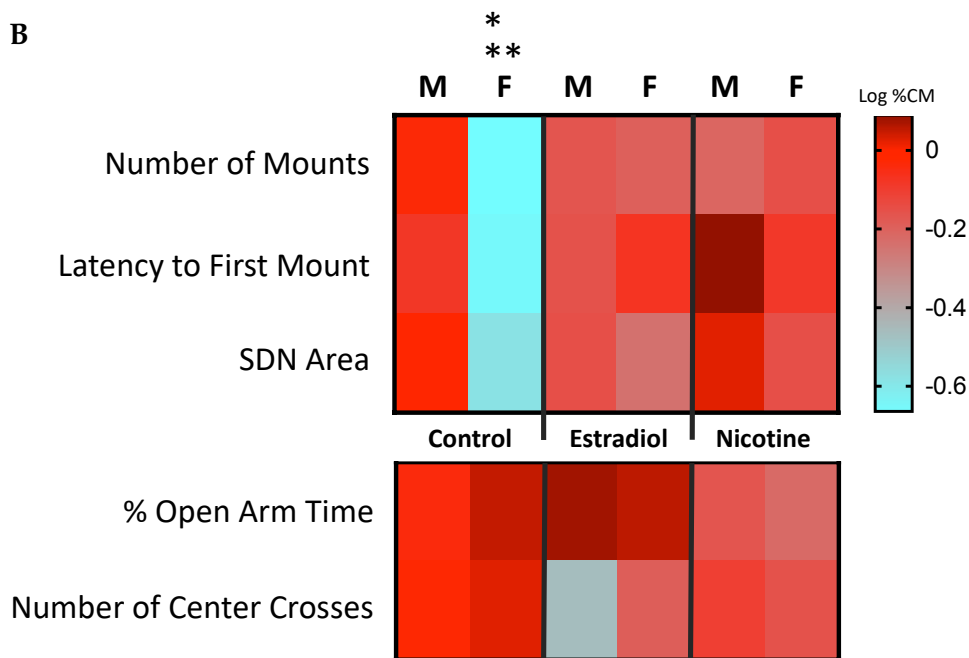


Figure 10: Novel methods for assessing masculinization of the rat POA.

Novel methods for assessing masculinization of the rat POA. A) Schematic outlining statistical approaches to comprehensively assess POA masculinization, including repeated measures analysis and masculinization index. B) Heat map representing normalized and log-transformed values for masculinization parameters, including male sex behavior (number of mounts, latency to first mount), and SDN area, as well as

negative control parameters, including anxiety-like behavior (% open arm time, number of center crosses) across individual animals. The normalized and log transformed values for masculinization parameters in control females significantly differed from all other groups and behaviors when assessed as a repeated measures three-way ANOVA (treatment*sex*measure $p=0.0234$, $F=3.853$) and masculinization index two-way ANOVA (treatment*sex $p=0.0357$, $F=3.5857$). Control $n=9$ male, $n=9$ female; Estradiol $n=9$ male, $n=9$ female; Nicotine $n=8$ male, $n=8$ female. ** $P < 0.02$ Student's t-test post hoc analysis following significant three-way repeated measures ANOVA, ** $P < 0.05$ Student's t-test post hoc analysis following significant two-way masculinization index ANOVA. N indicates the number of litters.*

Table 1: Pyrosequencing assays used in targeted DMR validation.

Gene Name	Forward Primer (5'-3')	Reverse Primer (5'-3')	Sequencing Primer (5'-3')	Sequence to Analyze (5'-3')	PCR Annealing Temp (°C)	# CpGs Analyzed
<i>Dlgap1</i>	TTTTTTAAAGGAA AATAAGAGAAAG	*ATCCCAACAAA AAATTAAACTCC	TTGTTTGTTTTG TTATTAG	TTYGTTATTYGTTTATT TATATTTATTTGTAGT	58	2
<i>Kcnn3</i>	AGGATTGTGTTTG TGGTTGAAG	*ACCAACATAAT AACCAAAACAC C	TGTTTGTGGTTG AAGG	GGTAATTYGTGAGAATTG ATATTTGGAGAGTTTGGT TTTTAAAGTGATTTTTTTT TGTTTTTTTTGGGGGTATT ATAGTGGGAGAGTTAGGT TTYGGGGAGGATTATTGT TTTTTAATTGGTGTTTT	62	2
<i>Nkain3</i>	*TTAAAGGATTTG TTGTGTTAGTG	CAAATAATTTTC CAATCTCCACA	AATACTAACTTT CTAAACCT	CRTACCACAAAATACAC ACACACACACACACACA CACACACACACACACAC RCATCTCTTTTAAAATATT TATCCTATTTACATAA	62	2
<i>Tab1</i>	AAGGATGGGATT TGGTAGATATG	*CCAATAACTC AAACACAAAAC CT	GTTTAAAGTTTA TTTAGTT	AYGATATAGTAAGAATGT TTTTGAGTGGGTTAGTAA AGTTAGGGAGGATTAAT ATTTTTTGGTTTATAGTGA TATAATTTTTGGYGTG TTGGTTATTIGTTGAGGTT T	62	2

*indicates biotin labeling

Table 2: Birth outcomes stratified by gestational exposure.

		N Total Litters	Litter Size	# Males	# Females
			Average Number of Pups \pm SEM	Average Number of Pups \pm SEM	Average Number of Pups \pm SEM
Gestational Treatment	<i>No Pump Control</i>	19	12.32 \pm 0.76	5.95 \pm 0.60	6.37 \pm 0.51
	<i>Vehicle Control (DMSO)</i>	25	13.08 \pm 0.53	6.96 \pm 0.47	6.12 \pm 0.46
	<i>Nicotine (2mg/kg/day)</i>	13	12.23 \pm 0.80	5.69 \pm 0.80	6.54 \pm 0.76
<i>P-Value</i>			0.6438 ^a	0.1167 ^b	0.8412 ^b

^a Kruskal-Wallis test across treatments

^b One-way ANOVA across treatments

Table 3: DAVID Functional Annotation Clustering of Top DMRs.

Functional Cluster Name	Enrichment Score	Genes	P-Value	Benjamini-adjusted P-value
Phox homologous domain	3.86	<i>Sh3pxd2a, Sh3pxd2b, Pik3c2b, Snx19, Snx7, Snx27</i>	1.9 e-5	5.8 e-3
Phosphatidylinositol-3-phosphate binding	3.86	<i>Dennd1a, Sh3pxd2b, Snx19, Snx27</i>	8.1 e-4	1.7 e-1
Phosphatidylinositol binding	1.05	<i>Sh3pxd2a, Sh3pxd2b, Sh3yl1, Pik3c2b, Snx7</i>	1.4 e-3	1.5 e-1

Data obtained from DAVID Functional Annotation Tool (DAVID Bioinformatics Resources 6.7, NIAID/NIH) [153, 154].

Table 4: Genomic location and function of target DMRs.

DMR^a Nearest Gene Name	Chromosome No.	Differential Methylation^b	# CpGs^c	Distance to Nearest Gene (bp)	Genomic Category	Gene Function
<i>Tab1</i>	7	0.93	2	0	INTRON	Kinase activator
<i>Nkain3</i>	5	0.86	2	0	INTRON	Sodium/potassium transporting ATPase
<i>Dlgap1</i>	9	0.72	10	0	INTRON	DLG associated protein 1; highly expressed in brain
<i>Kcnn3</i>	2	0.69	2	0	INTRON	Potassium calcium activated channel; interacts with 17-B estradiol

^a DMR= 250bp differentially-methylated region

^b Differential methylation calculated between control males and females.

^c Indicates number of CpGs within 250bp DMR.

3. Maternal tobacco smoke exposure alters DNA methylation at genomic regions implicated in neurobehavioral disorders

3.1 Introduction

Maternal tobacco smoke (TS) exposure has been associated with a host of adverse developmental outcomes in exposed offspring [80, 81, 86], including low birth weight [72-78] and neurobehavioral and cognitive impairments [77, 79-86, 178].

Neurodevelopmental disorders like attention-deficit hyperactivity disorder (ADHD) and autism spectrum disorder (ASD) have been well studied in the context of maternal TS exposure, and ample evidence supports that both ADHD [25-28, 77, 81, 87-89, 179, 180] and ASD [179, 181, 182] are associated with smoking during pregnancy. ADHD and ASD are the most common neurodevelopmental disorders among children [183], and are both characterized by social impairment, hyperactivity, and impulsivity [184]. Both disorders often co-occur [185], with nearly 50% of children with ADHD displaying signs of ASD, and up to 80% of children with ASD displaying ADHD-like symptoms [185]. These parallels support the idea of shared developmental etiology. Although an exact cause has yet to be determined, the etiology of both ASD and ADHD has been long suspected to involve a strong genetic component in addition to a poorly understood environmental component [184].

Several animal and human studies have associated adverse outcomes of maternal TS exposure with alterations in DNA methylation during early development. For

example, low birth weight in male offspring of smoking mothers was associated with increased DNA methylation at the growth mitogen insulin-like growth factor II (*IGF2*) [18]. The affected region was further shown to have marked effects on *IGF2* transcription, with a 1% change in methylation leading to a halving (increased methylation) or doubling (decreased methylation) of transcript levels [18].

Developmental alterations to DNA methylation have also been associated with neurobehavioral disorders, like ADHD, as a result of gestational TS-exposure. In rats, developmental nicotine exposure induced ADHD-like behavioral changes in both the F1 and F2 exposed generations that were associated with global CpG hypomethylation in the adolescent striatum and cortex [140]. In humans, peripheral blood DNA methylation levels in the aryl hydrocarbon receptor repressor (*AHRR*) and the growth-factor independent 1 transcriptional repressor (*GFI1*) were associated with ADHD scores in children between 6 and 12 years of age who were exposed to developmental TS [21].

Independent of behavioral and birth weight outcomes, epigenome-wide alterations have also been associated with *in utero* TS exposure in humans [16, 17, 19, 22, 24]. Altered DNA methylation at 26 CpGs across ten genes in infant cord blood was associated with smoking during pregnancy [16, 17]. Affected genes included the aryl hydrocarbon receptor repressor (*AHRR*) and the cytochrome P450 family 1 subfamily A member 1 (*CYP1A1*), both of which play a role in the metabolism and excretion of TS constituents [17]. Similar associations were observed in adolescents [24] and adults [19, 22, 24] who were developmentally exposed to TS, supporting the persistence of the

epigenome-wide alterations established during development as a result of maternal TS exposure.

Umbilical cord blood and peripheral blood are commonly obtained to examine epigenetic endpoints in the context of developmental TS exposure in humans [16, 17, 20]. While associations have been established between blood DNA methylation levels and incidence of neurobehavioral disorders [20, 186], few studies have investigated corresponding changes to DNA methylation in the brain [187, 188]. This is likely due to the difficulty associated with examining DNA methylation in the human brain, which requires *post-mortem* sampling methods. Recently, an online database was developed to examine correlations between DNA methylation changes in the blood and brain in humans (available at: <https://epigenetics.essex.ac.uk/bloodbrain/>) [187]. This *in silico* database reports DNA methylation levels measured using the Illumina 450k BeadChip Array in matched blood and *post-mortem* brain tissue samples (prefrontal cortex, entorhinal cortex, superior temporal gyrus, and cerebellum) taken from adults who suffered from neurological diseases [187]. Despite these efforts, obtaining accurate exposure information associated with *post-mortem* samples is challenging. As such, associations in DNA methylation changes across blood and brain within the context of TS exposure in humans remains elusive. A recent study associating maternal TS exposure to changes in DNA methylation levels in human conceptual brain tissue [6] is the only known study to make these associations [6].

Animal models not only allow for concurrent examination of molecular outcomes across multiple tissues, but also behavioral outcomes, under a controlled

exposure setting. Given the evidence supporting associations between DNA methylation changes in blood and incidence of neurodevelopmental disorders like ASD and ADHD [7], questions remain as to whether DNA methylation patterns observed in blood correspond to changes in the brain in the context of TS exposure, particularly in brain regions associated with behaviors that are impaired by maternal TS exposure.

Resolving these questions allows determination of blood biomarkers of developmental exposure, and particularly those that reflect corresponding changes in the brain, is of utmost importance. Epigenetic biomarkers related to TS exposure have been previously described. For example, in blood samples taken from adolescents, maternal TS exposure was associated with increased DNA methylation of the gene encoding brain-derived neurotropic factor (*BDNF*) [23], a gene that was also found to serve as a methylation biomarker for depression [189]. In saliva taken from children aged 7-12, DNA methylation levels at the vasoactive intestinal peptide receptor 2 (*VIPR2*) were correlated to incidence of ADHD [190]. However, in all of these studies, correlations between DNA methylation levels in the brain were not assessed. Thus, identification of stable biomarkers of exposure that reflect changes in the brain is critical in order to better predict the likelihood of neurobehavioral disorder incidence as a result of early developmental exposure.

Here, we used a controlled animal study to examine maternal TSE-exposure induced alterations to DNA methylation levels in the blood and brain of developmentally-exposed offspring, particularly those who displayed signs of ADHD-like behavior in adulthood [142]. We specifically employed whole genome bisulfite

sequencing (WGBS) techniques to identify epigenome-wide DNA methylation changes in the peripheral blood, cortex, and hippocampus of male rats that were exposed *in utero* to low-dose tobacco-smoke extract (TSE; containing 0.2mg/kg/day of nicotine), low-dose nicotine (0.2mg/kg/day) or high-dose nicotine (2mg/kg/day) as compared to controls [142]. We chose to solely examine male rats given the increased prevalence of neurodevelopmental disorders like ADHD and ASD in males versus females [191, 192]. Using nearest gene name (with no preference for upstream or downstream) as a proxy for identified differentially methylated regions (DMRs), we identified DMRs in common across these three tissue types in male rats of all gestational treatment groups. We examined these common DMRs by functional annotation using the Database for Annotation, Visualization, and Integrated Discovery (DAVID)[153, 154], and identified genes involved in synapse formation as the most highly enriched within each treatment group. We next compared these regions to DMRs identified via reduced representation bisulfite sequencing (RRBS) in human cord blood taken from TS-exposed and unexposed newborn males (NEST Cohort), and found 306 DMRs in common with the TSE-exposed rats. Adding the DMRs identified in the nicotine exposure groups, we found DMRs in common between humans and rats of all three treatment groups, nearly half of which are implicated in ASD and/or ADHD. Our findings are the first to suggest a relationship between developmental TS exposure-induced changes to DNA methylation in the blood and brain that validate across species and correlate to both behavioral deficits [142] and neurodevelopmental disorder-relevant functional pathways. Furthermore, these associations were similar across both low- and high-dose

TS/nicotine-exposure models in rats, suggesting that developmental TS exposure across a range of exposure levels impacts the same genes and pathways, many of which bear direct relevance to common neurodevelopmental disorders.

3.2 Materials and Methods

3.2.1 Animal Husbandry and Gestational Treatment

All experiments involving the handling of animals or processing of animal tissues were conducted in compliance with Duke's Division of Laboratory Animal Resources policies and with approval from the Duke University Institutional Animal Care and Use Committee [142]. Young adult male and female Sprague-Dawley rats between the weights of 225-250g were ordered from Charles River Laboratories (Wilmington, MA, USA). Following two weeks of acclimation, females were anesthetized (60 mg/kg ketamine + 0.15 mg/kg dexmedetomidine administered i.p., followed by 0.15mg/kg atipamezole + 5 mg/kg ketoprofen administered s.c.) [142] and subcutaneously implanted with an Alzet 2ML4 mini-osmotic infusion pump (Durect Corp.; Cupertino, CA, USA) delivering either vehicle (dimethyl sulfoxide; DMSO), nicotine (nicotine hydrogen tartrate salt, Sigma-Aldrich; Saint Louis, MO, USA) at a dose of either 0.2 or 2 milligrams per kilogram body weight per day (2mg/kg/day), or tobacco smoke extract (TSE, Arista Laboratories, Richmond, VA, USA) at a dose containing 0.2 milligrams per kilogram body weight nicotine per day via subcutaneous diffusion. TSE was obtained from Arista Laboratories (Richmond, Virginia) and was prepared from Kentucky Reference cigarettes (KY3R4F) on a Rotary Smoke Machine under ISO

(International Organization for Standardization) smoke conditions [142]. Following surgery, females were allowed to recover for three days, and subsequently housed with a drug-naïve male rat for five days to allow for mating. Females were kept in isolation throughout pregnancy and allowed to undergo normal birthing processes. Parturition occurred around day 22 of gestation, and the day of birth was considered PND0. At PND1, litters were culled to achieve a total of 8-10 pups with an equal number of males and females. Animals were weaned at PND21 and housed in same sex groups of two or three. Following behavioral assessments of cognition and hyperactivity as reported previously [142], hippocampus, cortex, and peripheral blood were collected from males of all four treatment groups on PND90 for examination of epigenetic endpoints.

Our study included four treatment groups: vehicle control (DMSO), low-dose nicotine (0.2mg/kg/day), high-dose nicotine (2.0mg/kg/day) and TSE containing low dose nicotine (0.2mg/kg/day). Both nicotine and TSE doses were calculated based on the weight of the dam on the day of surgery, and nicotine dose was adjusted for tartrate salt weight. Due to the fact that maternal body weight increased during gestation, our doses decreased by approximately 33% during gestation, but recovered to initial values following post-partum weight loss. Our doses were chosen to model secondhand smoke exposure (0.2mg/kg/day nicotine, 0.2mg/kg/day TSE) and moderate maternal smoking (2.0mg/kg/day) based on previous reports that a subcutaneous dose of 1.5-6 mg/kg/day nicotine by osmotic mini-pump produces plasma nicotine levels in rats similar to humans who are moderate to heavy smokers [143-145]. A continuous infusion model of nicotine and TSE exposure was chosen to eliminate issues of hypoxia and ischemia that

are associated with nicotine injections [113, 116] and the confound of maternal stress that accompanies forced smoke inhalation in rodents [53, 117]. All animals were maintained on a reverse 12-hour light/dark cycle and provided with food and water *ad libitum*.

3.2.2 Study Population: NEST

Pregnant women were recruited from central North Carolina for the Newborn Epigenetics Study (NEST) from prenatal clinics at Duke University Hospital and Durham Regional Hospital obstetrics facilities between 2005 and 2011. All participants spoke English and/or Spanish and were at least 18 years of age. Women completed a questionnaire in English or Spanish at the time of recruitment, which assessed sociodemographic characteristics including age, race, marital status, and level of education. There were 2,640 women who participated in the study. For our current analyses, a subset of 26 male participants were randomly chosen based on maternal plasma cotinine levels measured during gestation (described below) to achieve an equal distribution of smoke-exposed (N=13 males) and unexposed (N=13 males). NEST study protocols were approved by the Duke University Institutional Review Board (Pro00014548). All enrolled women provided written informed consent for themselves and their child prior to participation in any study activities.

3.2.2.1 NEST Maternal Plasma Cotinine Measurement & Cord Blood Collection

Venous maternal blood was collected from NEST participants during pregnancy. Blood samples were collected into EDTA-containing lavender top vacutainer tubes, and subsequently separated by centrifugation into RBCs, plasma, and buffy coat as previously described [10]. Blood fractions were aliquoted and stored at -80°C until

analysis for cotinine levels. Cotinine is a relatively stable metabolite of nicotine and serves as a widely used blood biomarker of TS use and exposure [193]. Due to their hydrophobicity, both nicotine and cotinine readily cross the placenta [194] and accumulate in the fetus if exposure is sustained throughout pregnancy [195]. Cotinine (ng/mL plasma) was measured by Dr. JunFeng Zhang's Laboratory at Duke University via methods previously described [196] using high-performance liquid chromatography with tandem mass spectrometry (HPLC-MS-MS). The limit of detection was 0.05 ng/mL, with reproducibility greater than 94%. Based on measured cotinine levels, participants were dichotomized into two exposure categories, congruent with previous NEST studies [196] and studies examining passive smoke exposure during pregnancy [197, 198]: 1) "no exposure", or women with plasma cotinine levels below 1ng/mL; and 2) "active smoking", or women with plasma cotinine levels greater than 3ng/mL. Venous umbilical cord blood samples were collected at the time of birth from 26 male NEST participants either exposed or unexposed to maternal TS (exposure determined based on maternal plasma cotinine measurements; N=13 exposed, N=13 unexposed). Cord blood samples were collected into EDTA-containing lavender top vacutainer tubes, and subsequently separated by centrifugation into RBCs, plasma, and buffy coat as previously described [10]. Cord blood fractions were aliquoted and stored at -80°C until required for analysis.

3.2.3 DNA Isolation

Genomic DNA was extracted from rat tissue samples using the Qiagen AllPrep DNA/RNA Mini Kit (Qiagen; Valencia, CA) (Figure 11). Genomic DNA was extracted from the buffy coat of infant cord blood samples using the Qiagen QIAamp DNA Mini

kit (Qiagen; Valencia, CA). DNA samples were eluted in nuclease-free water and nucleic acid concentration and purity were assessed using a NanoDrop 2000 spectrophotometer (Thermo Fisher Scientific; Waltham, MA).

3.2.4 Whole Genome Bisulfite Sequencing (WGBS) of Rat Hippocampus, Cortex, and Peripheral Blood

WGBS was performed by Zymo Research (Irvine, CA, USA) using bisulfite-treated DNA samples isolated from male rat hippocampus, cortex, and peripheral blood. Samples were sequenced in two pools of six males each from each treatment group. Sequencing data was analyzed at the Duke Center for Genomic and Computational Biology (Duke University; Durham, NC, USA).

3.2.4.1 Methyl-MaxiSeq® library construction

Methyl-MaxiSeq® libraries were prepared from 300 ng of genomic DNA digested with 2 units of Zymo Research's (ZR) dsDNA Shearase™ Plus (Cat#: E2018-50). The fragments produced were end-blunted and 3'-terminal-A extended, then purified using the Zymo Research (ZR) DNA Clean & Concentrator™ – 5 kit (Cat#: D4003). The A-tailed fragments were ligated to pre-annealed adapters containing 5'-methyl-cytosine instead of cytosine and adapter-ligated fragments were filled-in. Bisulfite treatment of the fragments was done using the EZ DNA Methylation – Lightning kit (ZR, Cat#: D5030). PCR was performed with Illumina TruSeq indices and the size and concentration of the fragments were confirmed on the Agilent 2200 TapeStation, then sequenced on an Illumina HiSeq instrument.

3.2.4.2 Methyl-MaxiSeq® sequence alignments and data analysis

Sequence reads from bisulfite-treated EpiQuest libraries were identified using standard Illumina base-calling software and then analyzed using a Zymo Research proprietary analysis pipeline written in Python and using Bismark (<http://www.bioinformatics.babraham.ac.uk/projects/bismark/>) as the alignment software for analysis. Index files were constructed by *bismark_genome_preparation* command using the entire reference genome. *--non_directional* and all other default parameters were applied while running Bismark. The methylation level of each sampled cytosine was estimated as the number of reads reporting a C, divided by the total number of reads reporting a C or T.

3.2.5 Reduced Representation Bisulfite Sequencing (RRBS) of NEST Cord Blood

RRBS was performed by Zymo Research using bisulfite-treated DNA samples extracted from NEST cord blood buffy coat specimens. Individual libraries were constructed for all samples (N=13 exposed males, N=13 unexposed males) so they could be individually deconvoluted during analysis. Samples were pooled randomly prior to sequencing to account for batch effects. RRBS paired-end reads were processed using the TrimGalore toolkit (available at: http://www.bioinformatics.babraham.ac.uk/projects/trim_galore), which employs Cutadapt to trim low-quality bases and Illumina sequencing adapters from the 3' end of the reads. The following TrimGalore parameters specific to RRBS data were used: *--rrbs --non-directional --trim1*. Only reads that were 20nt or longer after trimming were kept

for further analysis. Reads were mapped to the GRCh37 (hg19) version of the human genome [199] using Bismark [151]. Percent methylation was called via both Bismark Methylation Extractor (for QC purposes only) and via the methylKit [152] package in R (for analysis). Methylation sites with fewer than four reads or more than 100 reads and not found in at least 10 samples per group were excluded from statistical analyses. Picard Tools CollectInsertSizeMetrics was used to confirm that the libraries conformed with the expected insert size distribution, and CollectHsMetrics was used to confirm that the aligned RRBS data targeted the expected *MspI* bed regions. Statistical analyses were conducted in the R statistical programming environment. PCA and hierarchical clustering analysis utilizing the top 25% most variable sites were performed to assess for the presence of outlier samples. For univariate analysis, percent methylation sites with zero variance were removed, and t-tests were used to assess for differences between groups (Hi and Lo); p-values were adjusted using the FDR correction.

3.2.6 Data Analysis

Using thresholds described above for calculating differential methylation in WGBS and RRBS, the top 10k differentially methylated CpGs were identified in each treatment group and tissue type relative to controls, and mapped to the nearest gene. Nearest gene name was used as a proxy for differentially methylated region (DMR). Overlap between DMRs across rat hippocampus, cortex, and peripheral blood was assessed for each treatment (0.2, 2.0 mg/kg/day nicotine and 0.2 mg/kg/day nicotine in TSE), and displayed as Venn Diagrams using Microsoft Excel. DMRs that were common to all three tissue types within each treatment group were then compared to each other

to determine DMR's commonly affected by TS and its constituents in rats. Overlapping DMRs within treatment groups were then compared to DMRs identified via RRBS of human cord blood, and common DMRs across species were identified. Overlapping DMR lists from rat tissues were assessed for functional clusters using the DAVID Functional Annotation Tool (DAVID Bioinformatics Resources 6.7, NIAID/NIH) [153, 154]. Genes (DMRs) implicated in autism were obtained from the Autism Tissue Program (ATP) Informatics Portal [200] and those implicated in attention deficit hyperactivity disorder (ADHD) were obtained from ADHDGene [201]. A subset of 8 genes (DMRs) implicated in both ASD and ADHD were further prioritized in targeted analyses using the rat WGBS data to assess tissue-specific correlations between the number of differentially methylated CpGs within each target DMR, as well as the percentage of CpGs mapping to functional genomic regions. To calculate this percentage, CpGs across each DMR were characterized as either intragenic (falling within an intron, exon, 5'-UTR, or 3'-UTR) or intergenic. The percentage of intragenic CpGs within each DMR was then evaluated. Prior to all statistical analyses, data sets were assessed for normality using the Shapiro Wilk's test. Normally-distributed data were analyzed using parametric statistics, including analysis of variance (ANOVA) and t-tests. Data that were not normally distributed were analyzed using non-parametric tests including the Kruskal-Wallis test. *Student's t-test* was used in *post hoc* analyses of multiple comparisons when appropriate. Statistical analyses were performed using JMP Pro Version 13.0 (SAS Institute Inc.; Cary, NC, USA).

3.3 Results

3.3.1 Overlap in genomic targets of altered methylation across peripheral blood, hippocampus, and cortex elicited by developmental TSE and nicotine exposure in male rats

DNAs extracted from peripheral blood, hippocampus, and cortex tissue samples were sequenced using whole-genome bisulfite sequencing (WGBS) in order to examine epigenome-wide exposure effects in adult male rats developmentally exposed to either TSE (dosed based on nicotine levels at 0.2 mg/kg/day; low-dose), 0.2 mg/kg/day nicotine (low-dose), or 2.0 mg/kg/day nicotine (high-dose) relative to vehicle (DMSO) controls. Differentially methylated CpGs were identified in each tissue by exposure type based on thresholds for differential methylation described in methods ($\geq 50\%$ difference in methylation relative to controls). In this study, the name of the nearest gene to each differentially methylated CpG was used to designate a DMR. Within each of the three treatment groups, DMRs across peripheral blood, hippocampus, and cortex were compared to identify the number of overlapping DMRs across tissues (Figure 12A-C). Across all three tissue types, there were 1,797 DMRs in common among rats exposed to low-dose TSE (Figure 12A), 2,153 DMRs were in common in rats exposed to low-dose nicotine (Figure 12B), and 2,010 DMRs were in common in rats exposed to high-dose nicotine (Figure 12C). Common DMR lists across each treatment were then overlapped to reveal 609 DMRs common across all tissue types and treatments (Figure 12D).

3.3.2 Developmental TSE and nicotine exposure-associated DMRs correlate to common functional clusters in male rats

In order to determine functional relevance, we clustered overlapping DMRs by functional annotation clustering using the Database for Annotation, Visualization, and Integrated Discovery (DAVID)[153, 154]. DMRs corresponding to genes involved in synapse formation were the most highly enriched in each treatment group (low-dose TSE-exposed Enrichment Score (ES)=12.31, Benjamini-corrected $p=1.4e-12$ (Table 5); low-dose nicotine exposed ES=12.52, Benjamini-corrected $p=1.1e-17$, (Table 6); high-dose nicotine-exposed ES=14.46, Benjamini-corrected $p=3.5e-14$, (Table 7), and across all treatment groups (overlap across treatments ES=11.23, Benjamini-corrected $p=3.7e-14$, (Table 8).

3.3.3 Overlap in genomic targets of altered methylation associated with developmental TS exposure in rats and humans

Epigenome-scale CpG methylation was assessed in human umbilical cord blood samples using reduced representation bisulfite sequencing (RRBS). DMRs were identified in cord blood samples taken from N=13 newborn males whose mothers smoked tobacco during pregnancy and N=13 males unexposed to maternal smoking. There were 309 DMRs in common when comparing the human data to the TSE-exposed rat data (Figure 13A). When extending the analysis to include data from the rats exposed to the low and high doses of nicotine, 115 DMRs were common to rats of all three treatment groups (and all three tissue types) and to the maternal TS-exposed humans (Figure 13B). Within this overlapping group of 115 DMRs, 45 DMRs (39%) are

implicated in ASD and/or ADHD: 33 implicated in ASD, 4 implicated in ADHD, with 8 implicated in both ASD and ADHD (**Table 9**) [200, 201]. This demonstrates a highly significant over-representation of genes involved in ASD and ADHD among the identified DMRs as compared to the number of genes implicated in both disorders (Chi-squared test statistic=146.9776, $p<0.0001$) [202].

3.3.4 Developmental TSE exposure induces tissue-specific changes in the number of differentially methylated CpGs within DMRs common to rats and humans

Tissue-specific differences in the number of differentially methylated (DM) CpGs and their genomic locations were evaluated across 8 target DMRs which were functionally implicated in both ASD and ADHD (Table 9). These DMRs were prioritized based on their implicated disease relevance and enrichment in neurological functional pathways, such as synapse formation. DM CpGs were examined using WGBS data obtained from peripheral blood, hippocampal, and cortical tissues taken from adult male rats exposed developmentally to low-dose nicotine (0.2 mg/kg/day), high-dose nicotine (2.0mg/kg/day) or low-dose TSE (0.2mg/kg/day). Across all target DMRs, the number of DM CpGs was significantly higher in cortical tissue compared to blood and hippocampal tissue in rats developmentally exposed to low-dose TSE (one-way ANOVA $p=0.0008$) (Figure 14A). When stratified by target DMR, tissue-specific trends in the number of DM CpGs were similar in TSE-exposed animals, but not other treatment groups (Figure 14B). In combining treatment groups, significant differences in DM CpG count were resolved between cortical and hippocampal, but not in blood (one-way

ANOVA $p=0.0149$) (Figure 14C). CpGs across each DMR were characterized as either intragenic (falling within an intron, exon, 5'-UTR, or 3'-UTR) or intergenic. Using these characteristics, relative genomic location was assessed and represented as the percentage of intragenic CpGs within each DMR. A heat map outlining these distributions revealed an enrichment of DM CpGs within functional genomic locations of DMRs assessed in TSE-exposed hippocampal tissue (Figure 14D).

3.4 Discussion

Maternal smoking is associated with a variety of neurobehavioral disorders in exposed offspring, such as autism and ADHD [25-28, 77, 81, 87-89, 179-182]. These adverse outcomes have been further associated with exposure-induced alterations to DNA methylation during early development. However, few studies have examined whether or not these alterations occur specifically in the brain, and particularly in brain regions responsible for mediating behaviors that are impaired by gestational TS exposure. In order to better understand the epigenetic links between gestational TS exposure and adverse behavioral outcomes, as well as to improve risk detection, it is critical to identify regions of the epigenome that can be used as biomarkers and that are particularly vulnerable to developmental TS exposure in both blood and brain tissue. Here, we used genome-scale sequencing techniques (WGBS, RRBS) to identify DMRs across the epigenome of rats and humans exposed developmentally to TS (TSE) or its major toxic constituent (nicotine). In rats, we identified common DMRs between the peripheral blood, hippocampus, and cortex of adult males who had been

developmentally exposed to either low-dose TSE, low-dose nicotine, or high-dose nicotine and exhibited altered cognitive and/or behavioral function as adults [142]. Of the DMRs identified across all tissue and treatment groups in rats, 115 overlapped with those also identified in humans via RRBS of cord blood from NEST newborns. Strikingly, nearly 40% of these overlapping DMRs are strongly implicated in autism and/or ADHD. Our results are the first to identify these associations, and suggest that developmental TS-exposure across a range of exposure levels can alter DNA methylation at common regions in blood and brain tissue, which we were able to validate across species.

We additionally investigated the correlation of the frequency and relative genomic location of differentially methylated CpGs within 8 target DMRs, corresponding to those implicated in both ASD and ADHD. While we did not resolve tissue-specific differences in DMR CpG count across both low-and high-dose nicotine treated animals, CpG count was significantly higher in the DMRs within cortical tissue of animals developmentally exposed to TSE. Further, when stratified by DMR, these tissue-specific trends showed little variability among TSE-exposed animals. The percentage of DMR-associated CpGs mapping to functional genomic regions was also significantly enriched in TSE-exposed animals, particularly in the hippocampus. Together, these findings support the targeted role of TSEs in altering DNA methylation, particularly in functional genomic regions. These effects were more pronounced than either of the nicotine-treated groups, suggesting that non-nicotine constituents of TSE drive changes at the CpG level. These findings align with the behavioral studies

conducted on these animals, in which a larger magnitude of adverse behavioral outcomes were associated with developmental TSE exposure, as compared to low-and high-dose nicotine [142].

Investigating functional pathways that were associated with DMRs identified from all treatment groups and tissue types in rats revealed contrasting results. Although DMRs common to all tissue types and exposure groups in male rats were enriched with genes involved in synapse formation, the strength of these enrichments was higher in the high-dose nicotine-exposed animals compared to those exposed to low-dose nicotine and TSE. Contrary to our results on the CpG level, functional clustering revealed that nicotine is a powerful driver of associations on the gene level. Across all treatment groups combined, synapse formation pathways were again significantly enriched, although to a lesser degree. This is likely due to the fewer number of DMRs common to all three treatment groups.

Deficiencies in synapse regulation have been reported in neurobehavioral disorders like ADHD [203] and ASD, particularly via interactions between discs-large associated proteins (DLGAPs 1-4) in the post-synaptic density (PSD) [204]. Comprising large scaffolding proteins like DLGAPs, the PSD is largely responsible for resetting the synapse following synaptic excitation via glutaminergic neurotransmission [204]. In our study, DMRs associated with genes encoding both DLGAP1 and DLGAP2 were common among rats and humans exposed to maternal TS, indicating TS exposure-induced targeting of altered DNA methylation at regions associated with the PSD. Although widely associated with ASD, DLGAP1 was recently associated with ADHD-

like behavior in children, specifically via its interaction with the glutaminergic NMDA receptor [205]. Further, alterations to DNA methylation at *Dlgap2* have been reported in rats as a result of post-traumatic stress [206]. Supporting these mechanisms, genes involved in glutaminergic receptor signaling were also highly enriched among our common DMR list. *Gria2*, *Gria3*, *Grid2*, *Grik2*, *Grik4*, and *Grm8* comprise glutaminergic receptor subunits [207], and were all among our list of 115 overlapping DMRs. Apart from *Grm8*, these DMRs were further enriched for synapse formation. Of note, mutations in several of these genes are implicated in neurodevelopmental disorders like ASD and ADHD [207]. Nearly half of the DMR-associated genes implicated in both ADHD and ASD are either active in the PSD or are involved in PSD-related signaling. This is perhaps unsurprising due to the involvement of the PSD in the etiology of ASD [208] and the strong correlation between ASD and ADHD-associated behaviors [184].

Like *Dlgap2*, several of our overlapping DMRs have reported DNA methylation differences associated with developmental smoke exposure, or exposure-related diseases. DNA methylation at dipeptidyl peptidase-like 10 (*Dpp10*), another gene implicated in autism, was correlated to ADHD-like behavior in boys [209]. DNA methylation at contactin associated protein like-2 (*Cntnap2*), a gene also implicated in autism [210], was found to be differentially methylated in blood samples taken from 5 year old children exposed to developmental TS [20]. Although we found no commonalities between our identified overlapping DMRs and genes implicated in ADHD as revealed by recent large-scale human GWAS [211], this study only identified 12

ADHD-associated genes after multiple corrections for false discovery, resulting in a vast underrepresentation of the large number of genes currently implicated in ADHD [202].

Our study had several limitations. For the rat data, each N represented six pooled samples, with two independent pools sequenced for each exposure. Thus, we were not able to resolve individual-specific methylation levels in the WGBS results, limiting the depth of our analysis. We also utilized a more inclusive approach by defining DMRs by nearest gene name rather than by individual CpG location. This was done to allow for identification of commonly affected genes across species, since individual CpG sites are not always conserved. The primary objective of our study within the NICHEs Children's Center was to determine if DNA methylation explains increased risk of ADHD that has been reported with TS exposure during pregnancy. We therefore restricted our examination to male offspring in both rats and humans due to the increased prevalence of ADHD in males. Thus, our focus on males limited our ability to identify exposure-related DMRs in females.

Our study had several strengths, notably the use of comprehensive sequencing techniques to assess epigenome-wide alterations to DNA methylation across species and tissue types. By combining data obtained from WGBS in rats and RRBS in humans, we were able to identify 115 common DMRs across species and tissues that are altered by developmental exposure to TSE or nicotine. Further, due to the timing of sample collection, these common DMRs were identified in samples taken both during early life in humans (umbilical cord blood), and adulthood in rat (cortex, hippocampus, and

peripheral blood), demonstrating the likelihood of persistence of this exposure-related epigenetic patterning across the life course.

In conclusion, our results indicate that developmental exposure to the full complement of TS constituent compounds and to nicotine alone are capable of altering DNA methylation in rats and humans at shared genomic targets. Of note, these DMRs are detectable in rat brain regions that are both implicated in neurobehavioral disorders and collected from animals that displayed signs of altered behavior as a result of developmental TS exposure [142]. The fact that we also detected these same DMRs in rat blood likely indicates that the altered methylation was established during post-fertilization reprogramming and before germ layer specification, as the changes were present in both ectodermally-derived and mesodermally-derived tissues. Moreover, on the CpG level, we observed tissue-and treatment-specific associations in the frequency and genomic distribution of differentially methylated CpGs. Developmental TSE-exposure induced alterations to methylation of CpGs across tissues in a pattern that was highly conserved in all DMRs examined. Moreover, methylation at CpGs altered by TSE at target DMRs was particularly enriched in functional genomic regions. These results support the potential use of CpGs within the 8 identified DMRs as biomarkers of exposure and as tools to assess risk of neurodevelopmental disorders, at least in males. Our data further support that genes involved in the PSD are selectively targeted by developmental TSE and nicotine exposure at both low and high doses, providing additional mechanistic insights into the neuro-selectivity of TS-induced epigenetic alterations over a range of exposure levels. Due to the prevalence of developmental TS-

related neurobehavioral disorders like ASD and ADHD [183], it will be important to correlate our identified exposure-related DMRs with prevalence of these disorders in humans to establish these as biomarkers and to determine if and how these methylation changes might be ameliorated or prevented in the context of maternal tobacco smoke exposure during pregnancy.

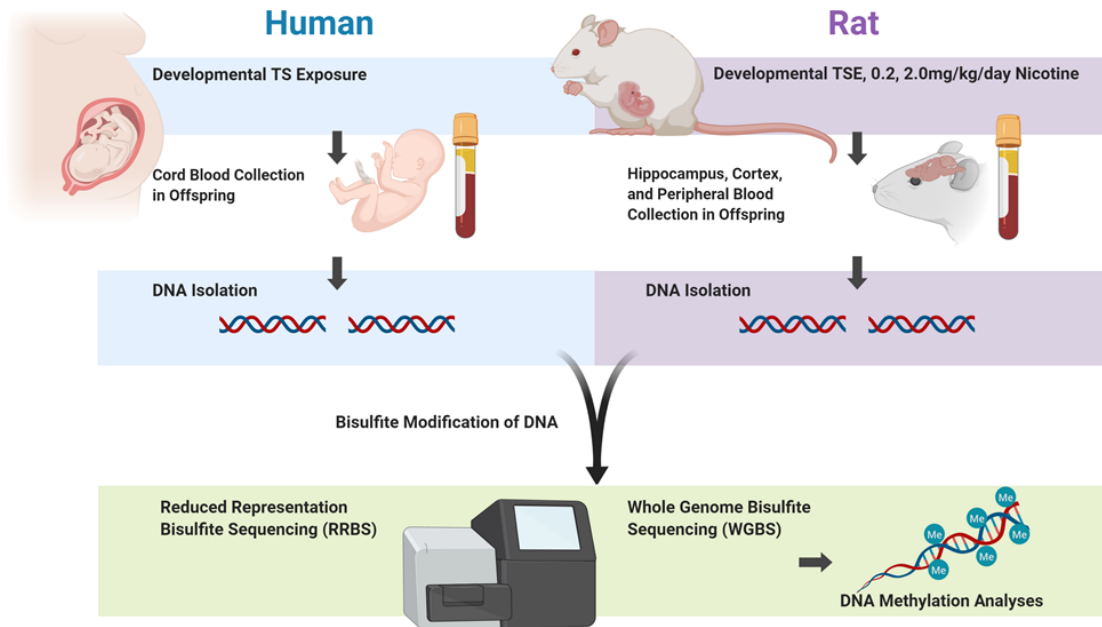


Figure 11: Schematic of tissue collection for bisulfite sequencing in humans and rats exposed *in utero* to TS or its constituents.

Umbilical cord blood was collected from 26 male NEST participants (13 TS-exposed, 13 unexposed). Peripheral blood, hippocampus, and cortex were harvested from adult male rats developmentally exposed to either low dose TSE (N=12), low-dose nicotine (N=12), or high-dose nicotine (N=12). DNA was extracted from all tissues for subsequent methylation detection analyses. Rat DNA samples were processed for whole-genome bisulfite sequencing (WGBS), and human DNA samples were processed for reduced representation bisulfite sequencing (RRBS). Image created with BioRender.

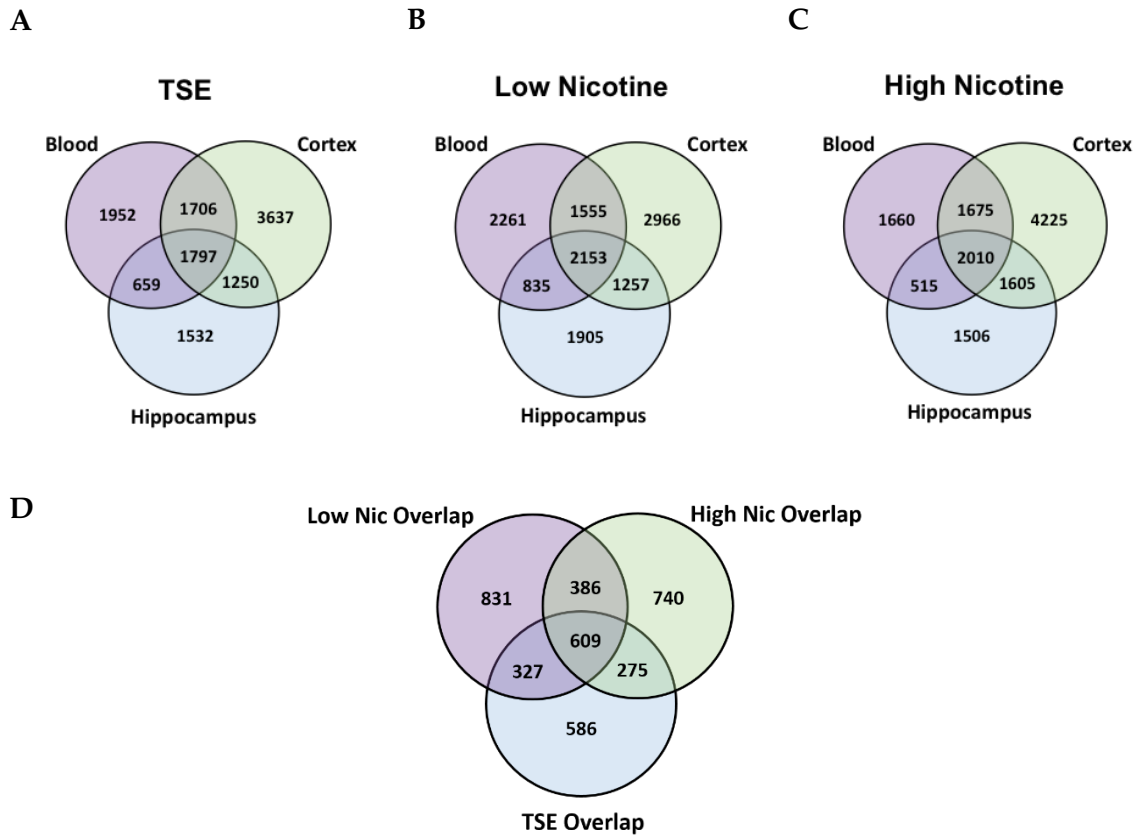


Figure 12: Overlapping DMRs identified through WGBS across peripheral blood, hippocampus, and cortical tissue in male rats developmentally exposed to TSE or nicotine.

Differential methylation across tissue types from animals developmentally exposed to A) 0.2 mg/kg/day TSE, B), 0.2 mg/kg/day nicotine, and C) 2.0 mg/kg/day nicotine was determined relative to vehicle controls (DMSO) as described in methods. D) Overlap between DMRs common to each treatment type. A-D) Nearest gene name was used to define a DMR. N= 2 (pools of 6 animals each) for each tissue type obtained from male rats developmentally exposed to: 0.2 mg/kg/day TSE, 0.2 mg/kg/day nicotine, 2.0 mg/kg/day nicotine, or vehicle control (DMSO).

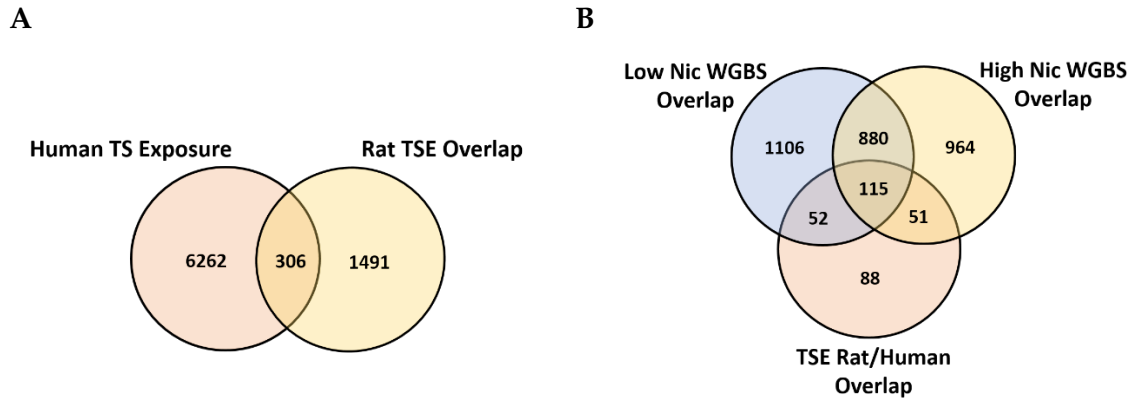


Figure 13: Overlapping DMRs identified through WGBS and RRBS in rat tissues and human umbilical cord blood.

A) Overlapping DMRs between those identified in human NEST cord blood via RRBS and those identified as common between peripheral blood, hippocampus, and cortex in adult male rats developmentally exposed to low-dose TSE. B) Overlapping DMRs across two developmental treatment groups in rats (low-dose nicotine, and high-dose nicotine) and the 306 DMRs common to TS-exposed rats and humans, as defined in A. A-B) Nearest gene name was used to define a DMR. Differential methylation was defined as described in methods. Rat: N= 2 (pools of 6 animals each) for each tissue type obtained from male rats developmentally exposed to: 0.2 mg/kg/day TSE, 0.2 mg/kg/day nicotine, 2.0 mg/kg/day nicotine, or vehicle control (DMSO). Human: N=13 TS-exposed males, N=13 unexposed males.

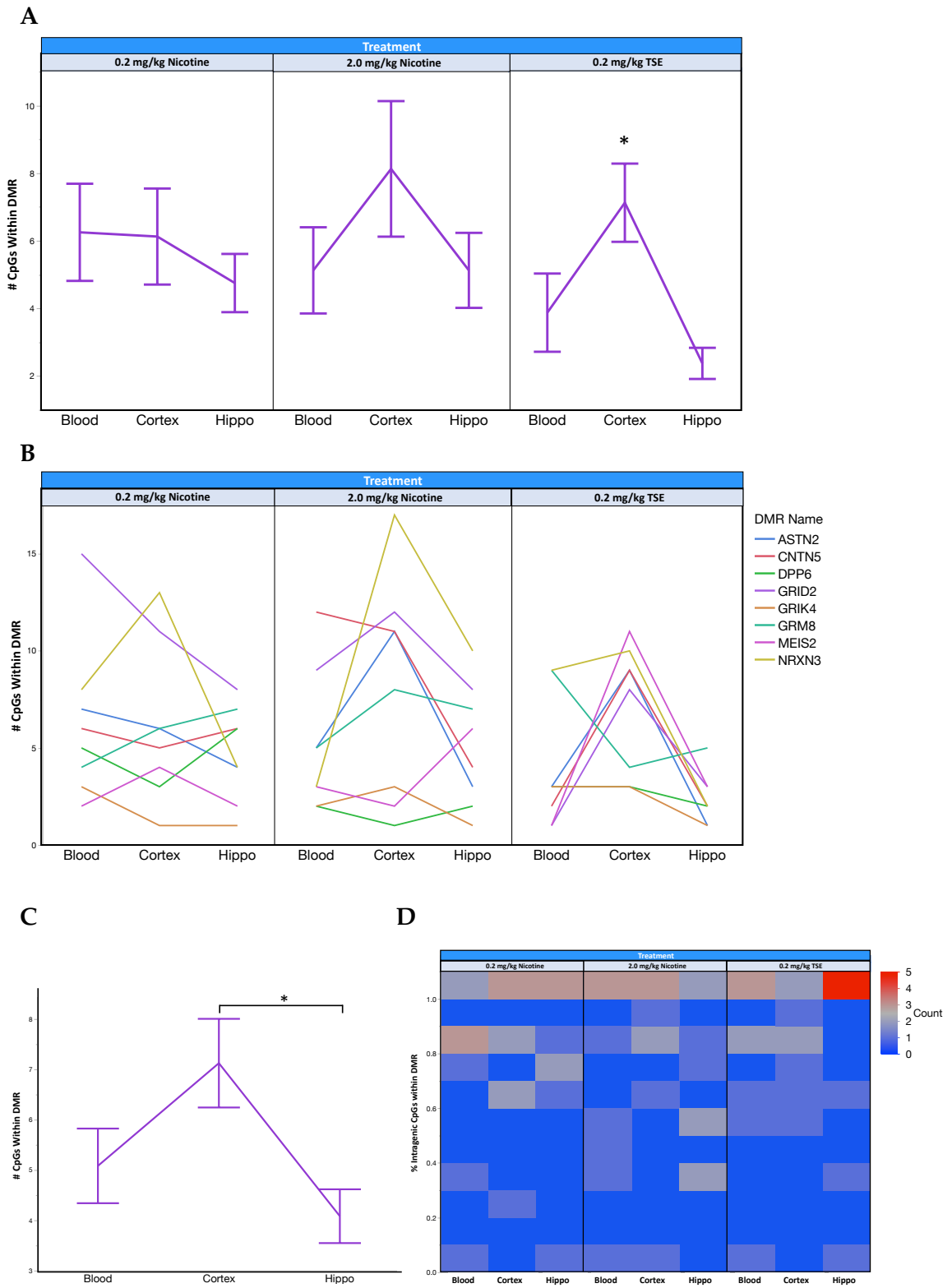


Figure 14: Frequency and Relative Genomic Location of CpGs within Target DMRs.

Number of differentially methylated (DM) CpGs from 8 target DMRs across peripheral blood, hippocampal, and cortical tissues taken from adult male rats developmentally exposed to low-dose nicotine (0.2 mg/kg/day), high-dose nicotine (2.0mg/kg/day) and low-dose TSE (0.2mg/kg/day) A) across all target DMRs, B) with individual target DMRs indicated, and C) across all target DMRs and treatment types. A) Across all target DMRs, the number of DM CpGs was significantly higher in cortical tissue compared to blood and hippocampal tissue in rats developmentally exposed to low-dose TSE (one-way ANOVA $p=0.0008$). C) Across all treatment groups and target DMRs, the number of DM CpGs were higher in cortical tissue compared to hippocampal tissue, but not blood (one-way ANOVA $p=0.0149$). D) Heat map representing the distribution of differentially methylated CpGs across functional genomic regions. CpGs across each DMR were characterized as either intragenic (falling within an intron, exon, 5'-UTR, or 3'-UTR) or intergenic. Genomic location was represented as the percentage of intragenic CpGs within each DMR. A) Rat: N= 2 (pools of 6 animals each) for each tissue type obtained from male rats developmentally exposed to: 0.2 mg/kg/day TSE, 0.2 mg/kg/day nicotine, 2.0 mg/kg/day nicotine, or vehicle control (DMSO). A-C) $*P < 0.05$, Student's *t*-test post hoc analysis for multiple comparisons following significant one-way ANOVA. Error bars represent standard error of the mean.

Table 5: DAVID Functional Annotation Clustering of DMRs Common to Peripheral Blood, Hippocampus, and Cortex of Male Rats Developmentally Exposed to 0.2 mg/kg/day TSE.

Functional Annotation Term	Cluster Enrichment Score	Gene Count	P-Value	Benjamini-adjusted P-value
Synapse	12.31	56	1.3 e -14	1.4 e -12
Postsynaptic membrane	12.31	44	4.8 e -14	6.7 e -12
Cell junction	12.31	70	9.7 e -13	7.9 e -11
Cell junction	12.31	64	2.2 e -12	1.8 e -10
Postsynaptic cell membrane	12.31	34	2.2 e -11	1.4 e -9

Data obtained from DAVID Functional Annotation Tool (DAVID Bioinformatics Resources 6.7, NIAID/NIH) [153, 154].

Table 6: DAVID Functional Annotation Clustering of DMRs Common to Peripheral Blood, Hippocampus, and Cortex of Male Rats Developmentally Exposed to 0.2 mg/kg/day Nicotine.

Functional Annotation Term	Cluster Enrichment Score	Gene Count	P-Value	Benjamini-adjusted P-value
Synapse	12.52	71	3.2 e -20	1.1 e -17
Cell junction	12.52	90	1.5 e -18	2.5 e -16
Postsynaptic membrane	12.52	48	4.6 e -14	7.0 e -12
Cell junction	12.52	73	2.4 e -13	2.9 e -11
Postsynaptic cell membrane	12.52	39	1.4 e -12	9.6 e -11
Ligand-gated ion channel	12.52	20	1.5 e -7	5.6 e -6
Neuroactive ligand-receptor interaction	12.52	43	1.9 e -6	7.2 e -5

Data obtained from DAVID Functional Annotation Tool (DAVID Bioinformatics Resources 6.7, NIAID/NIH) [153, 154].

Table 7: DAVID Functional Annotation Clustering of DMRs Common to Peripheral Blood, Hippocampus, and Cortex of Male Rats Developmentally Exposed to 2.0 mg/kg/day Nicotine.

Functional Annotation Term	Cluster Enrichment Score	Gene Count	P-Value	Benjamini-adjusted P-value
Synapse	14.46	63	6.6 e -17	3.5 e -14
Cell junction	14.46	82	3.2 e -16	5.3 e -14
Postsynaptic membrane	14.46	49	4.4 e -16	8.2 e -14
Postsynaptic cell membrane	14.46	39	1.4 e -13	9.2 e -12
Cell junction	14.46	69	3.6 e -13	4.0 e -11

Data obtained from DAVID Functional Annotation Tool (DAVID Bioinformatics Resources 6.7, NIAID/NIH) [153, 154].

Table 8: DAVID Functional Annotation Clustering of DMRs Common Across Blood, Hippocampus, and Cortex of Rats Developmentally Exposed to 0.2 mg/kg/day Nicotine, 2.0 mg/kg/day Nicotine, and 0.2 mg/kg/day TSE.

Functional Annotation Term	Cluster Enrichment Score	Gene Count	P-Value	Benjamini-adjusted P-value
Synapse	11.23	35	8.9 e -17	3.7 e -14
Cell junction	11.23	39	1.5 e -13	1.8 e -11
Synapse	11.23	31	2.0 e -13	1.6 e -11
Postsynaptic membrane	11.23	25	1.2 e -12	1.0 e -10
Cell junction	11.23	33	4.3 e -11	2.0 e -9
Postsynaptic cell membrane	11.23	20	1.2 e -10	5.6 e -9
Neuroactive ligand-receptor interaction	11.23	19	1.5 e -5	6.4 e -4

Data obtained from DAVID Functional Annotation Tool (DAVID Bioinformatics Resources 6.7, NIAID/NIH) [153, 154].

Table 9: 115 DMRs Common to Rats and Humans Developmentally Exposed to TSE or Components of TS, Stratified by Neurodevelopmental Disorder Implication.

	DMRs Implicated in ASD^a	DMRs Implicated in ADHD^b	Other DMRs
Gene Name	<i>ASTN2, CADPS2, CAMTA1, CHD7, CNTN5, CNTNAP2, CTNND2, DIAPH3, DLGAP1, DLGAP2, DMD, DPP6, DPP10, EPHA6, FER, GABBR2, GABRG3, GRID2, GRIK2, GRIK4, GRM8, KCNMA1, MDGA2, MEIS2, NELL1, NFIA, NFIB, NRG1, NTRK3, NRXN3, NUAK1, PCDH9, PRICKLE2, PSD3, PTPRT, RBFOX1, RELN, RIT2, ROBO2, SATB2, WWOX</i>	<i>ASTN2, CCSER1, CNTN5, DPP6, GRID2, GRIK4, GRM8, MAGI2, MEIS2, NRXN3, NTM, SORCS1,</i>	<i>ADAMTSL1, ALK, BACH2, BCOR, CALN1, CDH6, COBL, DACH1, DCC, DGKI, DNMT3, DOCK3, DOK5, ERC2, ESRRG, FAT3, FGF13, FMN1, FREM2, FRY, FSTL4, FSTL5, GRIA2, GRIA3, GULP1, HACE1, ITGA8, KALRN, KCNH5, KLHL29, LRRTM4, MAF, MAGEB16, MYO10, NCAM2, NEB, NEK10, OPCML, OXR1, PARD3, PBX3, PCDH17, PDZRN4, PHACTR3, PIEZO2, PLXNA2, PREP, PTPN14, PTPRD, PTPRM, RBPJ, RPS29, RSU1, RYR2, SAMD12, SATB1, SCAPER, SHISA6, SLIT2, SNTG1, SOX6, STIM2, TENM3, TIAM1, TMEFF2, TRPM3, U1, U3, WBSR17, ZMAT4</i>

^aData obtained from the Autism Tissue Program (ATP) Informatics Portal [200].

^bData obtained from ADHDGene [201].

Bolded genes are implicated in both ASD and ADHD [200, 201].

4. Maternal tobacco smoke is associated with increased DNA methylation at human metastable epialleles in infant cord blood

4.1 Introduction

Metastable epialleles (MEs) were first identified in mammals in 2002 as regions of the genome that are expressed variably in genetically identical individuals as a result of epigenetic modifications, particularly DNA methylation [64]. Methylation is stochastically established at these loci during development. The term “epiallele” refers to an allele that can exist in a number of epigenetic states. “Metastable” refers to the variable establishment of epigenetic marks, like DNA methylation, at epialleles during early development, before the specification of the germ layers [64]. Once established, the methylation level at MEs is somatically heritable and stable across the life course. As such, ME methylation patterns are consistent in all tissue types derived from the mesoderm, endoderm, and ectoderm. However, due to the randomly determined nature of the initial methylation establishment, MEs are also characterized by strong interindividual variation [62, 64-67].

The developmental window during which methylation levels at mammalian MEs are established is particularly vulnerable to environmental stressors [62, 63, 65-67, 212, 213]. Recently, multiple MEs were identified in humans [65] and found to exhibit methylation patterns that were associated with nutritional challenges faced by the

mother during the periconceptual period [65, 67], in agreement with prior rodent studies [62, 66]. However, little is known about the vulnerability of human MEs to non-nutritional exposures, including the impact of tobacco smoke (TS) exposure during pregnancy.

In addition to the adverse behavioral outcomes associated with developmental TS exposure elaborated upon previously in Chapter 1, and their respective associations with alterations in DNA methylation as elaborated upon in Chapters 1 and 2, maternal smoking has also been associated with altered levels of various micronutrients that are essential for healthy fetal development [214-216]. Folate, vitamins B12 and B6 are necessary components of the one-carbon metabolism pathway that generates methyl groups used for DNA methylation and other cellular methylation reactions. Maternal serum levels of these and other micronutrients, such as vitamin D, are lower in pregnant smokers [214-216]. While substantial evidence exists supporting the interaction between maternal micronutrient levels and fetal DNA methylation patterns [217], little is known about how smoking-related alterations in micronutrient levels impact DNA methylation at MEs.

Here, we leveraged multiple human tissue sources to validate putative human MEs and examine ME DNA methylation within the context of TS exposure [65, 67]. Using male and female conceptual tissues derived from mesoderm, endoderm, and ectoderm, we validated ME status for three previously identified human MEs and

examined tissue-specific functional relationships between ME DNA methylation and gene expression during early fetal development. We then used paired maternal blood and infant cord blood from Newborn Epigenetic Study (NEST) participants to examine the impact of developmental TS exposure on the establishment of DNA methylation at human MEs. Given the negative association between TS exposure and micronutrient levels, we further investigated potential associations between developmental TS exposure, maternal micronutrient levels, and DNA methylation at the putative human MEs: bola family member 3 (*BOLA3*), paired box 8 (*PAX8*) and zinc finger FYVE-type containing 28 (*ZFYVE28*).

4.2 Materials and Methods

4.2.1 Study Specimens: Human Conceptual Tissues

Human brain, liver, and kidney conceptual tissues (six male, six female) were obtained between the years of 1999 and 2010 from the NIH-supported Laboratory of Developmental Biology at the University of Washington and used under a protocol approved by the Duke University Institutional Review Board (Pro00014066). Tissue specimens were stored at -80°C until required for DNA and RNA extraction.

4.2.2 Study Population: NEST

Pregnant women were recruited from central North Carolina for the Newborn Epigenetics Study (NEST) from prenatal clinics at Duke University Hospital and

Durham Regional Hospital obstetrics facilities between 2005 and 2011. All participants spoke English and/or Spanish and were at least 18 years of age. Women completed a questionnaire in English or Spanish at the time of recruitment, which assessed sociodemographic characteristics including age, race, marital status, level of education, as well as self-reported cigarette smoking and/or exposure to tobacco smoke. There were 2,640 women who participated in the study. For our current analyses, a subset of 90 participants were randomly chosen based on maternal plasma cotinine levels measured during gestation (described below) to achieve a roughly equal distribution of smokers (N=48) and nonsmokers (N=42). Of these 90, five had a BMI indicative of being underweight (<18.5). Because our small sample size in this category did not give us the ability to control for potential confounding by underweight status, these samples were excluded from the final analyses, giving a final sample size of 85. NEST study protocols were approved by the Duke University Institutional Review Board (Pro00014548). All enrolled women provided written informed consent for themselves and their child prior to participation in any study activities.

4.2.2.1 Maternal Plasma Cotinine Measurement

Veinous maternal blood was collected in EDTA-containing lavender top vacutainer tubes from NEST participants during pregnancy (mean gestational age of sampling in 85 samples examined=120 days). Blood samples were then separated by centrifugation into RBCs, plasma, and buffy coat as previously described [10]. Blood

fractions were then aliquoted and stored at -80C until analysis for cotinine levels. Cotinine (ng/mL plasma) was measured by Dr. JunFeng Zhang's Laboratory at Duke University via methods previously described [196] using high-performance liquid chromatography with tandem mass spectrometry (HPLC-MS-MS). The limit of detection was 0.05 ng/mL, with reproducibility greater than 94%. Based on measured cotinine levels, participants were dichotomized into two exposure categories, congruent with previous NEST studies [196] and studies examining passive smoke exposure during pregnancy [197, 198]: 1) "no exposure", or women with plasma cotinine levels below 1ng/mL; and 2) "active smoking", or women with plasma cotinine levels greater than 3ng/mL.

4.2.2.2 Maternal Whole Blood Micronutrient Measurement

Red-blood cell (RBC) folate levels were estimated from maternal whole blood samples collected at the time of enrolment into the study using a commercial kit, with concentrations accounting for hematocrit levels, as previously described [10]. Maternal plasma vitamin B12 levels were measured using a commercially-available immunoassay, as previously described [218]. Plasma vitamins B6 pyridoxal 5'-phosphate (PLP) and pyridoxic acid (PA), as well as homocysteine levels were measured using high performance liquid chromatography (HPLC) techniques, as previously described [218]. Plasma 25-hydroxyvitamin D [25(OH)D] levels were also measured using a commercially available immunoassay, as previously described [219].

4.2.2.3 Umbilical Cord Blood Collection

Venous umbilical cord blood samples were collected at the time of birth for NEST participants. Samples collected into EDTA-containing lavender top vacutainer tubes were then separated by centrifugation into RBCs, plasma and buffy coat as previously described [10]. Cord blood fractions were aliquoted and stored at -80C until further processed for DNA extraction.

4.2.2.4 Umbilical Cord Fractionation

Polymorphonuclear cells (PMNs) and peripheral blood mononuclear cells (PBMCs) were fractionated from newborn umbilical cord blood as previously described [70]. In brief, specimens were fractionated using Lympholyte®-poly (Cedarlane Laboratories Limited, Burlington, NC, USA) to separate and collect the PMN and PBMC fractions. Fraction purity was assessed following Giemsa staining.

4.2.3 DNA/RNA Isolation and Bisulfite Modification

Both genomic DNA and total RNA were extracted from conceptual tissue samples using the Qiagen AllPrep DNA/RNA Mini Kit (Qiagen). Genomic DNA was extracted from the buffy coat of infant cord blood samples and PMN/PBMC fractions using the Qiagen QIAamp DNA Mini kit (Qiagen; Valencia, CA). DNA and RNA samples were eluted in nuclease-free water and nucleic acid concentration and purity were assessed using a NanoDrop 2000 Spectrophotometer (Thermo Fisher Scientific; Waltham, MA). Genomic DNA (800ng) was modified by bisulfite treatment for subsequent DNA

methylation analysis using the Zymo EZ DNA Methylation Kit (Zymo Research, Inc.; Irvine, CA) and eluted in 40 μ L nuclease-free water for a final concentration of 20 ng/ μ L bisulfite-treated DNA, assuming complete conversion.

4.2.4 DNA Methylation Analyses

Bisulfite pyrosequencing was used to analyze CpG methylation as previously described [18] for the following MEs: *BOLA3*, *PAX8*, *SLITRK1*, and *ZFYVE28* using primers and PCR protocols of previously published assays for these loci [65]. Primers were ordered from Sigma Aldrich (Sant Louis, MO; Table S1). All pyrosequencing assays were performed using a Qiagen PyroMark Q96 MD Pyrosequencer and validated for quantitative performance using methylation standards (Qiagen EpiTect Control DNA Set, Human Cat No. 59568) of defined proportions (0%, 25%, 50%, 75%, and 100% methylated). These defined standards were used to validate the linearity and range of the ME assays (Figure 15). Average methylation was calculated across all CpGs within each ME region analyzed using PyroQ CpG Software (Qiagen) and these averages were used as the unit of measurement, consistent with prior reports [65]. Each pyrosequencing assay contained 7 μ L PCR product generated using the following conditions for *BOLA3*, *PAX8*, *SLITRK1*, and *ZFYVE28*: 95°C for 15m, then 55 cycles of 94°C for 30s, [assay-specific] annealing temperature for 30s, 72°C for 30s, followed by 72°C for 10m. Annealing temperatures were as follows: *BOLA3*, 64°C; *PAX8*, 67°C; *SLITRK1*, 61°C; *ZFYVE28*, 59°C (Table 10).

4.2.5 Gene Expression Analyses

PAX8 transcript levels were measured in conceptual brain, liver, and kidney tissues via TaqMan Reverse Transcription Real-Time PCR using the Applied Biosystems QuantStudio 6 Flex Real-Time PCR System (Thermo Fisher Scientific). One-step cDNA synthesis was performed using the qScript XLT One-Step RT-qPCR Kit from Quanta BioSciences (Beverly, MA) and the following thermal cycler conditions: 50°C for 10m, 95°C for 1m. Real-time PCR cycling immediately followed using the following thermal cycler conditions: 40 cycles of 95°C for 10s, then 60°C for 60s. TaqMan assays used were as follows: *PAX8*: Hs00247586_m1, *B2M*: Hs00187842_m1 (Thermo Fisher Scientific). *PAX8* transcript levels were calculated as difference in cycle threshold (Ct) values relative to beta-2 microglobulin (*B2M*). *PAX8* transcript levels were correlated to DNA methylation levels for each sample using Spearman's Correlation.

4.2.6 Statistics

Preliminary analyses examining the distributions of all outcomes indicated that many outcomes were not normally distributed, so we used non-parametric statistical models to assess associations where appropriate. We first examined associations between sociodemographic variables and maternal nutrient levels, smoking status, and ME methylation using Spearman's correlation analyses, linear regression models, and chi-squared tests. Maternal sociodemographic variables examined included: race, education, preconceptional BMI, and age and were categorized as listed in Table 10. We

examined the effects of smoking exposure on individual ME methylation status using generalized linear models, accounting for potential confounding by sociodemographic characteristics and maternal nutrition. We next looked at methylation across all MEs using a mixed modeling approach [65]. In this model, ME name and individual were run as random effects. Maternal sociodemographic factors and micronutrient levels were considered as possible confounding variables in regression analyses; although none of the confounders under consideration were associated with both exposure (TS) and ME methylation in bivariate analyses, we conducted multivariate analyses using a backwards covariate selection approach and retained covariates that were significantly associated with ME methylation in adjusted models. All statistical analyses were performed using JMP Pro Version 13.0.

4.3 Results

4.3.1 Validation of metastable epialleles at BOLA3, PAX8, and ZFYVE28

Upon successful validation of metastable epiallele (ME) pyrosequencing assays previously published [65] (Figure 15, Table 10), we confirmed ME status for *BOLA3*, *PAX8*, and *ZFYVE28* in human conceptual brain, liver, and kidney tissues (Figure 16). We found significant within-individual inter-tissue correlation ($p < 0.02$) for all three MEs examined except at *ZFYVE28* in brain tissue. However, due to the high correlation between *ZFYVE28* CpG methylation in liver and kidney tissues, strong interindividual

variation, and congruence with previous determinations for comprising an ME [65], our data support that *ZFYVE28* comprises an ME. We also examined *SLITRK1*, another putative human ME [65], for ME status and were able to demonstrate strong inter-tissue correlation but rather minimal inter-individual variation (range ~3%, Figures 172A-B). While methylation at *SLITRK1* was highly correlated in liver versus brain comparisons, correlations were weaker for kidney versus liver and kidney versus brain, with one outlying data point driving the associations. Further, examination of *SLITRK1* ME methylation in cord blood showed overall very low levels of methylation with little inter-individual variation (Figure 17C), altogether inconsistent with ME status for *SLITRK1*.

4.3.2 NEST maternal demographics and smoking status

The maternal sociodemographic breakdown of NEST women in our study sample is outlined in Table 11, and additional gestational characteristics are described in Table 12. Samples examined were derived from predominantly black (56%) or white (41%) mothers with a wide distribution of education levels, preconceptional BMIs, and ages (Table 11). Offspring were 40% male and 60% female (Table 12). Maternal plasma was collected during pregnancy at a mean gestational age of 119.6 \pm 8.7 days (SEM; Table 12). Mean plasma cotinine across all women was 55.9 \pm 8.5 ng/mL (SEM). Among women defined as “unexposed,” (N=38), gestational mean plasma cotinine was 0.17 \pm 0.04 ng/mL, and for “exposed,” (N=47), 100.9 \pm 11.7 ng/mL. The distribution of cotinine

values within the subset of samples examined (N=85) was highly correlated to that of the samples within the entire cohort for which cotinine values were measured (N=855) ($R_s=0.36$, $p=0.0007$) (Table 13).

Maternal education, commonly used as a proxy for socioeconomic status (SES), was strongly associated with maternal smoking status ($p<0.0001$, two-sided Chi-square test, Table 11). Maternal smoking status was also significantly associated with lower infant birth weight ($p=0.0053$, Table 14), congruent with previous findings [18].

4.3.3 Maternal micronutrient levels, smoking status, and sociodemographic variables

Micronutrient measurements were available for 41 to 44 of the N=85 samples examined. Mean plasma micronutrient levels were as follows: RBC folate, 218.6 \pm 11.9 μ g/L; vitamin B6 pyridoxal 5'-phosphate 9.6 \pm 1.2 nmol/L; vitamin B6 pyridoxic acid, 6.0 \pm 1.1 nmol/L; vitamin B12, 524.1 \pm 36.9 ng/L; 25(OH)D, 16.13 \pm 0.9 ng/mL; and homocysteine, 0.8 \pm 0.03 μ g/mL. Smoking exposure was significantly associated with reduced levels of RBC folate ($p=0.02$), plasma vitamin B6 pyridoxal 5'-phosphate ($p=0.05$), and plasma vitamin B12 ($p=0.007$, Table 15), as expected based on previous studies [215, 216]. Correspondingly, smoking exposure was also associated with increased plasma homocysteine levels ($p=0.02$, Table 15), a common indicator of low B vitamin levels, including folate [3].

The micronutrients folate, vitamins B6, and B12 are critical for generation of methyl groups for DNA methylation and normal embryonic and fetal development [3,

217, 218, 220], and all are recommended to be taken as dietary supplements before and during pregnancy [220]. The Institute of Medicine (IoM) has defined RBC folate deficiency as levels less than 140 µg/L, and plasma or serum vitamin B12 deficiency as levels less than 200 ng/L [221]. Vitamin B6 pyridoxal 5'-phosphate (PLP), the most commonly measured vitamin B6 derivative and indicator of B6 status, is considered deficient in the plasma at levels less than 20 nmol/L [220], and vitamin D 25(OH)D is considered deficient in the plasma at levels less than 20 ng/mL [222]. Using these deficiency thresholds, we found 2.27% of pregnant women examined to be vitamin B12 deficient, 13.95% to be folate deficient, 76.74% to be vitamin D deficient, and a staggering 90.91% to be PLP deficient. Smoking exposure was significantly associated with PLP deficiency ($p=0.015$, two-sided Chi-square test of micronutrient deficiency status vs. smoking exposure status), and less so with RBC folate or vitamin D deficiencies ($p=0.06$ and $p=0.12$, respectively).

Upon examination of relationships between sociodemographic covariates and micronutrient levels independent of smoking status, education (SES) most strongly associated with micronutrient levels (Table 16). Mothers who received less than a college education had significantly lower total folate ($p=0.03$), vitamin B6 pyridoxal phosphate ($p=0.0002$), and vitamin B6 pyridoxic acid ($p=0.003$) compared to those with at least some college education, as well as higher homocysteine ($p=0.01$), an indicator of reduced vitamin B levels (Table 16). Mothers with a pre-pregnancy BMI indicative of overweight

or obesity status (>25) had significantly less plasma vitamin B6 pyridoxal phosphate (p=0.04) and vitamin B12 (p=0.003, Table 17) than those with a normal BMI (18.5-25). Further, mothers who identified as nonwhite had significantly lower vitamin D levels (p=0.0036) than those who identified as white (Table 18). Racial disparities in maternal vitamin D levels have previously been reported [223-225] and associated with lower birth weight [224]. Finally, vitamin B12 levels significantly differed by maternal age, with mothers over the age of 30 years having higher vitamin B12 levels than younger mothers (p=0.03, Table 19).

4.3.4 Maternal tobacco smoke exposure is associated with increased infant ME DNA methylation

To address the possibility that there might be differences in DNA methylation at the metastable epialleles in the major leucocyte blood cell fractions found in umbilical cord blood, [226], we evaluated variability in CpG methylation at BOLA3, PAX8, and ZFYVE28 in the two major leukocyte fractions, polymorphonuclear cells (PMNs: basophils, neutrophils, and eosinophils) and peripheral blood mononuclear cells (PBMCs: monocytes and lymphocytes) using the validated ME pyrosequencing assays. CpG methylation was highly correlated across cord blood PMN and PBMC fractions for all three MEs (BOLA3 RS=0.91, p<0.001; PAX8, RS=0.93, p<0.001; and ZFYVE28, RS=0.97, p<0.001; Figure 18A-B). These strong correlations not only further support the ME status of BOLA3, PAX8, and ZFYVE28, but also justify examination of ME DNA methylation in mixed leukocyte populations in unfractionated umbilical cord blood.

In order to determine if there is a relationship between maternal smoking and infant ME DNA methylation, we measured ME methylation in DNA isolated from NEST infant cord blood buffy coat. DNA methylation was significantly increased in the exposed compared to unexposed group for the *PAX8* ME ($p=0.04$, Figure 18D-E). Using a mixed regression model, we found a significant overall effect of smoking exposure on DNA methylation across all three MEs ($p=0.04$, Figure 18D-E). Exposure was related to an average 2.4% increase in methylation across all three MEs (95% CI: 0.14% to 4.64% methylation).

4.3.5 *PAX8* and *BOLA3* methylation are negatively associated with maternal micronutrient levels

Due to the divergent associations observed between maternal smoking status versus plasma micronutrient levels and ME DNA methylation, we investigated potential relationships between maternal micronutrient levels and cord blood ME DNA methylation in the 85 NEST samples examined. We observed trending negative associations between maternal micronutrient levels and ME DNA methylation at *PAX8* for folate (*PAX8* % ME methylation versus total folate: $R_s=-0.25$, $p=0.10$) and at *BOLA3* for vitamin D (*BOLA3* % ME methylation versus vitamin D: $R_s=-0.36$, $p=0.02$; Table 20). In contrast to prior reports for ME methylation and nutritional availability [65, 67], our findings indicate that maternal smoking-associated hypermethylation at MEs is established despite methyl-donor micronutrient availability.

4.3.6 PAX8 mRNA levels are negatively associated with DNA methylation

Due to the significant effect of smoking exposure on DNA methylation at *PAX8*, we sought to determine if there was a potential functional relationship between *PAX8* ME DNA methylation and *PAX8* gene expression. Using reverse-transcription real-time PCR of total RNA derived from conceptual brain, liver, and kidney tissues and normalized for RNA input, we found significantly higher levels of *PAX8* mRNA transcripts in the kidney relative to liver tissue ($p < 0.0001$, Figure 19A). Due to the increased expression in kidney, we next evaluated a potential functional relationship between *PAX8* mRNA content and ME DNA methylation in conceptual kidney tissues. Normalized *PAX8* mRNA levels were negatively associated with *PAX8* ME DNA methylation in kidney, however this association was not statistically significant (Figure 19B). Using the slope of the correlation curve and assuming complete doubling in each PCR cycle, we found that, on average, a 21.4% change in *PAX8* ME methylation in the kidney corresponded to a halving or doubling of *PAX8* mRNA content ($p = 0.0767$, Figure 19C). These data support that the normal distribution of *PAX8* ME methylation is associated with a fourfold range of *PAX8* expression, and that the random establishment of methylation at this locus naturally produces wide, inherent variation between individuals in the expression of this functionally important gene.

4.4 Discussion

The periconceptual establishment of DNA methylation at human MEs can be vulnerable to environmental factors. Because DNA methylation at MEs is highly correlated across all tissue types, perturbations to their establishment can result in somatic-wide effects. While environmental influences, like the preconceptional availability of nutrients, have been shown to alter DNA methylation at MEs [65, 67], little is known about their vulnerability to *in utero* exposures like tobacco smoke (TS). Our data indicates that nearly 21% of women of childbearing age smoke while pregnant in Central North Carolina, and around 15% of pregnant women are exposed to second-hand smoke (SHS) (Table 13) [196]. Compared to nation-wide estimates based on self-report, smoking during pregnancy is nearly three times more common in our study sample [227]. Given the prevalence of maternal smoking (Table 13) as well as known associations between developmental TS exposure and alterations in infant cord blood DNA methylation [14, 17, 18, 23, 29], we examined relationships between developmental TS exposure and DNA methylation at human MEs. Because maternal smoking is also associated with decreased micronutrient levels [215, 216], particularly those that function in the generation of methyl group donors, we further examined the potential effects of smoking-related maternal micronutrient reductions on methylation at infant MEs. This is the first study to demonstrate the vulnerability of DNA methylation

establishment at human MEs to developmental TS exposure within the context of TS exposure-related maternal micronutrient reductions.

Here, we leveraged multiple human tissue sources to validate three previously-identified putative human MEs (*BOLA3*, *PAX8*, and *ZFYVE28*) and examined ME DNA methylation within the context of TS exposure [65, 67]. Access to human conceptual tissues allowed for examination of ME DNA methylation in mesodermal-, endodermal-, and ectodermally-derived prenatal tissues without the potential confounds of *ex utero* exposures. In these tissues, we observed similar ranges of ME DNA methylation as has been reported in previous adult human ME studies [65, 67], corroborating the notion that the early establishment of DNA methylation at MEs leads to methylation levels that are stable throughout germ layer specification, tissue differentiation, and during subsequent somatic cell division throughout the life course. These tissues additionally enabled us to examine the tissue-specific, functional roles of ME DNA methylation during fetal development.

Availability of the NEST samples enabled us to examine infant ME methylation in the context of matched maternal micronutrient levels, as well as sociodemographic variables like race, maternal education level, and pre-pregnancy BMI. From these data sets, we examined the potential confounding effects of sociodemographic variables and micronutrient levels on infant cord blood ME DNA methylation. For example, methylation at *PAX8* was significantly associated with maternal age and vitamin D

levels, underscoring the importance of collectively examining these covariates in human DNA methylation studies (Figure 18D-E).

Among the sociodemographic variables analyzed, education level, an indicator of socioeconomic status (SES), was most strongly associated with maternal smoke exposure status as has been previously shown [18, 196] (Table 11). Upon cross-examination of sociodemographic variables and maternal micronutrient levels independent of exposure status, education level was again most strongly associated with decreased micronutrient levels, significantly impacting three of the five micronutrient levels examined. Correspondingly, education level was significantly associated with increased homocysteine levels (Table 16). Within the context of our study, these findings position SES as the most impactful sociodemographic confounder within the context of smoking and maternal micronutrient levels.

After adjusting for potential confounding by sociodemographic factors, maternal TS exposure status was significantly correlated with reduced gestational levels of RBC folate (consistent with previous findings [196]), vitamin B6 pyridoxal 5'-phosphate, and vitamin B12, as well as increased levels of homocysteine, an indicator of low vitamin B and total folate levels (Table 15). All of these micronutrients are involved in one-carbon metabolism, a metabolic pathway that generates substrates used for methylation reactions in the cell, including DNA methylation [3]. Methyl group-generating micronutrients are essential for normal development [3, 217, 218, 220] and the

prevention of neurodevelopmental abnormalities like neural tube defects. As such, women of childbearing age are strongly recommended to fortify their diets with adequate levels of vitamins B6, B12, and folate when planning pregnancy and throughout gestation. Despite these efforts, many women of childbearing age do not receive adequate levels of methyl-donor micronutrients through their diet alone [220]. Therefore, in 1998 the US Food and Drug Administration required the fortification of enriched grain products with folic acid to help ensure adequate levels in the event a woman becomes pregnant. This requirement was put in effect in part due to nearly half of all pregnancies, at least in the US, being unplanned [220]. In addition, the post-fertilization period of epigenetic reprogramming requires an adequate supply of methyl groups to support the remethylation of the genome in the embryo. This reprogramming occurs well before most women suspect they may be pregnant. Micronutrient dilution during pregnancy-related blood volume gain exacerbates this deficit.

Based on the IOM's defined thresholds for micronutrient sufficiency, more than three quarters of women examined in our study were deficient for both vitamin D and PLP. Vitamin D deficiencies during pregnancy have been associated with miscarriage, preeclampsia, and stunted fetal growth [219, 223, 224, 228]. Although PLP deficiency is considered rare due to the nearly ubiquitous presence of B6-rich foods, deficiency is higher among obese and pregnant individuals [229]. As the majority of pregnant women examined were obese (61.73%), the widespread PLP deficiency (90.9%) we observed is

perhaps unsurprising. In line with previous findings [230], PLP deficiency was significantly associated with smoking status ($p=0.0148$), with lower plasma PLP levels in mothers exposed to TS. Vitamin B6 is critical to neurotransmitter synthesis and normal fetal neurodevelopment. As such, vitamin B6 deficiency has been associated with the development of neurological disorders, such as seizure disorder [229]. However, adverse clinical outcomes due to PLP deficiency in infants remains contested and poorly characterized [220].

We are the first to identify a significant association between maternal smoking and elevated DNA methylation at the *PAX8* ME ($p=0.037$, Figure 18D-E) and across all three MEs collectively ($p=0.038$, Figure 18D-E) in infant cord blood. The observed additive effect on DNA methylation across multiple ME regions suggests their enhanced vulnerability to the early life *in utero* environment and maternal exposures. These findings are consistent with previous reports of enhanced exposure effects across multiple ME regions [65, 67], and together support the vulnerability of MEs to environmental exposures as collective, rather than targeted. As all associations were corrected for the potential confounding effects of maternal micronutrient levels, they stand independent of smoking-related decreases in maternal micronutrient levels.

Increasing methylation at both *PAX8* and *BOLA3* were associated with decreasing maternal levels of total folate and vitamin D, respectively. While higher maternal micronutrient levels, especially those involved in one-carbon metabolism, have

been associated with increased infant DNA methylation at imprinted loci [218, 231], this is not always the case [3, 10, 11, 65, 67, 217, 232]. Maternal folate levels were negatively associated with fetal DNA methylation at several imprinted loci in the NEST cohort [10, 11] and at putative human MEs [65, 67]. Our findings corroborate these studies, and indicate that increased DNA methylation can occur under developmental conditions of maternal methyl-donor deprivation. Such paradoxical findings have also been reported in cancer models, and suggest that the effects of folate levels on DNA methylation are site specific rather than epigenome-wide [233, 234]. While developmental vitamin D depletion has been generally associated with hypomethylation [71, 235], these associations were locus-specific [219]. Our findings are the first to demonstrate an inverse relationship between developmental vitamin D levels and DNA methylation at MEs. The inverse relationships we observed between DNA methylation at MEs and micronutrient availability versus maternal TS exposure merits further study into the mechanisms behind which developmental exposure alters DNA methylation at MEs in the early developing fetus, especially within the context of methyl donor deprivation.

Since methylation at *PAX8* indicated the strongest independent association to exposure ($p=0.038$, Figure 18D-E) we further explored its functional role in conceptual tissues derived from the three germ layers (mesoderm-kidney, ectoderm-brain, endoderm-liver). Additionally, due to the proximity between *PAX8*'s ME region, transcriptional start site, and large, intragenic CpG island [212], we hypothesized that

DNA methylation at the *PAX8* ME may functionally contribute to regulation of gene expression. *PAX8* is part of the paired-box transcription factor family, a group of genes involved in organogenesis during development [236, 237], and has specifically been associated with thyroid, brain, and kidney development [236, 237]. As such, *PAX8* has also been implicated in promoting tumor cell growth in adults [236, 238], and its expression has been linked to thyroid cancer [236], kidney cancer [236, 237, 239], and even ovarian cancer [236, 238, 240]. *PAX8*'s established role in a number of cancers [236-240] provided additional impetus to investigate a potential relationship between *PAX8* ME methylation and gene expression within the context of developmental TS exposure, especially since TS exposure itself is an established cancer risk factor.

Although *PAX8* ME methylation was highly correlated across tissues (Figure 16), we resolved a tissue-specific differences in *PAX8* gene expression, which may be important depending on gene function and the inter-individual distributional range of ME DNA methylation (Figures 16, 19). *PAX8* transcript levels were highest in conceptual kidney ($p < 0.0001$), relative to liver, which had the lowest expression levels [241] (Figure 19A). These results were unsurprising given the developmental role of *PAX8* in kidney formation [236, 237] and in cancer of the kidneys [236, 237, 239]. *PAX8* transcript levels were negatively associated with ME DNA methylation in conceptual kidney tissues as lower methylation corresponded to higher levels of *PAX8* transcription. Normalized *PAX8* cycle threshold (Ct) values indicated that a methylation change of 21.4% in the

kidney correspond to a doubling/halving of *PAX8* mRNA content. While this correlation was not statistically significant, it corroborates the notion that changes in ME DNA methylation across a methylation range that endogenously spans from ~20% to ~90% at *PAX8* could potentially have a substantial impact on gene expression levels. This is of particular significance given the role of *PAX8* in cancer [236-240], and a recent finding that suggests non-CpG island DNA methylation in *PAX8* can serve as a methylation biomarker for squamous cell lung cancer [242]. It would be of interest to determine if individuals with lower baseline levels of methylation at the *PAX8* ME locus are at increased risk of cancer or have a more aggressive course of disease.

Our study was primarily limited by low sample number for some analyses, especially after adjusting for covariates. Due to limited sample availability, we were also under-powered in our gene expression analyses in conceptual tissues, which likely accounts for the inability to resolve statistical significance. In addition, while we observed emerging correlative trends between *PAX8* ME DNA methylation and gene expression, we did not use reporter constructs to validate these findings. Further work is needed to better understand how ME DNA methylation may functionally contribute to gene expression, perhaps through mediating transcription factor binding.

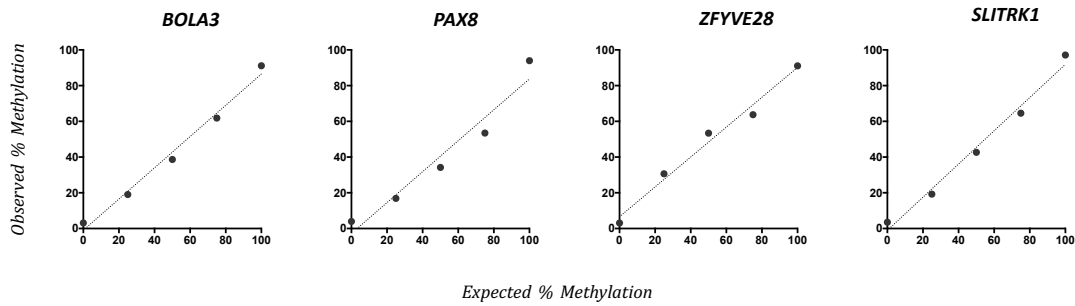
Our study had several notable strengths. First, we employed quantitative sequencing methodology to validate and assess CpG methylation at putative human MEs across multiple human tissues sets, including human conceptual tissues and

umbilical cord blood. Examining ME methylation in human conceptual tissues provided a unique insight into human *in utero* ME methylation levels, about which little is known. The fact that we observed similar ranges of ME methylation in conceptual tissue as has been previously observed in human adult tissue [65, 67] further corroborates the notion that ME methylation is stable throughout life. Access to infant cord blood samples with corresponding maternal sociodemographic information and micronutrient levels enabled an integrative analysis of exposure-related associations between micronutrient status and infant ME DNA methylation—an assessment which has not been previously performed. We were further able to cross-examine maternal sociodemographic variables with micronutrient levels to gain a better understanding of exposure-independent factors that influenced the *in utero* environment during the time of sampling.

In conclusion, our research revealed the potential for developmental TS exposure to alter DNA methylation in the developing fetus at vulnerable regions of the epigenome. Our findings not only support *BOLA3*, *PAX8*, and *ZFYVE28* as human MEs, but further indicate their individual and collective vulnerability to TS exposure during a critical early developmental window. Our integrative analyses of matched maternal sociodemographic information and micronutrient levels revealed exposure-related and -independent interactions with infant DNA methylation at human MEs, further underscoring the importance of considering these factors in epigenetic studies. While we identified a trending functional relationship between *PAX8* ME DNA methylation

and gene expression, more work is needed to better understand how TS exposure mechanistically contributes to hypermethylation at MEs, and how these changes might potentially alter risk of disease and/or its course. Further, a better understanding on the potential interaction between pre-and peri-conceptional maternal micronutrient availability and environmental exposures is paramount given the micronutrient-independent effects we observed from maternal smoking on infant ME methylation. We find these gaps in the literature critical to address in order to better understand this potential new route to developmental origins of disease.

A



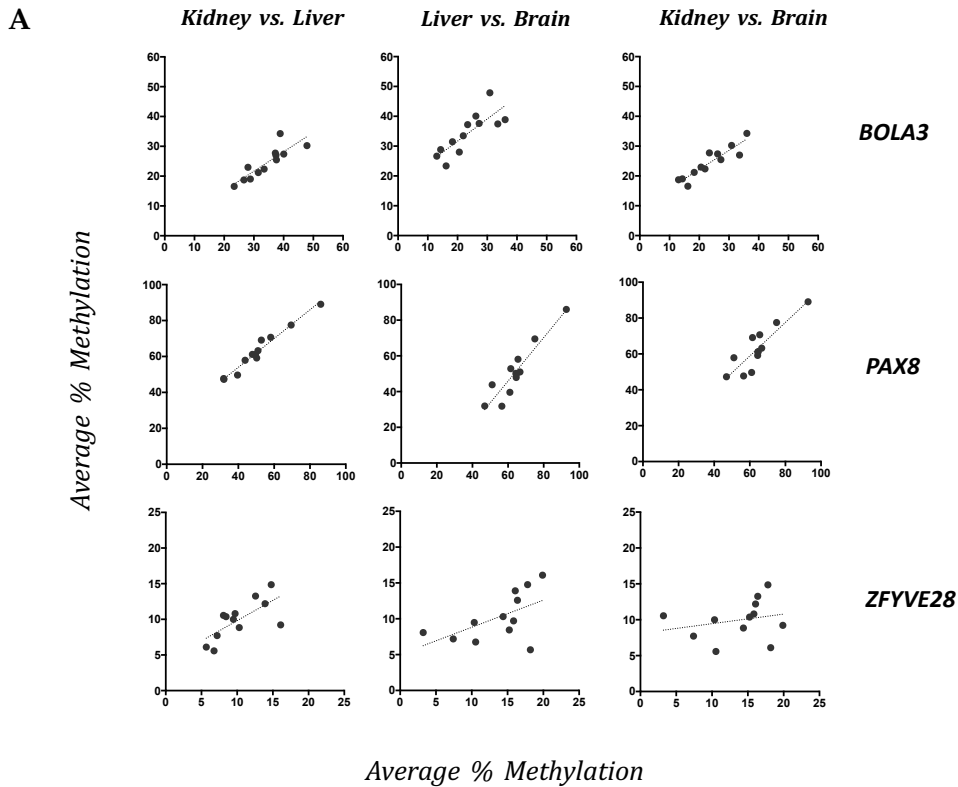
B

Observed vs. Expected			
		R_p	P
Metastable Epialleles	<i>BOLA3</i>	0.9931	0.0007
	<i>PAX8</i>	0.9726	0.0054
	<i>ZFYVE28</i>	0.9911	0.0010
	<i>SLITRK1</i>	0.9926	0.0008

R_p =Pearson's Correlation, P=p value

Figure 15: Pyrosequencing assay validations for human MEs.

A. Human DNA methylation standards serially diluted to 0%, 25%, 50%, 75%, and 100% were used to generate standard curve correlations between measured ME DNA methylation and the human DNA methylation standards for each ME assay. Error bars represent standard error of the mean (SEM). B. All assays examined displayed significant correlation between expected and observed % methylation across human DNA methylation standards (*BOLA3* $R=0.99$, $p=0.0007$, *PAX8* $R=0.97$, $p=0.0054$, *ZFYVE28* $R=0.99$, $p=0.0010$, *SLITRK1* $R=0.99$, $p=0.0008$). Correlation assessed using Pearson's Correlation Coefficient (R_p).



B

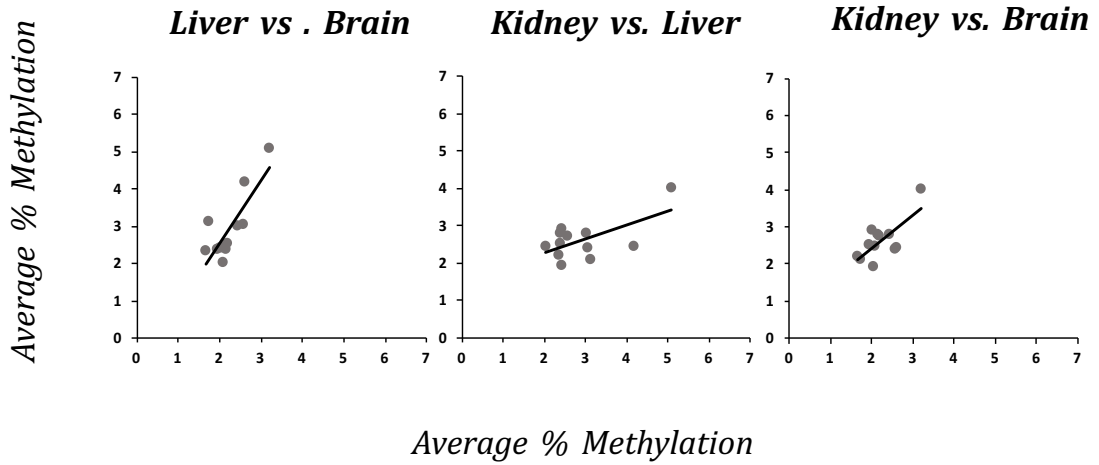
		Kidney vs. Liver		Liver vs. Brain		Kidney vs. Brain	
		R_s	P	R_s	P	R_s	P
Metastable Epialleles	<i>BOLA3</i>	0.8811	0.0002	0.8601	0.0003	0.8881	0.0001
	<i>PAX8</i>	0.9650	<0.0001	0.8601	0.0003	0.8881	0.0001
	<i>ZFYVE28</i>	0.6643	0.0185	0.5175	0.0849	0.2448	0.4433

R_s =Spearman's Correlation, P=p value, N=12 individuals (fetal conceptual)

Figure 16: Inter-tissue correlation and inter-individual variation verify BOLA3, PAX8, and ZFYVE28 as human metastable epialleles (MEs).

A: Scatter plots depict inter-individual variation and inter-tissue correlation in DNA methylation (represented as average % methylation) at PAX8, BOLA3, and ZFYVE28 in brain, liver and kidney tissue, representing all embryonic germ tissue layers. N=6 male, N=6 female. B: Pairwise comparisons across conceptual tissues reveal strong inter-tissue correlation at MEs. Correlations assessed using Spearman's Correlation (R_s).

A



B

	Liver vs. Brain		Kidney vs. Liver		Kidney vs. Brain	
	R_s	P	R_s	P	R_s	P
SLITRK1	0.6340	0.0268	0.1193	0.7119	0.4273	0.1659

R_s =Spearman's Correlation. P=p value, N=12 individuals (fetal conceptual)

C

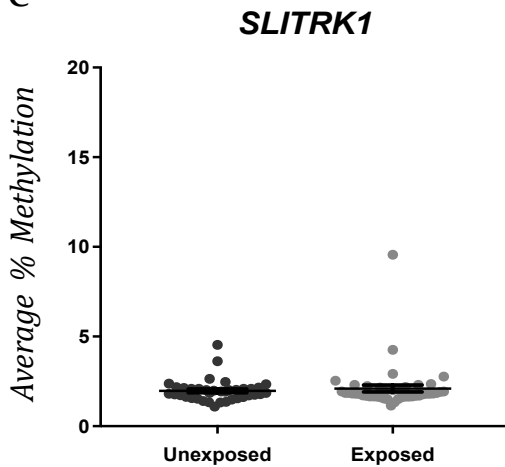
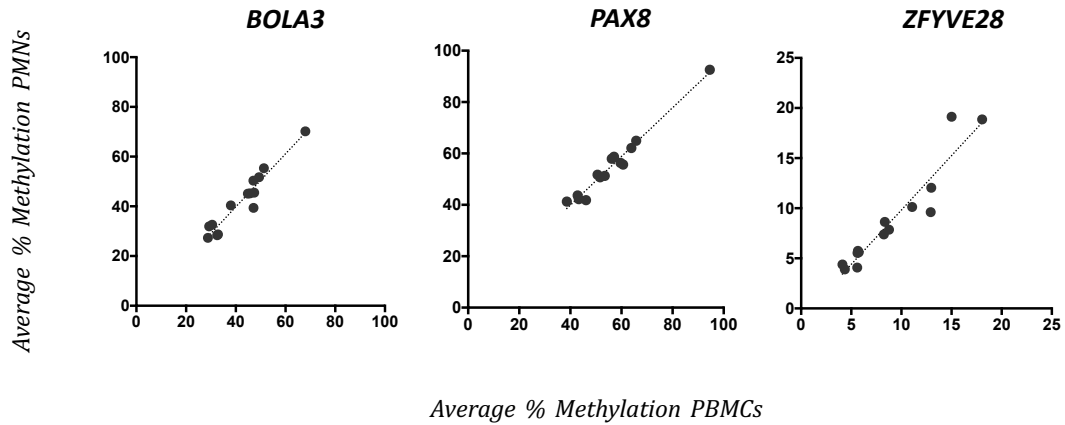


Figure 17: Characterization of ME status for the putative human ME SLITRK1.

A-B: SLITRK1 displays trending intertissue correlation across conceptual brain, liver, and kidney tissue (Liver vs. Brain, $R_s=0.63$, $p=0.03$; Kidney vs. Liver, $R_s=0.12$, $p=0.71$; Kidney vs. Brain, $R_s=0.43$, $p=0.17$; $N=6$ male, $N=6$ female). Correlations assessed using Spearman's Correlation Coefficient (R_s). C. Exposure to tobacco smoke in utero is not associated with cord blood DNA methylation at SLITRK1. "Unexposed" samples identified by maternal plasma cotinine levels $<1\text{ng/mL}$. "Exposed" samples identified by maternal plasma cotinine levels $>3\text{ng/mL}$. $N=38$ unexposed, $N=44$ exposed, $p=0.56$ for comparison between ME % methylation and maternal smoke exposure. Error bars represent standard error of the mean (SEM).

A



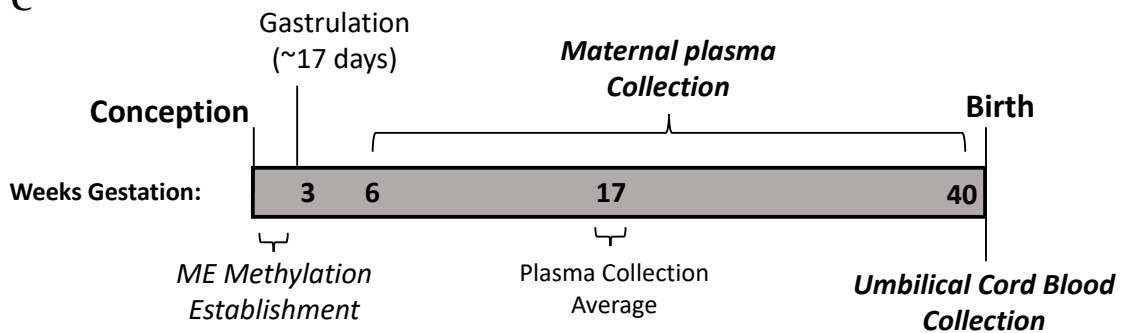
B

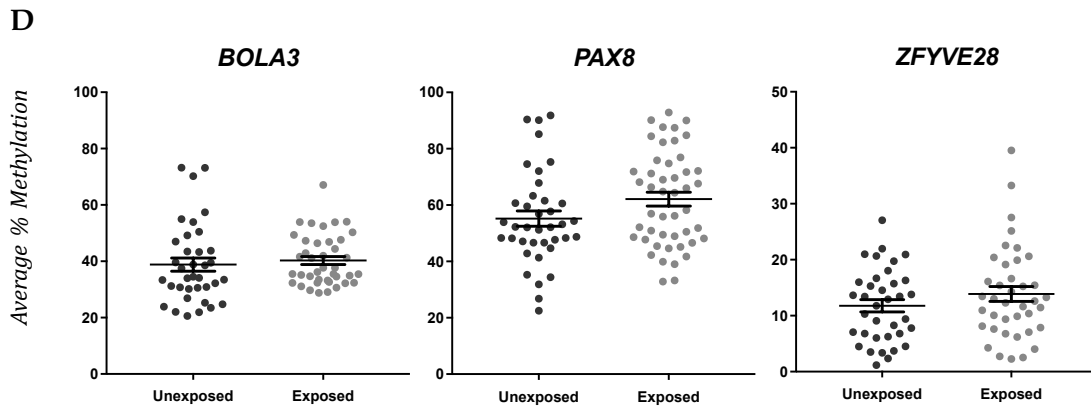
PMN vs. PBMC

		R_s	P
Metastable Epialleles	<i>BOLA3</i>	0.91	<0.0001
	<i>PAX8</i>	0.93	<0.0001
	<i>ZFYVE28</i>	0.97	<0.0001

R_s =Spearman's Correlation, P=p value, N=14 individuals (fetal conceptual)

C



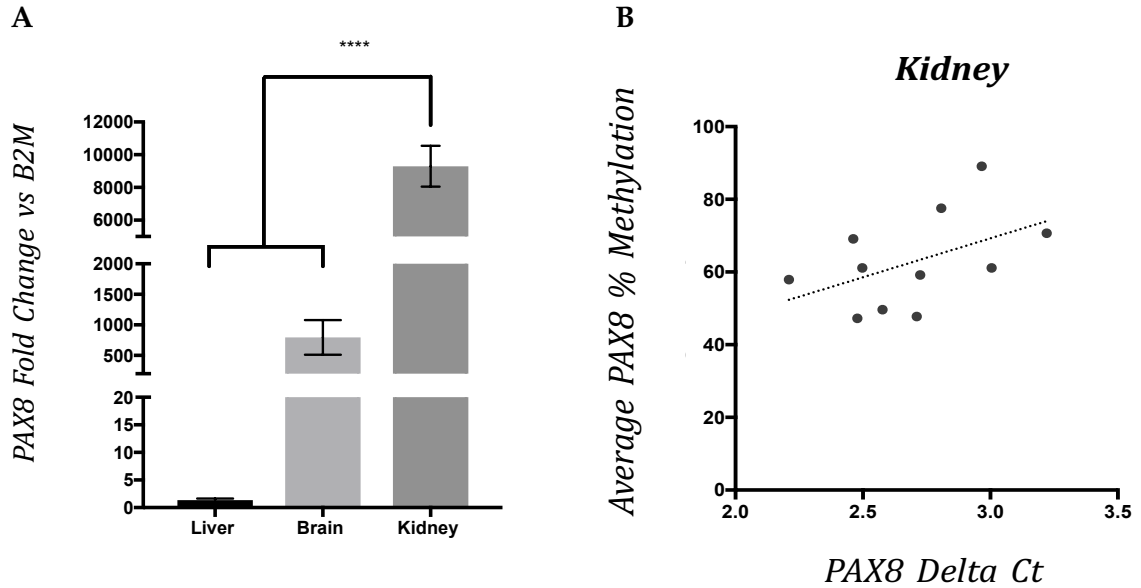


E

Unexposed vs. Exposed		
		*P
Metastable Epialleles	<i>BOLA3</i>	0.5922
	<i>PAX8</i>	0.0371
	<i>ZFYVE28</i>	0.2281
	<i>All Three</i>	0.0378

Figure 18: NEST maternal tobacco smoke (TS) exposure is associated with increased infant cord blood DNA methylation at MEs.

A-B: Correlations in DNA methylation at *BOLA3*, *PAX8*, and *ZFYVE28* across polymorphonuclear and mononuclear cell fractions (PMNs and PBMCs), supporting whole buffy coat sampling methods ($p < 0.0001$, Spearman's correlations). C: Timeline for NEST maternal plasma and cord blood sample collection in the context of ME establishment. D-E: Average % DNA methylation at ME loci in NEST infant cord blood stratified by maternal tobacco smoke exposure status. "Unexposed" samples identified by maternal plasma cotinine levels $< 1\text{ng/mL}$. "Exposed" samples identified by maternal plasma cotinine levels $> 3\text{ng/mL}$. *PAX8*: $N=38$ unexposed, $N=47$ exposed, $p=0.037$, *BOLA3*: $N=36$ unexposed, 40 exposed, $p=0.59$, *ZFYVE28*: $N=36$ unexposed, 39 exposed, $p=0.23$. Error bars represent the standard error of the mean (SEM). *PAX8* association adjusted for maternal age and plasma vitamin D levels. Repeated measures association across all three MEs adjusted for maternal vitamin B6 pyridoxic acid levels. * p -value for comparison between infant average ME % methylation and maternal smoke exposure status using linear regression models (*PAX8*, *BOLA3*, *ZFYVE28*), or mixed models with repeated measures (All Three MEs).



C

**Average PAX8 % Methylation
vs. Delta Ct in Kidney**

		R_s	P	$y = m(x) + b$
Tissue Type	Kidney	0.5545	0.0767	$y = 21.43x + 4.988$

R_s =Spearman's Correlation, P=p value, N=11 individuals (fetal conceptual)

Figure 19: Association of PAX8 mRNA levels and ME DNA methylation in conceptual kidney tissue.

PAX8 mRNA levels were calculated as the difference in cycle threshold (Delta Ct) between PAX8 and B2M following reverse transcription real-time PCR. A: PAX8 mRNA levels differed significantly across tissue types, with the highest mRNA content in kidney (**** $p < 0.0001$, two-way ANOVA followed by Tukey's HSD post-hoc test). Error bars represent the standard error of the mean (SEM). N=6 male, N=6 female. B-C: Correlation of PAX8 ME average % DNA methylation and Delta Ct in kidney conceptual tissue. Correlations assessed using Spearman's Correlation (R_s). N= 6 male, N=5 female.

Table 10: Pyrosequencing assays for human metastable epialleles.

Metastable Epiallele	Forward Primer (5'-3')	Reverse Primer (5'-3')	Sequencing Primer (5'-3')	Sequence to Analyze (5'-3')	PCR Annealing Temp (°C)	# CpGs Analyzed
<i>BOLA3</i>	GGTGTATTTAAGT ATAGAG AAGGTGGAGAT	*AAAACAACATA AACTCACAAACC ACTACTA	GTGGAGATGG AGGGA	YGGGAGGGGGTTTTY GTTGTTTTYGATTTTTY GGGTTTAGAYGTTGT TGGAGAGTAGTAAG	64	5
<i>PAX8</i>	GGGGTGGATGAGA TTGAGGTTAGA	*CCTTCAATACCT TTCCCCATACTAC C	GGTTTGTTTTG AGGAT	TTYGTTTTATTYGY GTTATAGTTGTATGG TTYGGGATTTTTTTG TYGTATTTGAGAGGA GGGTTTGGTT	67	5
<i>ZFYVE28</i>	TTTAGTAGGGGYG GYGTAGTTTTAGTT ATA	*AAACCTAACRCC TAAAAAATAACC	GGYGTAGTTTT AGTTAT AGAGT	YGGGGTGTTTYGGGY GTAYGYGGGGGTTA	59	5
<i>SLITRK1</i>	*GGTGAAGGYGGA GGTGATAAA	CTCCAACCTCTAC CTAAACACC	CCTAAACACC AACAAAAT	ATCCATCTCRATATT AATCCCRAAACTACT	61	2

*indicates biotin labeling

Primer sequences provided by Rob Waterland and his laboratory, as used in Dominguez-Salas et al, 2014.

Table 11: NEST cohort maternal sociodemographic data stratified by plasma cotinine levels.

		Full Sample		Unexposed ^a		Exposed ^b		*P
		N (%)	Cotinine Mean in ng/mL ± SEM ^c	N (%)	Cotinine Mean in ng/mL ± SEM ^c	N (%)	Cotinine Mean in ng/mL ± SEM ^c	
Race	<i>White</i>	34 (40.00)	54.07 ± 12.76	19 (50.00)	0.22 ± 0.07	15 (31.92)	122.28 ± 16.59	
	<i>Black^d</i>	48 (56.47)	59.62 ± 11.94	17 (44.74)	0.14 ± 0.04	31 (65.96)	92.24 ± 15.67	
	<i>Hispanic^d</i>	2 (2.35)	24.00 ± 24.00	1 (2.63)	0.00	1 (2.13)	48.00	
	<i>Other^d</i>	1 (1.18)	0.01	1 (2.63)	0.01	0	-	
Education	<i>No College</i>	39 (45.88)	90.06 ± 14.25	8 (21.05)	0.20 ± 0.08	31 (65.96)	113.25 ± 15.37	<0.0001
	<i>At Least Some College</i>	46 (54.12)	26.87 ± 7.80	30 (78.95)	0.17 ± 0.04	16 (34.04)	76.94 ± 16.40	
BMI	<i>18.5 < x < 25 (Normal)</i>	31 (38.27)	55.33 ± 13.04	15 (40.54)	0.18 ± 0.07	16 (36.36)	107.04 ± 17.04	0.8192
	<i>> 25 (Overweight)</i>	50 (61.73)	47.53 ± 9.62	22 (59.46)	0.17 ± 0.05	28 (63.64)	84.74 ± 13.55	
Age	<i>< 25 y.o.</i>	28 (32.94)	46.68 ± 12.21	11 (28.95)	0.11 ± 0.05	17 (36.17)	76.81 ± 16.42	0.3103
	<i>25-30 y.o.</i>	31 (36.47)	71.72 ± 16.83	12 (31.58)	0.27 ± 0.07	19 (40.43)	116.85 ± 21.86	
	<i>> 30 y.o.</i>	26 (30.59)	46.84 ± 13.76	15 (39.47)	0.14 ± 0.07	11 (23.40)	110.53 ± 20.37	

^a Unexposed: maternal plasma cotinine < 1 ng/mL.

^b Exposed: maternal plasma cotinine >3 ng/mL.

^c Non-transformed cotinine values presented.

^d Races combined in statistical analyses as "Nonwhite."

*p-value for two-sided Chi-square test of maternal sociodemographic variable (race, education, BMI, Age) vs smoke exposure status (exposed or unexposed).

Table 12: NEST gestational characteristics stratified by tobacco smoke exposure status.

	<i>Trimester</i>	Full Sample ^a		Unexposed ^b		Exposed ^c	
		N (%)	Cotinine Mean in ng/mL ± SEM ^d	N (%)	Cotinine Mean in ng/mL ± SEM ^d	N (%)	Cotinine Mean in ng/mL ± SEM ^d
Gestational Age at Sampling	<i>1st (0-13 weeks)</i>	48 (56.47)	44.65 ± 10.47	28 (73.68)	0.19 ± 0.05	20 (42.55)	106.89 ± 17.36
	<i>2nd (14-27 weeks)</i>	20 (23.53)	45.24 ± 14.91	9 (23.68)	0.13 ± 0.06	11 (23.40)	82.15 ± 21.57
	<i>3rd (28-40 weeks)</i>	17 (20.00)	100.02 ± 22.53	1 (2.63)	0.00	16 (34.04)	106.27 ± 23.05
Infant Sex	<i>Male</i>	32 (37.65)	47.03 ± 13.65	16 (50.00)	0.17 ± 0.07	16 (50.00)	93.89 ± 21.84
	<i>Female</i>	53 (62.35)	61.20 ± 10.82	22 (41.51)	0.17 ± 0.05	31 (58.49)	104.50 ± 14.01

^aN Total=85.

^bUnexposed: maternal plasma cotinine < 1 ng/mL.

^cExposed: maternal plasma cotinine >3 ng/mL.

^dNon-transformed cotinine values presented.

Table 13: Maternal plasma cotinine distribution in the full NEST cohort.

Exposure Category	Full Sample ^a	
	N (%)	Cotinine Mean in ng/mL \pm SEM ^b
<i>Unexposed</i> (Cotinine <1ng/mL)	534 (62.46)	0.36 \pm 0.01
<i>Passive Exposure</i> (Cotinine 1< x< 3ng/mL)	136 (15.91)	1.56 \pm 0.04
<i>Active Exposure</i> (Cotinine >3ng/mL)	185 (21.64)	71.92 \pm 5.82

^a N Total=855.

^b Non-transformed cotinine values presented.

Table 14: NEST infant birth weight stratified by maternal tobacco smoke exposure status.

	N Total	Unexposed ^a		Exposed ^b		*P
		N (%)	Birth Weight Mean ± SEM	N (%)	Birth Weight Mean ± SEM	
<i>Birth Weight (g)</i>	47	24 (51.06)	3481.58 ± 137.43	23 (48.94)	3004.83 ± 84.28	0.0053

^aUnexposed: maternal plasma cotinine < 1 ng/mL.

^bExposed: maternal plasma cotinine >3 ng/mL.

*p-value for comparison between infant birth weight and maternal smoke exposure status.

Table 15: NEST cohort maternal micronutrient levels stratified by tobacco smoke exposure.

	N Total	Unexposed ^a		Exposed ^b		*P
		N (%)	Nutrient Mean \pm SEM ^c	N (%)	Nutrient Mean \pm SEM ^c	
<i>Total Folate (μg/L)</i>	43	22 (51.16)	246.38 \pm 13.09	21 (48.84)	189.41 \pm 18.33	0.0147
<i>B6 Pyridoxal Phosphate (nmol/L)^{d,e}</i>	44	22 (50.00)	13.27 \pm 2.00	22 (50.00)	5.93 \pm 1.01	0.0497
<i>B6 Pyridoxic Acid (nmol/L)^{d,e}</i>	44	22 (50.00)	7.71 \pm 1.54	22 (50.00)	4.35 \pm 1.50	0.4434
<i>Vitamin D (ng/mL)^f</i>	43	21 (48.84)	17.62 \pm 1.32	22 (51.16)	14.70 \pm 1.16	0.3087
<i>Vitamin B12 (ng/L)</i>	44	22 (50.00)	620.41 \pm 54.94	22 (50.00)	427.77 \pm 40.83	0.0074
<i>Homocysteine (μg/mL)^{d,e}</i>	41	20 (48.78)	0.70 \pm 0.04	21 (51.22)	0.79 \pm 0.05	0.0193

^a Unexposed: maternal plasma cotinine < 1 ng/mL.

^b Exposed: maternal plasma cotinine >3 ng/mL

^c Non-transformed micronutrient values presented.

^d B6 pyridoxal phosphate, B6 pyridoxic acid, and homocysteine values were natural log transformed after adding a constant prior to statistical testing to increase normality.

^e B6 pyridoxal phosphate, B6 pyridoxic acid, and homocysteine associations adjusted for maternal education.

^f Vitamin D association adjusted for maternal race.

*p-value for comparison between maternal micronutrient level and smoke exposure status.

Table 16: NEST maternal micronutrient levels stratified by education level.

	No College ^a			College ^b		*P
	N Total	N (%)	Nutrient Mean \pm SEM ^c	N (%)	Nutrient Mean \pm SEM ^c	
<i>Total Folate ($\mu\text{g/L}$)</i>	43	17 (39.53)	186.61 \pm 19.75	26 (60.47)	239.45 \pm 13.61	0.0279
<i>B6 Pyridoxal Phosphate (nmol/L)^d</i>	44	17 (38.64)	4.45 \pm 0.94	27 (61.36)	12.85 \pm 1.66	0.0002
<i>B6 Pyridoxic Acid (nmol/L)^d</i>	44	17 (38.64)	2.45 \pm 0.46	27 (61.36)	8.28 \pm 1.62	0.0030
<i>Vitamin D (ng/mL)^e</i>	43	17 (39.53)	16.05 \pm 1.53	26 (60.47)	16.18 \pm 1.12	0.2688
<i>Vitamin B12 (ng/L)</i>	44	17 (38.64)	433.04 \pm 47.52	27 (61.36)	575.13 \pm 50.31	0.0810
<i>Homocysteine ($\mu\text{g/mL}$)^{d,f}</i>	41	15 (36.59)	0.68 \pm 0.03	26 (63.41)	0.79 \pm 0.05	0.0116

^a No College: High school/General Equivalency Degree (GED) or less.

^b College: At least some college education.

^c Non-transformed micronutrient values presented.

^d B6 pyridoxal phosphate, B6 pyridoxic acid, and homocysteine values were natural log transformed after adding a constant prior to statistical testing to increase normality.

^e Vitamin D association adjusted for race.

^f Homocysteine association adjusted for maternal smoking status.

*p-value for comparison between maternal micronutrient level and education level.

Table 17: NEST maternal micronutrient levels stratified by pre-conceptional BMI.

	Normal Weight ^a			Overweight ^b		*P
	N Total	N (%)	Nutrient Mean \pm SEM ^c	N (%)	Nutrient Mean \pm SEM ^c	
<i>Total Folate ($\mu\text{g/L}$)</i>	43	20 (46.51)	221.70 \pm 19.13	23 (53.49)	215.82 \pm 15.12	0.8083
<i>B6 Pyridoxal Phosphate (nmol/L)^{d,e}</i>	44	20 (45.45)	12.29 \pm 2.02	24 (54.55)	7.37 \pm 1.41	0.0348
<i>B6 Pyridoxic Acid (nmol/L)^{d,e}</i>	44	20 (45.45)	6.34 \pm 1.43	24 (54.55)	5.77 \pm 1.64	0.7619
<i>Vitamin D (ng/mL)^f</i>	43	19 (44.19)	17.71 \pm 1.30	24 (55.81)	14.87 \pm 1.19	0.1982
<i>Vitamin B12 (ng/L)</i>	44	20 (45.45)	639.02 \pm 62.73	24 (54.55)	428.31 \pm 32.79	0.0033
<i>Homocysteine ($\mu\text{g/mL}$)^{d,g}</i>	41	18 (43.90)	0.72 \pm 0.04	23 (56.10)	0.77 \pm 0.05	0.7436

^a Normal weight individuals identified by BMI between 18.5 and 25.

^b Overweight individuals identified by BMI >25.

^c Non-transformed micronutrient values presented.

^d B6 pyridoxal phosphate, B6 pyridoxic acid, and homocysteine values were natural log transformed after adding a constant prior to statistical testing to increase normality.

^e Vitamin B6 pyridoxal phosphate and B6 pyridoxic acid associations adjusted for maternal education.

^f Vitamin D association adjusted for race.

^g Homocysteine association adjusted for maternal smoking status and maternal education.

*p-value for comparison between maternal micronutrient level and pre-pregnancy BMI.

Table 18: NEST maternal micronutrient levels stratified by predominant race.

	N Total	White		Nonwhite ^a		*P
		N (%)	Nutrient Mean \pm SEM ^b	N (%)	Nutrient Mean \pm SEM ^b	
<i>Total Folate ($\mu\text{g/L}$)</i>	43	18 (41.86)	243.87 \pm 12.57	25 (58.14)	200.33 \pm 17.65	0.0702
<i>B6 Pyridoxal Phosphate (nmol/L)^{c,d}</i>	44	18 (40.91)	13.14 \pm 2.12	26 (59.09)	7.15 \pm 1.33	0.1529
<i>B6 Pyridoxic Acid (nmol/L)^{c,d}</i>	44	18 (40.91)	7.30 \pm 1.54	26 (59.09)	5.15 \pm 1.52	0.7882
<i>Vitamin D (ng/mL)</i>	43	17 (39.53)	19.25 \pm 1.36	26 (60.47)	14.08 \pm 1.02	0.0036
<i>Vitamin B12 (ng/L)</i>	44	18 (40.91)	557.05 \pm 69.69	26 (59.09)	501.28 \pm 40.26	0.4637
<i>Homocysteine ($\mu\text{g/mL}$)^{c,e}</i>	41	17 (41.46)	0.70 \pm 0.03	24 (58.54)	0.78 \pm 0.05	0.0813

^a Nonwhite: Black, Hispanic, and Other races combined.

^b Non-transformed micronutrient values presented.

^c B6 pyridoxal phosphate, B6 pyridoxic acid, and homocysteine values were natural log transformed after adding a constant prior to statistical testing to increase normality.

^d Vitamin B6 pyridoxal phosphate and B6 pyridoxic acid associations adjusted for maternal education.

^e Homocysteine association adjusted for maternal smoking status and maternal education.

*p-value for comparison between maternal micronutrient level and predominant race.

Table 19: NEST maternal micronutrient levels stratified by maternal age.

	N Total	< 25 years		25-30 years		> 30 years		*P
		N (%)	Nutrient Mean \pm SEM ^a	N (%)	Nutrient Mean \pm SEM ^a	N (%)	Nutrient Mean \pm SEM ^a	
<i>Total Folate ($\mu\text{g/L}$)</i>	43	10 (23.26)	174.21 \pm 24.02	15 (34.88)	218.18 \pm 14.93	18 (41.86)	243.50 \pm 20.25	0.0758
<i>B6 Pyridoxal Phosphate (nmol/L)^{b,c}</i>	44	11 (25.00)	5.90 \pm 1.75	15 (34.09)	10.52 \pm 2.14	18 (40.91)	11.11 \pm 2.14	0.5846
<i>B6 Pyridoxic Acid (nmol/L)^{b,c}</i>	44	11 (25.00)	3.56 \pm 1.15	15 (34.09)	6.96 \pm 1.98	18 (40.91)	6.76 \pm 1.99	0.8338
<i>Vitamin D (ng/mL)^d</i>	43	11 (25.58)	14.47 \pm 1.58	15 (34.88)	15.29 \pm 1.53	17 (39.53)	17.93 \pm 1.47	0.2378
<i>Vitamin B12 (ng/L)</i>	44	11 (25.00)	407.80 \pm 63.90	15 (34.09)	471.99 \pm 42.61	18 (40.91)	638.58 \pm 65.61	0.0246
<i>Homocysteine ($\mu\text{g/mL}$)^{b,e}</i>	41	10 (24.39)	0.69 \pm 0.05	14 (34.15)	0.78 \pm 0.06	17 (41.46)	0.76 \pm 0.06	0.4638

^a Non-transformed micronutrient values presented.

^b B6 pyridoxal phosphate, B6 pyridoxic acid, and homocysteine values were natural log transformed after adding a constant prior to statistical testing to increase normality.

^c Vitamin B6 pyridoxal phosphate and B6 pyridoxic acid associations adjusted for maternal education.

^d Vitamin D association adjusted for race.

^e Homocysteine association adjusted for maternal smoking status and maternal education.

*p-value for comparison between maternal micronutrient level and age.

Table 20: DNA methylation at human metastable epialleles stratified by NEST maternal micronutrient levels.

	Average <i>PAX8</i> % Methylation			Average <i>BOLA3</i> % Methylation			Average <i>ZFYVE28</i> % Methylation		
	N Total	R _s	P	N Total	R _s	P	N Total	R _s	P
<i>Total Folate (µg/L)</i>	43	-0.2508	0.1047	39	-0.0642	0.6979	40	-0.1478	0.3626
<i>B6 Pyridoxal Phosphate (nmol/L)^a</i>	44	-0.0909	0.5573	40	-0.0120	0.9414	41	-0.1686	0.2919
<i>B6 Pyridoxic Acid (nmol/L)^a</i>	44	0.0293	0.8502	40	-0.0505	0.7571	41	-0.0991	0.5375
<i>Vitamin D (ng/mL)</i>	43	0.1722	0.2696	40	-0.3617	0.0218	41	-0.0439	0.7852
<i>Vitamin B12 (ng/L)</i>	44	-0.1674	0.2773	40	-0.2355	0.1436	41	-0.1178	0.4634
<i>Homocysteine (µg/mL)^a</i>	41	-0.0664	0.6798	38	0.0018	0.9917	39	-0.0337	0.8384

R_s=Spearman's Correlation

^a B6 pyridoxal phosphate, B6 pyridoxic acid, and homocysteine values were natural log transformed after adding a constant prior to statistical testing to increase normality.

5. Conclusion

5.1 Summary

The goals of this dissertation research were broadly to identify alterations in DNA methylation patterning in the brain as a result of maternal TS exposure, and investigate their neurodevelopmental significance. Despite the extensive literature supporting the ability of TS and its constituents to induce epigenetic alterations in the developing fetus, particularly if exposure occurs during vulnerable windows of developmental reprogramming, the mechanisms by which these alterations occur remain elusive. This is largely due to the fact that most studies examining these associations are purely correlative. Moreover, sampling techniques in human studies almost exclusively rely on sampling of peripheral or umbilical cord blood, from which functional relevance is difficult to derive, especially pertaining to neurodevelopmental consequences. As such, I sought out to specifically examine whether developmental TS exposure could induce epigenetic alterations in the exposed fetus that 1) altered larger neurodevelopmental processes like brain sexualization, 2) contributed to behavioral outcomes later in life, and 3) occurred in brain regions implicated TS-exposure related behaviors. Moreover, whether or not these alterations in the brain corresponded to those in the blood was a question of utmost relevance in order to derive translational implications and correlations with humans.

In chapter 2, we investigated the effects of maternal TS exposure on neurodevelopmental processes that rely on DNA methylation events occurring early in development, namely the sexual differentiation of the brain. Given previous work identifying interactions between nicotine and estradiol in the brain, and given estradiol's critical role in brain masculinization, we hypothesized that developmental nicotine exposure would upregulate brain masculinization. We chose to specifically examine these interactions in the POA, a region of the brain that displays robust sexual dimorphism. Our results indicated that developmental nicotine exposure is capable of triggering masculinization of the female POA, potentially via epigenetic mechanisms. These results highlight nicotine's ability to alter the neurodevelopmental process of brain sexualization, an association that has not been previously examined.

In chapter 3, we examined epigenome-wide alterations to DNA methylation in the rodent brain as a result of developmental TS-exposure, particularly in brain regions associated with TS-exposure implicated behaviors. We further chose to examine these changes solely in males, given the established sex bias of incidence in neurodevelopmental disorders, like ASD and ADHD. Because previous associations have been made between developmental TS-exposure and epigenetic alterations, we hypothesized that developmental TS exposure would induce widespread changes to the epigenome. Further, as most research in this field has relied on the examination of blood samples, we sought out to identify an association between DNA methylation changes in

the blood and brain. Using a rat gestational exposure model for TSE and nicotine, we examined DNA methylation levels in the hippocampus, cortex, and peripheral blood of developmentally-exposed adult male rats, and found significant overlap in differentially methylated regions (DMRs) across all three tissues. Of interest, in examination of functional relevance, these DMRs significantly clustered to functional pathways critical to neurodevelopment, namely synapse formation. In order to determine translational significance, we further investigated the overlap between these target rat DMRs and human DMRs identified in the cord blood of children from the NEST cohort. In our investigation, we found 115 DMRs in common between rat and human tissue samples, indicating that developmental TS-exposure is capable of altering DNA methylation in regions common to rats and humans. Even more interesting is that these common DMRs were heavily implicated in neurobehavioral disorders associated with developmental TS-exposure, namely ASD and ADHD. Our findings corroborate existing behavioral data associating developmental TS with ASD and ADHD, and open new horizons to potential targets for biomarkers of exposure.

The research summarized in chapters 2 and 3 addressed the neurodevelopmental and epigenetic consequences of developmental TS-exposure. As both involved the use of a controlled, rodent gestational exposure model, we were able to closely examine exposure effects during windows of critical epigenetic reprogramming. However, due to the nature of our controlled studies, we were not able to pinpoint the exact epigenetic

reprogramming window that was affected by TS-exposure. In chapter 4, we examined DNA methylation alterations at human metastable epialleles, or regions that are specifically reprogrammed via stochastic establishment of DNA methylation during early development. Our results supported the notion that developmental TS-exposure is not only capable of altering DNA methylation during early development, but also at the earliest timepoint of epigenetic reprogramming (prior to gastrulation).

5.2 Implications, Limitations, and Future Directions

The results presented in this dissertation research supported two main conclusions: 1) Developmental exposure to TS and its constituents are capable of altering DNA methylation in epigenomic regions that are critical to neurodevelopmental processes and 2) Similar changes can be observed in human blood, underscoring the human translational implications of these findings. More specifically, by examining behavioral and molecular endpoints across multiple species, we discovered novel ways in which developmental exposure to TS and its constituents alter neurodevelopmental processes, and lead to epigenome-wide alterations that correlate to those examined in humans. Despite the multi-faceted and comprehensive analytical approaches employed in this research, we were limited by several factors. Firstly, in our brain sexualization study, the gestational exposure model we employed relied on exposure spanning from preconception through the end of lactation. As this exposure window is much broader than the window for brain sexualization, it is possible that the exposure effects we

observed were the result of off-target developmental effects. While this is unlikely, employing a gestational exposure model that spans strictly the window for brain sexualization would be ideal in future experiments. Second, based on our decision to only examine males in our DMR study, we were limited from observing exposure-related effects in females. This is of particular relevance given female's enhanced vulnerability to TS exposure, both during development and adolescence. Of interest would be examining sex differences in developmental TS-exposure induced epigenome-wide alterations. Finally, although we associated widespread exposure-induced changes to the epigenome with functional genomic regions implicated with human neurodevelopmental disorders, we did not make correlations to human behavior itself. Drawing correlations between behavior and epigenetic markers would be a critical next step in order to determine biomarkers of exposure, as proposed in chapter 3.

While such follow up studies would add to the findings presented here, the implications of this research are widespread, and collectively support a larger hypothesis elaborated upon below.

5.2.1 The Masculinizing Effects of Developmental TS Exposure

Although developmental TS exposure has been extensively associated with sex-specific effects in females, ranging from psychiatric to behavioral effects [93], the work presented in this dissertation supports that developmental nicotine exposure generally favors a masculinizing environment. Here, we showed that the female rodent POA was

masculinized by developmental nicotine exposure. Our results are corroborated by human studies linking maternal TS exposure to same-sex sexual behavior in females [176]. The male-biased incidence of other human behaviors associated with developmental TS-exposure, namely ASD and ADHD [184] further support this idea. In fact, ASD has been considered an “extreme” male brain phenotype [191]. These behavioral outcomes are further supported by molecular mechanisms. The nicotinic acetylcholine receptor facilitates molecular mechanisms that are in close alignment with those required for brain masculinization, namely its 1) direct interactions with estradiol in the brain [107], 2) downregulation of epigenetic modifying enzymes like Dnmts [141], 3) upregulation of anti-apoptotic proteins like *Bcl2* [162] that are required for the establishment of masculinized structural differences in the brain [118], and 4) facilitation of excitatory neurotransmission, also critical to normal brain masculinization [86].

Activation of these molecular mechanisms required for masculinization might be mediated via testosterone, as smoking during pregnancy has been associated with elevated maternal androgen production [243]. In rodents, the developing fetuses are protected from maternal circulating estrogen via expression of alpha fetoprotein, which favorably binds estrogen in the placenta. Rodent alpha fetoprotein has also been detected in the brain, with expression levels decreasing steeply at the end of gestation, right around the beginning of the critical window for brain sexualization [244]. Although alpha fetoprotein provides fetal protection from estrogen, it does not bind to

testosterone [244]. Thus, pups are vulnerable to fluctuations in maternal androgen levels, and potential downstream effects. Further investigation of this hypothesis would be of interest as the effects of developmental TS exposure have traditionally been thought to be female-specific. Perhaps these understandings simply need to be re-examined through the lens of masculinization.

Taken together, research presented in this dissertation not only identified novel neurodevelopmental consequences of maternal TS-exposure, but also created opportunities for new studies. Of interest would be further examining the role that the nAChR plays in brain sexualization, and whether or not its activity or expression is disrupted in the POA following developmental nicotine exposure. Of additional interest would be correlating changes in DNA methylation in cord blood, or other human blood samples, with behavioral outcomes. This question is actively being pursued by our laboratory in an effort to distinctly and comprehensively associate developmental TS-exposure with adverse neurobehavioral disorders like ASD and ADHD.

Such investigations are critical in order to better characterize the early developmental windows that are vulnerable to maternal TS exposure. Moreover, since underlying mechanisms to exposure-related outcomes are at least partly epigenetic, the possibility for transmission of effects to subsequent generations is of concern. The research summarized in this dissertation supports these notions, and merits continued work in this field in an effort to improve and protect human health.

References

1. Lee, K.W. and Z. Pausova, *Cigarette smoking and DNA methylation*. *Front Genet*, 2013. 4: p. 132.
2. Amateau, S.K. and M.M. McCarthy, *A novel mechanism of dendritic spine plasticity involving estradiol induction of prostaglandin-E2*. *J Neurosci*, 2002. 22(19): p. 8586-96.
3. Anderson, O.S., K.E. Sant, and D.C. Dolinoy, *Nutrition and epigenetics: an interplay of dietary methyl donors, one-carbon metabolism and DNA methylation*. *J Nutr Biochem*, 2012. 23(8): p. 853-9.
4. Bartolomei, M.S., *Genomic imprinting: employing and avoiding epigenetic processes*. *Genes Dev*, 2009. 23(18): p. 2124-33.
5. Cantone, I. and A.G. Fisher, *Epigenetic programming and reprogramming during development*. *Nat Struct Mol Biol*, 2013. 20(3): p. 282-9.
6. Chatterton, Z., et al., *In utero exposure to maternal smoking is associated with DNA methylation alterations and reduced neuronal content in the developing fetal brain*. *Epigenetics Chromatin*, 2017. 10: p. 4.
7. Dall'Aglio, L., et al., *The role of epigenetic modifications in neurodevelopmental disorders: A systematic review*. *Neurosci Biobehav Rev*, 2018. 94: p. 17-30.
8. Denis, H., M.N. Ndlovu, and F. Fuks, *Regulation of mammalian DNA methyltransferases: a route to new mechanisms*. *EMBO Rep*, 2011. 12(7): p. 647-56.
9. Feng, S., S.E. Jacobsen, and W. Reik, *Epigenetic reprogramming in plant and animal development*. *Science*, 2010. 330(6004): p. 622-7.
10. Hoyo, C., et al., *Erythrocyte folate concentrations, CpG methylation at genomically imprinted domains, and birth weight in a multiethnic newborn cohort*. *Epigenetics*, 2014. 9(8): p. 1120-30.
11. Hoyo, C., et al., *Methylation variation at IGF2 differentially methylated regions and maternal folic acid use before and during pregnancy*. *Epigenetics*, 2011. 6(7): p. 928-36.
12. Keverne, E.B. and J.P. Curley, *Epigenetics, brain evolution and behaviour*. *Front Neuroendocrinol*, 2008. 29(3): p. 398-412.

13. Meng, S., et al., *Epigenetics in Neurodevelopment: Emerging Role of Circular RNA*. *Front Cell Neurosci*, 2019. 13: p. 327.
14. Perera, F. and J. Herbstman, *Prenatal environmental exposures, epigenetics, and disease*. *Reprod Toxicol*, 2011. 31(3): p. 363-73.
15. Pacchierotti, F. and M. Spano, *Environmental Impact on DNA Methylation in the Germline: State of the Art and Gaps of Knowledge*. *Biomed Res Int*, 2015. 2015: p. 123484.
16. Joubert, B.R., et al., *Maternal smoking and DNA methylation in newborns: in utero effect or epigenetic inheritance?* *Cancer Epidemiol Biomarkers Prev*, 2014. 23(6): p. 1007-17.
17. Joubert, B.R., et al., *450K epigenome-wide scan identifies differential DNA methylation in newborns related to maternal smoking during pregnancy*. *Environ Health Perspect*, 2012. 120(10): p. 1425-31.
18. Murphy, S.K., et al., *Gender-specific methylation differences in relation to prenatal exposure to cigarette smoke*. *Gene*, 2012. 494(1): p. 36-43.
19. Richmond, R.C., et al., *DNA methylation as a marker for prenatal smoke exposure in adults*. *Int J Epidemiol*, 2018. 47(4): p. 1120-1130.
20. Rzehak, P., et al., *Maternal Smoking during Pregnancy and DNA-Methylation in Children at Age 5.5 Years: Epigenome-Wide-Analysis in the European Childhood Obesity Project (CHOP)-Study*. *PLoS One*, 2016. 11(5): p. e0155554.
21. Sengupta, S.M., et al., *Locus-specific DNA methylation changes and phenotypic variability in children with attention-deficit hyperactivity disorder*. *Psychiatry Res*, 2017. 256: p. 298-304.
22. Tehranifar, P., et al., *Maternal cigarette smoking during pregnancy and offspring DNA methylation in midlife*. *Epigenetics*, 2018. 13(2): p. 129-134.
23. Toledo-Rodriguez, M., et al., *Maternal smoking during pregnancy is associated with epigenetic modifications of the brain-derived neurotrophic factor-6 exon in adolescent offspring*. *Am J Med Genet B Neuropsychiatr Genet*, 2010. 153B(7): p. 1350-4.
24. Wiklund, P., et al., *DNA methylation links prenatal smoking exposure to later life health outcomes in offspring*. *Clin Epigenetics*, 2019. 11(1): p. 97.

25. Dong, T., et al., *Prenatal exposure to maternal smoking during pregnancy and attention-deficit/hyperactivity disorder in offspring: A meta-analysis*. *Reprod Toxicol*, 2018. 76: p. 63-70.
26. Huang, L., et al., *Maternal Smoking and Attention-Deficit/Hyperactivity Disorder in Offspring: A Meta-analysis*. *Pediatrics*, 2018. 141(1).
27. Linnet, K.M., et al., *Maternal lifestyle factors in pregnancy risk of attention deficit hyperactivity disorder and associated behaviors: review of the current evidence*. *Am J Psychiatry*, 2003. 160(6): p. 1028-40.
28. Milberger, S., et al., *Is maternal smoking during pregnancy a risk factor for attention deficit hyperactivity disorder in children?* *Am J Psychiatry*, 1996. 153(9): p. 1138-42.
29. Knopik, V.S., et al., *The epigenetics of maternal cigarette smoking during pregnancy and effects on child development*. *Dev Psychopathol*, 2012. 24(4): p. 1377-90.
30. Seisenberger, S., et al., *Reprogramming DNA methylation in the mammalian life cycle: building and breaking epigenetic barriers*. *Philos Trans R Soc Lond B Biol Sci*, 2013. 368(1609): p. 20110330.
31. Waddington, C.H. and E. Robertson, *Selection for developmental canalisation*. *Genet Res*, 1966. 7(3): p. 303-12.
32. Rakyan, V.K., et al., *Epigenome-wide association studies for common human diseases*. *Nat Rev Genet*, 2011. 12(8): p. 529-41.
33. Ficiz, G., et al., *Dynamic regulation of 5-hydroxymethylcytosine in mouse ES cells and during differentiation*. *Nature*, 2011. 473(7347): p. 398-402.
34. Dahl, C., K. Gronbaek, and P. Guldberg, *Advances in DNA methylation: 5-hydroxymethylcytosine revisited*. *Clin Chim Acta*, 2011. 412(11-12): p. 831-6.
35. Jeltsch, A., *Molecular enzymology of mammalian DNA methyltransferases*. *Curr Top Microbiol Immunol*, 2006. 301: p. 203-25.
36. Tang, M., et al., *Potential of DNMT and its Epigenetic Regulation for Lung Cancer Therapy*. *Curr Genomics*, 2009. 10(5): p. 336-52.
37. Han, L., et al., *CpG island density and its correlations with genomic features in mammalian genomes*. *Genome Biol*, 2008. 9(5): p. R79.

38. Eckhardt, F., et al., *DNA methylation profiling of human chromosomes 6, 20 and 22*. Nat Genet, 2006. 38(12): p. 1378-85.
39. Lander, E.S., et al., *Initial sequencing and analysis of the human genome*. Nature, 2001. 409(6822): p. 860-921.
40. Medvedeva, Y.A., et al., *Intergenic, gene terminal, and intragenic CpG islands in the human genome*. BMC Genomics, 2010. 11: p. 48.
41. Hackett, J.A. and M.A. Surani, *DNA methylation dynamics during the mammalian life cycle*. Philos Trans R Soc Lond B Biol Sci, 2013. 368(1609): p. 20110328.
42. Smith, Z.D. and A. Meissner, *DNA methylation: roles in mammalian development*. Nat Rev Genet, 2013. 14(3): p. 204-20.
43. Kuo, K.C., et al., *Quantitative reversed-phase high performance liquid chromatographic determination of major and modified deoxyribonucleosides in DNA*. Nucleic Acids Res, 1980. 8(20): p. 4763-76.
44. Song, L., et al., *Specific method for the determination of genomic DNA methylation by liquid chromatography-electrospray ionization tandem mass spectrometry*. Anal Chem, 2005. 77(2): p. 504-10.
45. Le, T., et al., *A sensitive mass spectrometry method for simultaneous quantification of DNA methylation and hydroxymethylation levels in biological samples*. Anal Biochem, 2011. 412(2): p. 203-9.
46. Liu, Z., et al., *Quantification of regional DNA methylation by liquid chromatography/tandem mass spectrometry*. Anal Biochem, 2009. 391(2): p. 106-13.
47. Quinlivan, E.P. and J.F. Gregory, 3rd, *DNA methylation determination by liquid chromatography-tandem mass spectrometry using novel biosynthetic [U-15N]deoxycytidine and [U-15N]methyldeoxycytidine internal standards*. Nucleic Acids Res, 2008. 36(18): p. e119.
48. So, M.Y., et al., *Gene expression profile and toxic effects in human bronchial epithelial cells exposed to zearalenone*. PLoS One, 2014. 9(5): p. e96404.
49. Li, P., et al., *An integrated workflow for DNA methylation analysis*. J Genet Genomics, 2013. 40(5): p. 249-60.

50. Kurdyukov, S. and M. Bullock, *DNA Methylation Analysis: Choosing the Right Method*. Biology (Basel), 2016. 5(1).
51. Lee, Y.K., et al., *Improved reduced representation bisulfite sequencing for epigenomic profiling of clinical samples*. Biol Proced Online, 2014. 16(1): p. 1.
52. Meissner, A., et al., *Reduced representation bisulfite sequencing for comparative high-resolution DNA methylation analysis*. Nucleic Acids Res, 2005. 33(18): p. 5868-77.
53. Chatterjee, A., et al., *Technical considerations for reduced representation bisulfite sequencing with multiplexed libraries*. J Biomed Biotechnol, 2012. 2012: p. 741542.
54. Nye, M.D., C. Hoyo, and S.K. Murphy, *In vitro lead exposure changes DNA methylation and expression of IGF2 and PEG1/MEST*. Toxicol In Vitro, 2015. 29(3): p. 544-50.
55. Wilhelm-Benartzi, C.S., et al., *Review of processing and analysis methods for DNA methylation array data*. Br J Cancer, 2013. 109(6): p. 1394-402.
56. Solomon, O., et al., *Comparison of DNA methylation measured by Illumina 450K and EPIC BeadChips in blood of newborns and 14-year-old children*. Epigenetics, 2018. 13(6): p. 655-664.
57. Mohn, F., et al., *Lineage-specific polycomb targets and de novo DNA methylation define restriction and potential of neuronal progenitors*. Mol Cell, 2008. 30(6): p. 755-66.
58. Seisenberger, S., J.R. Peat, and W. Reik, *Conceptual links between DNA methylation reprogramming in the early embryo and primordial germ cells*. Curr Opin Cell Biol, 2013. 25(3): p. 281-8.
59. Smith, Z.D., et al., *A unique regulatory phase of DNA methylation in the early mammalian embryo*. Nature, 2012. 484(7394): p. 339-44.
60. Elhamamsy, A.R., *Role of DNA methylation in imprinting disorders: an updated review*. J Assist Reprod Genet, 2017. 34(5): p. 549-562.
61. Tycko, B., *DNA methylation in genomic imprinting*. Mutat Res, 1997. 386(2): p. 131-40.
62. Dolinoy, D.C., et al., *Metastable epialleles, imprinting, and the fetal origins of adult diseases*. Pediatr Res, 2007. 61(5 Pt 2): p. 30R-37R.

63. Harris, R.A., D. Nagy-Szakal, and R. Kellermayer, *Human metastable epiallele candidates link to common disorders*. *Epigenetics*, 2013. 8(2): p. 157-63.
64. Rakyan, V.K., et al., *Metastable epialleles in mammals*. *Trends Genet*, 2002. 18(7): p. 348-51.
65. Waterland, R.A., et al., *Season of conception in rural gambia affects DNA methylation at putative human metastable epialleles*. *PLoS Genet*, 2010. 6(12): p. e1001252.
66. Dolinoy, D.C., et al., *Variable histone modifications at the A(vy) metastable epiallele*. *Epigenetics*, 2010. 5(7): p. 637-44.
67. Dominguez-Salas, P., et al., *Maternal nutrition at conception modulates DNA methylation of human metastable epialleles*. *Nat Commun*, 2014. 5: p. 3746.
68. Takizawa, T., et al., *DNA methylation is a critical cell-intrinsic determinant of astrocyte differentiation in the fetal brain*. *Dev Cell*, 2001. 1(6): p. 749-58.
69. Li, L., et al., *Regulation of maternal behavior and offspring growth by paternally expressed Peg3*. *Science*, 1999. 284(5412): p. 330-3.
70. Murphy, S.K., Z. Huang, and C. Hoyo, *Differentially methylated regions of imprinted genes in prenatal, perinatal and postnatal human tissues*. *PLoS One*, 2012. 7(7): p. e40924.
71. Xue, J., et al., *Maternal vitamin D depletion alters DNA methylation at imprinted loci in multiple generations*. *Clin Epigenetics*, 2016. 8: p. 107.
72. Brooke, O.G., et al., *Effects on birth weight of smoking, alcohol, caffeine, socioeconomic factors, and psychosocial stress*. *Bmj*, 1989. 298(6676): p. 795-801.
73. Picone, T.A., et al., *Pregnancy outcome in North American women. I. Effects of diet, cigarette smoking, and psychological stress on maternal weight gain*. *Am J Clin Nutr*, 1982. 36(6): p. 1205-13.
74. Picone, T.A., et al., *Pregnancy outcome in North American women. II. Effects of diet, cigarette smoking, stress, and weight gain on placentas, and on neonatal physical and behavioral characteristics*. *Am J Clin Nutr*, 1982. 36(6): p. 1214-24.
75. Meyer, M.B. and G.W. Comstock, *Maternal cigarette smoking and perinatal mortality*. *Am J Epidemiol*, 1972. 96(1): p. 1-10.

76. Matsubara, F., et al., *Maternal active and passive smoking and fetal growth: A prospective study in Nagoya, Japan*. J Epidemiol, 2000. 10(5): p. 335-43.
77. Ernst, M., E.T. Moolchan, and M.L. Robinson, *Behavioral and neural consequences of prenatal exposure to nicotine*. J Am Acad Child Adolesc Psychiatry, 2001. 40(6): p. 630-41.
78. Hardy, J.B. and E.D. Mellits, *Does maternal smoking during pregnancy have a long-term effect on the child?* Lancet, 1972. 2(7791): p. 1332-6.
79. Cornelius, M.D., et al., *Effects of prenatal cigarette smoke exposure on neurobehavioral outcomes in 10-year-old children of adolescent mothers*. Neurotoxicol Teratol, 2011. 33(1): p. 137-44.
80. Dunn, H.G. and A.K. McBurney, *Cigarette smoking and the fetus and child*. Pediatrics, 1977. 60(5): p. 772.
81. Naeye, R.L. and E.C. Peters, *Mental development of children whose mothers smoked during pregnancy*. Obstet Gynecol, 1984. 64(5): p. 601-7.
82. Rantakallio, P., *A follow-up study up to the age of 14 of children whose mothers smoked during pregnancy*. Acta Paediatr Scand, 1983. 72(5): p. 747-53.
83. Eskenazi, B. and R. Castorina, *Association of prenatal maternal or postnatal child environmental tobacco smoke exposure and neurodevelopmental and behavioral problems in children*. Environ Health Perspect, 1999. 107(12): p. 991-1000.
84. Fergusson, D.M., L.J. Horwood, and M.T. Lynskey, *Maternal smoking before and after pregnancy: effects on behavioral outcomes in middle childhood*. Pediatrics, 1993. 92(6): p. 815-22.
85. Wakschlag, L.S., et al., *Maternal smoking during pregnancy and the risk of conduct disorder in boys*. Arch Gen Psychiatry, 1997. 54(7): p. 670-6.
86. Dwyer, J.B., R.S. Broide, and F.M. Leslie, *Nicotine and brain development*. Birth Defects Res C Embryo Today, 2008. 84(1): p. 30-44.
87. Streissguth, A.P., et al., *Intrauterine alcohol and nicotine exposure: attention and reaction time in 4-year-old children*. Developmental Psychology, 1984. 20: p. 533-541.

88. Dunn, H.G., et al., *Maternal cigarette smoking during pregnancy and the child's subsequent development: II. Neurological and intellectual maturation to the age of 6 1/2 years.* Can J Public Health, 1977. 68(1): p. 43-50.
89. Kristjansson, E.A., P.A. Fried, and B. Watkinson, *Maternal smoking during pregnancy affects children's vigilance performance.* Drug Alcohol Depend, 1989. 24(1): p. 11-9.
90. Butler, N.R. and H. Goldstein, *Smoking in pregnancy and subsequent child development.* Br Med J, 1973. 4(5892): p. 573-5.
91. Fried, P.A., B. Watkinson, and R. Gray, *A follow-up study of attentional behavior in 6-year-old children exposed prenatally to marijuana, cigarettes, and alcohol.* Neurotoxicol Teratol, 1992. 14(5): p. 299-311.
92. Fried, P.A. and B. Watkinson, *36- and 48-month neurobehavioral follow-up of children prenatally exposed to marijuana, cigarettes, and alcohol.* J Dev Behav Pediatr, 1990. 11(2): p. 49-58.
93. Cross, S.J., K.E. Linker, and F.M. Leslie, *Sex-dependent effects of nicotine on the developing brain.* J Neurosci Res, 2017. 95(1-2): p. 422-436.
94. Scherman, A., J.E. Tolosa, and C. McEvoy, *Smoking cessation in pregnancy: a continuing challenge in the United States.* Ther Adv Drug Saf, 2018. 9(8): p. 457-474.
95. Schnoll, R.A., F. Patterson, and C. Lerman, *Treating tobacco dependence in women.* J Womens Health (Larchmt), 2007. 16(8): p. 1211-8.
96. Perkins, K.A., *Smoking cessation in women. Special considerations.* CNS Drugs, 2001. 15(5): p. 391-411.
97. Piper, M.E., et al., *Gender, race, and education differences in abstinence rates among participants in two randomized smoking cessation trials.* Nicotine Tob Res, 2010. 12(6): p. 647-57.
98. al'Absi, M., *Hypothalamic-pituitary-adrenocortical responses to psychological stress and risk for smoking relapse.* Int J Psychophysiol, 2006. 59(3): p. 218-27.
99. Xu, J., et al., *Gender effects on mood and cigarette craving during early abstinence and resumption of smoking.* Nicotine Tob Res, 2008. 10(11): p. 1653-61.

100. Cao, J., et al., *Locomotor and stress responses to nicotine differ in adolescent and adult rats*. *Pharmacol Biochem Behav*, 2010. 96(1): p. 82-90.
101. Gentile, N.E., et al., *Sexually diergic hypothalamic-pituitary-adrenal (HPA) responses to single-dose nicotine, continuous nicotine infusion, and nicotine withdrawal by mecamylamine in rats*. *Brain Res Bull*, 2011. 85(3-4): p. 145-52.
102. Valera, S., M. Ballivet, and D. Bertrand, *Progesterone modulates a neuronal nicotinic acetylcholine receptor*. *Proc Natl Acad Sci U S A*, 1992. 89(20): p. 9949-53.
103. Curtis, L., et al., *Potentiation of human alpha4beta2 neuronal nicotinic acetylcholine receptor by estradiol*. *Mol Pharmacol*, 2002. 61(1): p. 127-35.
104. Miller, M.M., J. Silver, and R.B. Billiar, *Effects of gonadal steroids on the in vivo binding of [125I]alpha-bungarotoxin to the suprachiasmatic nucleus*. *Brain Res*, 1984. 290(1): p. 67-75.
105. Paradiso, K., J. Zhang, and J.H. Steinbach, *The C terminus of the human nicotinic alpha4beta2 receptor forms a binding site required for potentiation by an estrogenic steroid*. *J Neurosci*, 2001. 21(17): p. 6561-8.
106. Jin, X. and J.H. Steinbach, *Potentiation of Neuronal Nicotinic Receptors by 17beta-Estradiol: Roles of the Carboxy-Terminal and the Amino-Terminal Extracellular Domains*. *PLoS One*, 2015. 10(12): p. e0144631.
107. Ke, L. and R.J. Lukas, *Effects of steroid exposure on ligand binding and functional activities of diverse nicotinic acetylcholine receptor subtypes*. *J Neurochem*, 1996. 67(3): p. 1100-12.
108. Konkle, A.T. and M.M. McCarthy, *Developmental time course of estradiol, testosterone, and dihydrotestosterone levels in discrete regions of male and female rat brain*. *Endocrinology*, 2011. 152(1): p. 223-35.
109. Rhoda, J., P. Corbier, and J. Roffi, *Gonadal steroid concentrations in serum and hypothalamus of the rat at birth: aromatization of testosterone to 17 beta-estradiol*. *Endocrinology*, 1984. 114(5): p. 1754-60.
110. Amateau, S.K., et al., *Brain estradiol content in newborn rats: sex differences, regional heterogeneity, and possible de novo synthesis by the female telencephalon*. *Endocrinology*, 2004. 145(6): p. 2906-17.

111. Amateau, S.K. and M.M. McCarthy, *Induction of PGE2 by estradiol mediates developmental masculinization of sex behavior*. *Nat Neurosci*, 2004. 7(6): p. 643-50.
112. He, Z., et al., *Development of the sexually dimorphic nucleus of the preoptic area and the influence of estrogen-like compounds*. *Neural Regen Res*, 2013. 8(29): p. 2763-74.
113. Lenz, K.M. and M.M. McCarthy, *Organized for sex - steroid hormones and the developing hypothalamus*. *Eur J Neurosci*, 2010. 32(12): p. 2096-104.
114. Lenz, K.M., B.M. Nugent, and M.M. McCarthy, *Sexual differentiation of the rodent brain: dogma and beyond*. *Front Neurosci*, 2012. 6: p. 26.
115. McCarthy, M.M., C.L. Wright, and J.M. Schwarz, *New tricks by an old dogma: mechanisms of the Organizational/Activational Hypothesis of steroid-mediated sexual differentiation of brain and behavior*. *Horm Behav*, 2009. 55(5): p. 655-65.
116. Schwarz, J.M. and M.M. McCarthy, *Cellular mechanisms of estradiol-mediated masculinization of the brain*. *J Steroid Biochem Mol Biol*, 2008. 109(3-5): p. 300-6.
117. Wright, C.L., et al., *Cellular mechanisms of estradiol-mediated sexual differentiation of the brain*. *Trends Endocrinol Metab*, 2010. 21(9): p. 553-61.
118. Wright, C.L. and M.M. McCarthy, *Prostaglandin E2-induced masculinization of brain and behavior requires protein kinase A, AMPA/kainate, and metabotropic glutamate receptor signaling*. *J Neurosci*, 2009. 29(42): p. 13274-82.
119. Lenz, K.M., et al., *Prostaglandin E(2) regulates AMPA receptor phosphorylation and promotes membrane insertion in preoptic area neurons and glia during sexual differentiation*. *PLoS One*, 2011. 6(4): p. e18500.
120. McCarthy, M.M., *Estradiol and the developing brain*. *Physiol Rev*, 2008. 88(1): p. 91-124.
121. McCarthy, M.M., S.K. Amateau, and J.A. Mong, *Steroid modulation of astrocytes in the neonatal brain: implications for adult reproductive function*. *Biol Reprod*, 2002. 67(3): p. 691-8.
122. McCarthy, M.M., A.M. Davis, and J.A. Mong, *Excitatory neurotransmission and sexual differentiation of the brain*. *Brain Res Bull*, 1997. 44(4): p. 487-95.
123. McCarthy, M.M., *Multifaceted origins of sex differences in the brain*. *Philos Trans R Soc Lond B Biol Sci*, 2016. 371(1688): p. 20150106.

124. Slotkin, T.A., et al., *Permanent, sex-selective effects of prenatal or adolescent nicotine exposure, separately or sequentially, in rat brain regions: indices of cholinergic and serotonergic synaptic function, cell signaling, and neural cell number and size at 6 months of age*. *Neuropsychopharmacology*, 2007. 32(5): p. 1082-97.
125. Mychasiuk, R., et al., *Long-term alterations to dendritic morphology and spine density associated with prenatal exposure to nicotine*. *Brain Res*, 2013. 1499: p. 53-60.
126. Damborsky, J.C., W.H. Griffith, and U.H. Winzer-Serhan, *Chronic neonatal nicotine exposure increases excitation in the young adult rat hippocampus in a sex-dependent manner*. *Brain Res*, 2012. 1430: p. 8-17.
127. Klein, L.C., et al., *Laternal nicotine exposure increases nicotine preference in periadolescent male but not female C57B1/6J mice*. *Nicotine Tob Res*, 2003. 5(1): p. 117-24.
128. Lichtensteiger, W. and M. Schlumpf, *Prenatal nicotine affects fetal testosterone and sexual dimorphism of saccharin preference*. *Pharmacol Biochem Behav*, 1985. 23(3): p. 439-44.
129. Chen, H., et al., *Gestational nicotine exposure reduces nicotinic cholinergic receptor (nAChR) expression in dopaminergic brain regions of adolescent rats*. *Eur J Neurosci*, 2005. 22(2): p. 380-8.
130. Dominguez, J.M., et al., *Mating activates NMDA receptors in the medial preoptic area of male rats*. *Behav Neurosci*, 2007. 121(5): p. 1023-31.
131. Hillarp, N.A., H. Olivecrona, and W. Silfverskiold, *Evidence for the participation of the preoptic area in male mating behaviour*. *Experientia*, 1954. 10(5): p. 224-5.
132. Larsson, K. and L. Heimer, *MATING BEHAVIOUR OF MALE RATS AFTER LESIONS IN THE PREOPTIC AREA*. *Nature*, 1964. 202: p. 413-4.
133. Markowski, V.P., et al., *A D1 agonist in the MPOA facilitates copulation in male rats*. *Pharmacol Biochem Behav*, 1994. 47(3): p. 483-6.
134. McCarthy, M.M. and A.P. Arnold, *Reframing sexual differentiation of the brain*. *Nat Neurosci*, 2011. 14(6): p. 677-83.
135. Gorski, R.A., *Sexual differentiation of the brain*. *Hosp Pract*, 1978. 13(10): p. 55-62.

136. Malsbury, C.W., *Facilitation of male rat copulatory behavior by electrical stimulation of the medial preoptic area*. *Physiol Behav*, 1971. 7(6): p. 797-805.
137. Dominguez-Salazar, E., et al., *Facilitation of male-like coital behavior in female rats by kindling*. *Behav Brain Res*, 2003. 140(1-2): p. 57-64.
138. Christensen, L.W., D.M. Nance, and R.A. Gorski, *Effects of hypothalamic and preoptic lesions on reproductive behavior in male rats*. *Brain Res Bull*, 1977. 2(2): p. 137-41.
139. Nugent, B.M., et al., *Brain feminization requires active repression of masculinization via DNA methylation*. *Nat Neurosci*, 2015. 18(5): p. 690-7.
140. Buck, J.M., et al., *Developmental nicotine exposure precipitates multigenerational maternal transmission of nicotine preference and ADHD-like behavioral, rhythmometric, neuropharmacological, and epigenetic anomalies in adolescent mice*. *Neuropharmacology*, 2019. 149: p. 66-82.
141. Satta, R., et al., *Nicotine decreases DNA methyltransferase 1 expression and glutamic acid decarboxylase 67 promoter methylation in GABAergic interneurons*. *Proc Natl Acad Sci U S A*, 2008. 105(42): p. 16356-61.
142. Hall, B.J., et al., *Cognitive and Behavioral Impairments Evoked by Low-Level Exposure to Tobacco Smoke Components: Comparison with Nicotine Alone*. *Toxicol Sci*, 2016. 151(2): p. 236-44.
143. Trauth, J.A., F.J. Seidler, and T.A. Slotkin, *An animal model of adolescent nicotine exposure: effects on gene expression and macromolecular constituents in rat brain regions*. *Brain Res*, 2000. 867(1-2): p. 29-39.
144. Murrin, L.C., et al., *Nicotine administration to rats: methodological considerations*. *Life Sci*, 1987. 40(17): p. 1699-708.
145. Benowitz, N.L. and P. Jacob, 3rd, *Daily intake of nicotine during cigarette smoking*. *Clin Pharmacol Ther*, 1984. 35(4): p. 499-504.
146. Slotkin, T.A., et al., *Effects of prenatal nicotine exposure on biochemical development of rat brain regions: maternal drug infusions via osmotic minipumps*. *J Pharmacol Exp Ther*, 1987. 240(2): p. 602-11.
147. Rees, S. and T. Inder, *Fetal and neonatal origins of altered brain development*. *Early Hum Dev*, 2005. 81(9): p. 753-61.

148. Slotkin, T.A., *Fetal nicotine or cocaine exposure: which one is worse?* J Pharmacol Exp Ther, 1998. 285(3): p. 931-45.
149. Franke, R.M., J.D. Belluzzi, and F.M. Leslie, *Gestational exposure to nicotine and monoamine oxidase inhibitors influences cocaine-induced locomotion in adolescent rats.* Psychopharmacology (Berl), 2007. 195(1): p. 117-24.
150. Oliveira, E., et al., *Nicotine exposure affects mother's and pup's nutritional, biochemical, and hormonal profiles during lactation in rats.* J Endocrinol, 2010. 205(2): p. 159-70.
151. Krueger, F. and S.R. Andrews, *Bismark: a flexible aligner and methylation caller for Bisulfite-Seq applications.* Bioinformatics, 2011. 27(11): p. 1571-2.
152. Akalin, A., et al., *methylKit: a comprehensive R package for the analysis of genome-wide DNA methylation profiles.* Genome Biol, 2012. 13(10): p. R87.
153. Huang da, W., B.T. Sherman, and R.A. Lempicki, *Systematic and integrative analysis of large gene lists using DAVID bioinformatics resources.* Nat Protoc, 2009. 4(1): p. 44-57.
154. Huang, D.W., et al., *DAVID Bioinformatics Resources: expanded annotation database and novel algorithms to better extract biology from large gene lists.* Nucleic Acids Res, 2007. 35(Web Server issue): p. W169-75.
155. Boehm, N., C. Lazarus, and C. Aron, *Interactions of testosterone with the olfactory system in the display of mounting behavior in the female rat.* Physiol Behav, 1991. 50(5): p. 1001-6.
156. Bertolini, A., M. Bernardi, and S. Genedani, *Effects of prenatal exposure to cigarette smoke and nicotine on pregnancy, offspring development and avoidance behavior in rats.* Neurobehav Toxicol Teratol, 1982. 4(5): p. 545-8.
157. Suzuki, K., *The developing world of DOHaD.* J Dev Orig Health Dis, 2018. 9(3): p. 266-269.
158. Chandra, M., et al., *Classification of the human phox homology (PX) domains based on their phosphoinositide binding specificities.* Nat Commun, 2019. 10(1): p. 1528.
159. Shin, N., et al., *Sorting nexin 9 interacts with dynamin 1 and N-WASP and coordinates synaptic vesicle endocytosis.* J Biol Chem, 2007. 282(39): p. 28939-50.

160. Binda, C.S., et al., *Sorting nexin 27 rescues neuroligin 2 from lysosomal degradation to control inhibitory synapse number*. *Biochem J*, 2019. 476(2): p. 293-306.
161. Mizutani, R., et al., *Expression of sorting nexin 12 is regulated in developing cerebral cortical neurons*. *J Neurosci Res*, 2012. 90(4): p. 721-31.
162. Grando, S.A., *Connections of nicotine to cancer*. *Nat Rev Cancer*, 2014. 14(6): p. 419-29.
163. Barbieri, R.L., J. Gochberg, and K.J. Ryan, *Nicotine, cotinine, and anabasine inhibit aromatase in human trophoblast in vitro*. *J Clin Invest*, 1986. 77(6): p. 1727-33.
164. Lenroot, R.K., et al., *Sexual dimorphism of brain developmental trajectories during childhood and adolescence*. *Neuroimage*, 2007. 36(4): p. 1065-73.
165. Yates, M.A. and J.M. Juraska, *Pubertal ovarian hormone exposure reduces the number of myelinated axons in the splenium of the rat corpus callosum*. *Exp Neurol*, 2008. 209(1): p. 284-7.
166. Herting, M.M., et al., *The role of testosterone and estradiol in brain volume changes across adolescence: a longitudinal structural MRI study*. *Hum Brain Mapp*, 2014. 35(11): p. 5633-45.
167. Herting, M.M., et al., *The impact of sex, puberty, and hormones on white matter microstructure in adolescents*. *Cereb Cortex*, 2012. 22(9): p. 1979-92.
168. Nunez, J.L., D.M. Lauschke, and J.M. Juraska, *Cell death in the development of the posterior cortex in male and female rats*. *J Comp Neurol*, 2001. 436(1): p. 32-41.
169. Nunez, J.L., J. Sodhi, and J.M. Juraska, *Ovarian hormones after postnatal day 20 reduce neuron number in the rat primary visual cortex*. *J Neurobiol*, 2002. 52(4): p. 312-21.
170. Willing, J. and J.M. Juraska, *The timing of neuronal loss across adolescence in the medial prefrontal cortex of male and female rats*. *Neuroscience*, 2015. 301: p. 268-75.
171. Pinos, H., et al., *The development of sex differences in the locus coeruleus of the rat*. *Brain Res Bull*, 2001. 56(1): p. 73-8.
172. England, L.J., et al., *Nicotine and the Developing Human: A Neglected Element in the Electronic Cigarette Debate*. *Am J Prev Med*, 2015. 49(2): p. 286-93.

173. Lister, R., et al., *Global epigenomic reconfiguration during mammalian brain development*. *Science*, 2013. 341(6146): p. 1237905.
174. Segarra, A.C. and F.L. Strand, *Perinatal administration of nicotine alters subsequent sexual behavior and testosterone levels of male rats*. *Brain Res*, 1989. 480(1-2): p. 151-9.
175. Gondim, R., F. Teles, and U. Barroso, Jr., *Sexual orientation of 46, XX patients with congenital adrenal hyperplasia: a descriptive review*. *J Pediatr Urol*, 2018. 14(6): p. 486-493.
176. Ellis, L. and S. Cole-Harding, *The effects of prenatal stress, and of prenatal alcohol and nicotine exposure, on human sexual orientation*. *Physiol Behav*, 2001. 74(1-2): p. 213-26.
177. Ganna, A., et al., *Large-scale GWAS reveals insights into the genetic architecture of same-sex sexual behavior*. *Science*, 2019. 365(6456).
178. Williams, G.M., et al., *Maternal cigarette smoking and child psychiatric morbidity: a longitudinal study*. *Pediatrics*, 1998. 102(1): p. e11.
179. Buck, J.M., H.C. O'Neill, and J.A. Stitzel, *Developmental nicotine exposure elicits multigenerational disequilibria in proBDNF proteolysis and glucocorticoid signaling in the frontal cortices, striata, and hippocampi of adolescent mice*. *Biochem Pharmacol*, 2019. 168: p. 438-451.
180. Button, T.M., B. Maughan, and P. McGuffin, *The relationship of maternal smoking to psychological problems in the offspring*. *Early Hum Dev*, 2007. 83(11): p. 727-32.
181. Golding, J., et al., *Grand-maternal smoking in pregnancy and grandchild's autistic traits and diagnosed autism*. *Sci Rep*, 2017. 7: p. 46179.
182. Lyall, K., R.J. Schmidt, and I. Hertz-Picciotto, *Maternal lifestyle and environmental risk factors for autism spectrum disorders*. *Int J Epidemiol*, 2014. 43(2): p. 443-64.
183. Doernberg, E. and E. Hollander, *Neurodevelopmental Disorders (ASD and ADHD): DSM-5, ICD-10, and ICD-11*. *CNS Spectr*, 2016. 21(4): p. 295-9.
184. Scandurra, V., et al., *Neurodevelopmental Disorders and Adaptive Functions: A Study of Children With Autism Spectrum Disorders (ASD) and/or Attention Deficit and Hyperactivity Disorder (ADHD)*. *Front Psychiatry*, 2019. 10: p. 673.

185. Rommelse, N.N., et al., *Shared heritability of attention-deficit/hyperactivity disorder and autism spectrum disorder*. Eur Child Adolesc Psychiatry, 2010. 19(3): p. 281-95.
186. van Mil, N.H., et al., *DNA methylation profiles at birth and child ADHD symptoms*. J Psychiatr Res, 2014. 49: p. 51-9.
187. Hannon, E., et al., *Interindividual methylomic variation across blood, cortex, and cerebellum: implications for epigenetic studies of neurological and neuropsychiatric phenotypes*. Epigenetics, 2015. 10(11): p. 1024-32.
188. van Dongen, J., et al., *Epigenome-wide Association Study of Attention-Deficit/Hyperactivity Disorder Symptoms in Adults*. Biol Psychiatry, 2019. 86(8): p. 599-607.
189. Fuchikami, M., et al., *DNA methylation profiles of the brain-derived neurotrophic factor (BDNF) gene as a potent diagnostic biomarker in major depression*. PLoS One, 2011. 6(8): p. e23881.
190. Wilmot, B., et al., *Methylomic analysis of salivary DNA in childhood ADHD identifies altered DNA methylation in VIPR2*. J Child Psychol Psychiatry, 2016. 57(2): p. 152-60.
191. Baron-Cohen, S., *The extreme male brain theory of autism*. Trends Cogn Sci, 2002. 6(6): p. 248-254.
192. Thapar, A., M. Cooper, and M. Rutter, *Neurodevelopmental disorders*. Lancet Psychiatry, 2017. 4(4): p. 339-346.
193. Dempsey, D.A., et al., *Determination of tobacco smoke exposure by plasma cotinine levels in infants and children attending urban public hospital clinics*. Arch Pediatr Adolesc Med, 2012. 166(9): p. 851-6.
194. Sastry, B.V., et al., *Formation and retention of cotinine during placental transfer of nicotine in human placental cotyledon*. Pharmacology, 1998. 57(2): p. 104-16.
195. Jauniaux, E. and B. Gulbis, *Placental transfer of cotinine at 12-17 weeks of gestation and at term in heavy smokers*. Reprod Biomed Online, 2001. 3(1): p. 30-33.
196. Schechter, J.C., et al., *Impact of Smoking Ban on Passive Smoke Exposure in Pregnant Non-Smokers in the Southeastern United States*. Int J Environ Res Public Health, 2018. 15(1).

197. Hawkins, S.S., et al., *Secondhand smoke exposure among nonsmoking pregnant women in New York City*. *Nicotine Tob Res*, 2014. 16(8): p. 1079-84.
198. Braun, J.M., et al., *Prenatal environmental tobacco smoke exposure and early childhood body mass index*. *Paediatr Perinat Epidemiol*, 2010. 24(6): p. 524-34.
199. Kersey, P.J., et al., *Ensembl Genomes: an integrative resource for genome-scale data from non-vertebrate species*. *Nucleic Acids Res*, 2012. 40(Database issue): p. D91-7.
200. Brimacombe, M.B., R. Pickett, and J. Pickett, *Autism post-mortem neuroinformatics resource: the autism tissue program (ATP) informatics portal*. *J Autism Dev Disord*, 2007. 37(3): p. 574-9.
201. Zhang, L., et al., *ADHDgene: a genetic database for attention deficit hyperactivity disorder*. *Nucleic Acids Res*, 2012. 40(Database issue): p. D1003-9.
202. Hayman, V. and T.V. Fernandez, *Genetic Insights Into ADHD Biology*. *Front Psychiatry*, 2018. 9: p. 251.
203. Sorokina, A.M., et al., *Striatal transcriptome of a mouse model of ADHD reveals a pattern of synaptic remodeling*. *PLoS One*, 2018. 13(8): p. e0201553.
204. Rasmussen, A.H., H.B. Rasmussen, and A. Silahatoglu, *The DLGAP family: neuronal expression, function and role in brain disorders*. *Mol Brain*, 2017. 10(1): p. 43.
205. Fan, Z., et al., *DLGAP1 and NMDA receptor-associated postsynaptic density protein genes influence executive function in attention deficit hyperactivity disorder*. *Brain Behav*, 2018. 8(2): p. e00914.
206. Chertkow-Deutsher, Y., et al., *DNA methylation in vulnerability to post-traumatic stress in rats: evidence for the role of the post-synaptic density protein Dlgap2*. *Int J Neuropsychopharmacol*, 2010. 13(3): p. 347-59.
207. Soto, D., et al., *Glutamate receptor mutations in psychiatric and neurodevelopmental disorders*. *Commun Integr Biol*, 2014. 7(1): p. e27887.
208. Gao, C., N.C. Tronson, and J. Radulovic, *Modulation of behavior by scaffolding proteins of the post-synaptic density*. *Neurobiol Learn Mem*, 2013. 105: p. 3-12.
209. Heinrich, H., et al., *Attention, cognitive control and motivation in ADHD: Linking event-related brain potentials and DNA methylation patterns in boys at early school age*. *Sci Rep*, 2017. 7(1): p. 3823.

210. Morrow, E.M., et al., *Identifying autism loci and genes by tracing recent shared ancestry*. *Science*, 2008. 321(5886): p. 218-23.
211. Demontis, D., et al., *Discovery of the first genome-wide significant risk loci for attention deficit/hyperactivity disorder*. *Nat Genet*, 2019. 51(1): p. 63-75.
212. Waterland, R.A., et al., *Maternal methyl supplements increase offspring DNA methylation at Axin Fused*. *Genesis*, 2006. 44(9): p. 401-6.
213. Kuhnen, P., et al., *Interindividual Variation in DNA Methylation at a Putative POMC Metastable Epiallele Is Associated with Obesity*. *Cell Metab*, 2016. 24(3): p. 502-509.
214. Lokki, A.I., et al., *Smoking during pregnancy reduces vitamin D levels in a Finnish birth register cohort*. *Public Health Nutr*, 2019: p. 1-5.
215. Prasodjo, A., et al., *Serum cotinine and whole blood folate concentrations in pregnancy*. *Ann Epidemiol*, 2014. 24(7): p. 498-503 e1.
216. Tuenter, A., et al., *Folate, vitamin B12, and homocysteine in smoking-exposed pregnant women: A systematic review*. *Matern Child Nutr*, 2018: p. e12675.
217. Joubert, B.R., et al., *Maternal plasma folate impacts differential DNA methylation in an epigenome-wide meta-analysis of newborns*. *Nat Commun*, 2016. 7: p. 10577.
218. McCullough, L.E., et al., *Maternal B vitamins: effects on offspring weight and DNA methylation at genomically imprinted domains*. *Clin Epigenetics*, 2016. 8: p. 8.
219. Benjamin Neelon, S.E., et al., *Maternal vitamin D, DNA methylation at imprint regulatory regions and offspring weight at birth, 1 year and 3 years*. *Int J Obes (Lond)*, 2018. 42(4): p. 587-593.
220. Simpson, J.L., et al., *Micronutrients and women of reproductive potential: required dietary intake and consequences of dietary deficiency or excess. Part I--Folate, Vitamin B12, Vitamin B6*. *J Matern Fetal Neonatal Med*, 2010. 23(12): p. 1323-43.
221. US, I.o.M., in *Dietary Reference Intakes for Thiamin, Riboflavin, Niacin, Vitamin B6, Folate, Vitamin B12, Pantothenic Acid, Biotin, and Choline*. 1998: Washington (DC).
222. Holick, M.F., *Vitamin D deficiency*. *N Engl J Med*, 2007. 357(3): p. 266-81.
223. Chawla, D., et al., *Early prenatal vitamin D concentrations and social-emotional development in infants*. *J Matern Fetal Neonatal Med*, 2019. 32(9): p. 1441-1448.

224. Burris, H.H., et al., *Plasma 25-hydroxyvitamin D during pregnancy and small-for-gestational age in black and white infants*. *Ann Epidemiol*, 2012. 22(8): p. 581-6.
225. Bodnar, L.M., et al., *High prevalence of vitamin D insufficiency in black and white pregnant women residing in the northern United States and their neonates*. *J Nutr*, 2007. 137(2): p. 447-52.
226. Adalsteinsson, B.T., et al., *Heterogeneity in white blood cells has potential to confound DNA methylation measurements*. *PLoS One*, 2012. 7(10): p. e46705.
227. Curtin, S.C. and T.J. Matthews, *Smoking Prevalence and Cessation Before and During Pregnancy: Data From the Birth Certificate, 2014*. *Natl Vital Stat Rep*, 2016. 65(1): p. 1-14.
228. Ideraabdullah, F.Y., et al., *Maternal vitamin D deficiency and developmental origins of health and disease (DOHaD)*. *J Endocrinol*, 2019.
229. Brown, M.J. and K. Beier, *Vitamin B6 Deficiency (Pyridoxine)*, in *StatPearls*. 2019: Treasure Island (FL).
230. Vermaak, W.J., et al., *Vitamin B-6 nutrition status and cigarette smoking*. *Am J Clin Nutr*, 1990. 51(6): p. 1058-61.
231. Ba, Y., et al., *Relationship of folate, vitamin B12 and methylation of insulin-like growth factor-II in maternal and cord blood*. *Eur J Clin Nutr*, 2011. 65(4): p. 480-5.
232. Stidley, C.A., et al., *Multivitamins, folate, and green vegetables protect against gene promoter methylation in the aerodigestive tract of smokers*. *Cancer Res*, 2010. 70(2): p. 568-74.
233. Kim, Y.I., *Nutritional epigenetics: impact of folate deficiency on DNA methylation and colon cancer susceptibility*. *J Nutr*, 2005. 135(11): p. 2703-9.
234. Crider, K.S., et al., *Folate and DNA methylation: a review of molecular mechanisms and the evidence for folate's role*. *Adv Nutr*, 2012. 3(1): p. 21-38.
235. Xue, J., et al., *Impact of vitamin D depletion during development on mouse sperm DNA methylation*. *Epigenetics*, 2018. 13(9): p. 959-974.
236. Laury, A.R., et al., *A comprehensive analysis of PAX8 expression in human epithelial tumors*. *Am J Surg Pathol*, 2011. 35(6): p. 816-26.

237. Poleev, A., et al., *PAX8, a human paired box gene: isolation and expression in developing thyroid, kidney and Wilms' tumors*. *Development*, 1992. 116(3): p. 611-23.
238. Hardy, L.R., A. Salvi, and J.E. Burdette, *UnPAXing the Divergent Roles of PAX2 and PAX8 in High-Grade Serous Ovarian Cancer*. *Cancers (Basel)*, 2018. 10(8).
239. Arva, N.C., et al., *Diagnostic Utility of Pax8, Pax2, and NGFR Immunohistochemical Expression in Pediatric Renal Tumors*. *Appl Immunohistochem Mol Morphol*, 2018. 26(10): p. 721-726.
240. Chai, H.J., et al., *PAX8 is a potential marker for the diagnosis of primary epithelial ovarian cancer*. *Oncol Lett*, 2017. 14(5): p. 5871-5875.
241. Fagerberg, L., et al., *Analysis of the human tissue-specific expression by genome-wide integration of transcriptomics and antibody-based proteomics*. *Mol Cell Proteomics*, 2014. 13(2): p. 397-406.
242. Anglim, P.P., et al., *Identification of a panel of sensitive and specific DNA methylation markers for squamous cell lung cancer*. *Mol Cancer*, 2008. 7: p. 62.
243. James, W.H., *Potential explanation of the reported association between maternal smoking and autism*. *Environ Health Perspect*, 2013. 121(2): p. a42.
244. Garcia-Garcia, A.G., et al., *Alpha-fetoprotein (AFP) modulates the effect of serum albumin on brain development by restraining the neurotrophic effect of oleic acid*. *Brain Res*, 2015. 1624: p. 45-58.

Biography

Rashmi Joglekar completed her Bachelor of Science degree, *summa cum laude*, in Biotechnology with a minor in chemistry from Indiana University in December, 2013. At Indiana University, Rashmi was inducted into the Phi Beta Kappa Society. She joined the Integrated Toxicology and Environmental Health Program at Duke University in the fall of 2014, and has since focused her doctoral research on investigating the neurodevelopmental consequences of smoking during pregnancy.

During her time at Duke, Rashmi was awarded several research grants and scholarships that supported her academic work. In 2016, she received an administrative supplemental grant totaling \$100,000 from the NIEHS and EPA, which was used to support the majority of her doctoral research. In 2018, Rashmi was awarded a competitive \$5,000 scholarship through the Environmental Health Scholars Program. Rashmi also earned additional awards for her research presentations and university service. She won a Distinguished Poster Award at the Environmental Health Scholars Program Fall Forum at Duke University in 2018, and placed first in the annual Nicholas School of the Environment Ph.D. Symposium 3-Minute Thesis Competition that same year. For her university service, primarily through serving as the President of the Graduate and Professional Student Council (GPSC), Rashmi was named one of Duke's Top 18 People to Know on Campus by the Duke Chronicle. She continues to work on

efforts addressing food insecurity among graduate and professional students at Duke, and hopes to transition to a career in science policy after receiving her doctorate.